Investigation of Steel Pile Foundations in Corrosively Active Areas

Final Report

March 1995

Richard P. Long, Professor
Joseph Badinter, Graduate Assistant
Papa Rao Kambala, Graduate Assistant

JHR 95-239 Project 92-4

This research was sponsored by the Joint Highway Research Advisory Council (JHRAC) of the University of Connecticut and the Connecticut Department of Transportation and was carried out in the Civil Engineering Department of the University of Connecticut.

Technical Report Documentation Page

1. Report No.	2. Government Accession No.	3. Recipient's Catalog No.
JHR 95-239		

4. Title and Subtitle	5. Report Date
Investigation of Steel Pile Foundations in Corrosively Active Areas	March 1995
	6. Performing Organization Code
7. Author(s) Richard P. Long, Joseph Badinter, and Papa Rao Kambala	8. Performing Organization Report No. JHR 95-239
9. Performing Organization Name and Address University of Connecticut Department of Civil Engineering 191 Auditorium Road, Box U-37 TI Storrs, CT 06269	10. Work Unit No. (TRAIS) 11. Contract or Grant No.
12. Sponsoring Agency Name and Address Connecticut Department of Transportation 280 West Street Rocky Hill, CT 06067-0207	13. Type of Report and Period Covered Final Report 14. Sponsoring Agency Code

15. Supplementary Notes

16. Abstract

Severely corroded steel H piles were discovered in 1988 when the new interchange between I-84 and I-91 in Hartford, CT, was under construction. Based on the findings of an earlier report, construction drawings of all bridges that contain steel piles were reviewed. Locations that showed subsurface conditions similar to those that produced the corrosion have been prioritized for further field and laboratory investigation. The techniques used to identify these locations are described. Laboratory investigation explored the characteristics of the macrocell which is the mechanism that caused the corrosion in Hartford. These experiments showed that in addition to the combination of layers of incineration products and clay above the groundwater table, a macrocell can form at the groundwater table in homogenous soil whose pore water has a resistivity below 1000 ohm-cm^{-1}. A soil probe is described that can be adapted to locate layers in the subsurface profile that will corrode steel piles.

17. Key Words	18. Distribution Statement
Steel piles, corrosion, macrocell corrosion, soil corrosion probe	No Restrictions

19. Security Classif. (of this report)	20. Security Classif. (of this page)	21. No. of Pages	22. Price
Unclassified	Unclassified	146	

Form DOT F 1700.7 (8-72) Reproduction of completed page authorized

SI* (MODERN METRIC) CONVERSION FACTORS

APPROXIMATE CONVERSIONS TO SI UNITS

Symbol	When You Know	Multiply By	To Find	Symbol
	LENGTH			
in	inches	25.4	millimetres	mm
ft	feet	0.305	metres	m
yd	yards	0.914	metres	m
mi	miles	1.61	kilometres	km
	AREA			
in^2	square inches	645.2	millimetres squared	mm^2
ft^2	square feet	0.093	metres squared	m^2
yd^2	square yards	0.836	metres squared	m^2
ac	acres	0.405	hectares	ha
mi^2	square miles	2.59	kilometres squared	km^2
	VOLUME			
fl oz	fluid ounces	29.57	millilitres	mL
gal	gallons	3.785	Litres	L
ft^3	cubic feet	0.028	metres cubed	m^3
yd^3	cubic yards	0.765	metres cubed	m^3

NOTE: Volumes greator than 1000 L shall be shown in m^3.

Symbol	When You Know	Multiply By	To Find	Symbol
	MASS			
oz	ounces	28.35	grams	g
lb	pounds	0.454	kilograms	kg
T	short tons (2000 lb)	0.907	megagrams	Mg
	TEMPERATURE (exact)			
°F	Fahrenheit temperature	5(F-32)/9	Celcius temperature	°C

*SI is the symbol for the International System of Measurement

APPROXIMATE CONVERSIONS TO SI UNITS

Symbol	When You Know	Multiply By	To Find	Symbol
	LENGTH			
mm	millimetres	0.039	inches	in
m	metres	3.28	feet	ft
m	metres	1.09	yards	yd
km	kilometres	0.621	miles	mi
	AREA			
mm^2	millimetres squared	0.0016	square inches	in^2
m^2	metres squared	10.764	square feet	ft^2
ha	hectares	2.47	acres	ac
km^2	kilometres squared	0.386	square miles	mi^2
	VOLUME			
mL	millilitres	0.034	fluid ounces	fl oz
L	litres	0.264	gallons	gal
m^3	metres cubed	35.315	cubic feet	ft^3
m^3	metres cubed	1.308	cubic yards	yd^3
	MASS			
g	grams	0.035	ounces	oz
kg	kilograms	2.205	pounds	lb
Mg	megagrams	1.102	short tons (2000 lb)	T
	TEMPERATURE (exact)			
°C	Celcius temperature	1.8C + 32	Fahrenheit temperature	°F

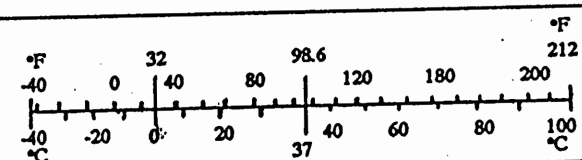

Table of Contents

List of Projects by Connecticut towns that were reviewed for steel piles in miscellaneous fill during this research project.

List of Figures

List of Tables

I. Introduction

Previous publications (1,2,3) addressed the corrosion of steel piles discovered during the reconstruction of the I-84 to I-91 Interchange in Hartford, CT. Briefly, the corrosion was caused by macrocells in the miscellaneous fill above the ground water table. Macrocells develop between layers in the miscellaneous fill having different aeration conditions; one layer is oxygen rich while the other is oxygen deficient. The strongest and most stable macrocells observed developed between a layer of clay and a layer of products of burning, such as ash, cinders and slag. The electrical current is generated by the contiguous layers but must flow through the steel pile to complete the circuit. The electrical current leaves the pile at the anode where it causes corrosion.

The work described here searches out other areas within the State of Connecticut in which corrosion as observed in Hartford might develop, and investigates various subsurface conditions that could support the development of macrocells.

II. Locating Corrosively Aggressive Areas

Corrosively aggressive areas can occur in miscellaneous fills because of the manner in which they were made and the materials used as fill. Each fill was made over a period of time with whatever material became available, and should be held in suspicion until it can be investigated. The subsurface profile consists of thin layers (30 to 60 cm) of all type soil from gravels to clays, and often includes other materials such as ashes, cinders, coal and construction debris. Each miscellaneous fill is different in both the materials used and their arrangement in the profile. The only known method at present of determining the capability of a fill to corrode steel piles is to retrieve continuous samples and test the electrical characteristics of contiguous layers. The sampling must be continuous so that no layers and no possible macrocell combinations are overlooked.

The U.S. Geological Survey prepares maps of surficial Geology that identify the type of soil near the surface. A special symbol is used on these maps to designate manmade fills. An example of a map with manmade fills is shown in Fig. 1. Every material that has been moved from elsewhere is designated manmade fill on these maps. Fills that follow the general shape of some constructed facility such as a highway probably contain granular fill and are relatively homogeneous. One can also see a fill that covers a large area such as "afl". This fill was probably not placed during construction of a specific structure and therefore is a good condidate for investigation.

Based on the location by town, the construction records of any highway that crosses the fill can be found in CONNDOT's records. Each structure on each project must be checked for the placement of steel piles through the miscellaneous fills. The construction drawings of all projects within the dotted outline of Fig. 2 were reviewed. The specific projects and structures are listed in Appendix A. The review examined available boring logs and construction drawings. There were several reasons that projects were eliminated from further investigation, the most obvious being that the foundations contained no steel piles. Projects that contained steel piles were examined further to determine the positions of the miscellaneous fill, the ground water table (GWT) and the elevation of the bottom of the pile cap.

If the bottom of the pile cap was below the ground water table, that structure was eliminated from further investigation because there is not enough oxygen below the GWT to support corrosion. The footing may have been placed below the bottom of the miscellaneous fill, which for the state of knowledge at the beginning of this project was sufficient to eliminate the site from further consideration as corrosively aggressive.

The locations that should receive additional investigation are listed in Table 1. Table 1 was prepared after reviewing the construction documents including the boring logs. Each project in this table has been assigned a priority, 1 through 5. All locations listed in Table 1 have potentially aggressive layers

Figure 1 **Section of Surficial Geology QR-18 U.S. Geological Survey, showing large areas of manmade fills along the shores of New Haven harbor**

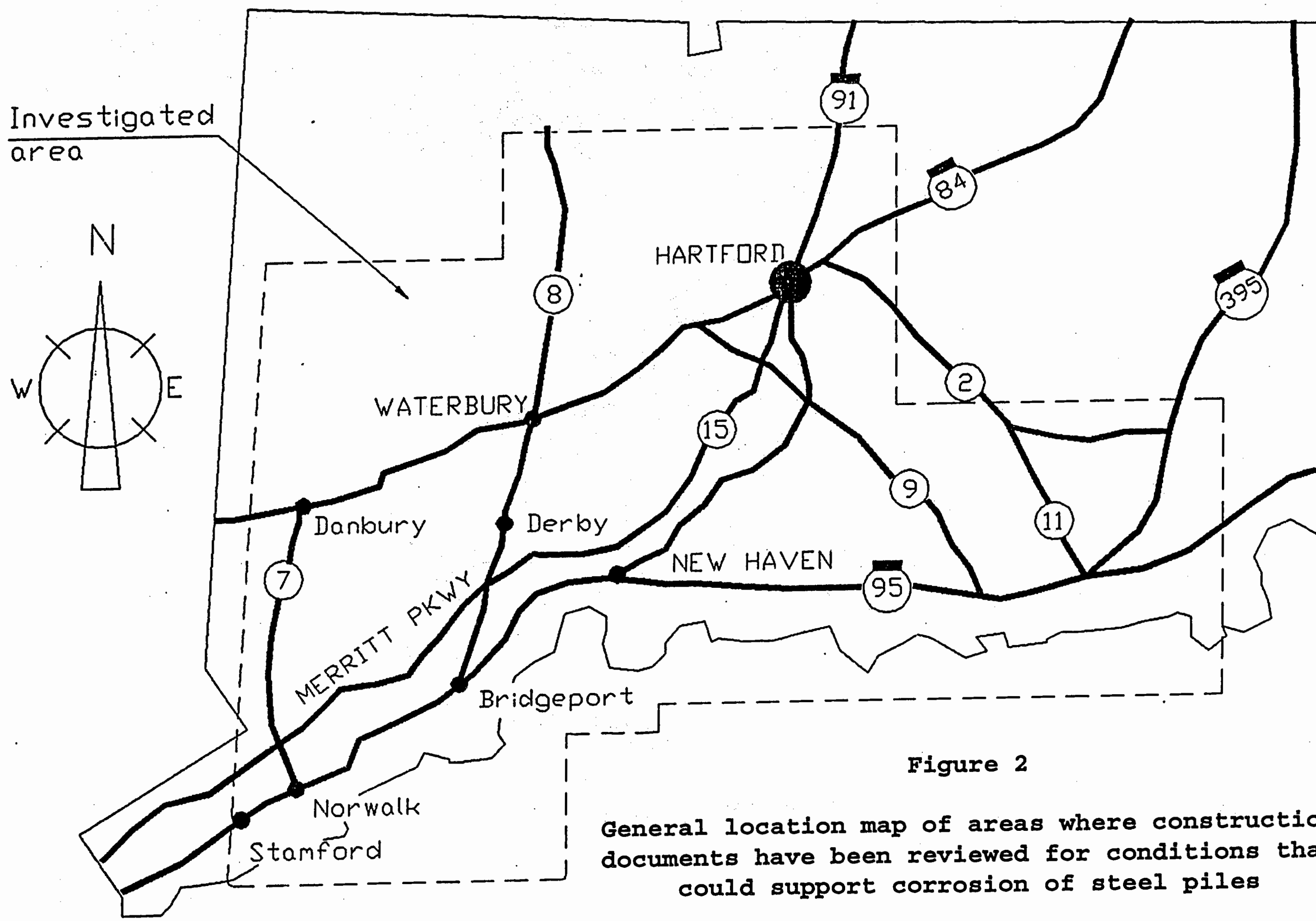

Figure 2

General location map of areas where construction documents have been reviewed for conditions that could support corrosion of steel piles

above the water table. The priorities were assigned as follows:

Priority	**Subsurface Conditions**
1	Ash against clay
2	Cinders, ash or misc. fill over 10' thick
3	Cinders, ash or misc. fill 5-10' thick
4	Cinders, ash or misc. fill 0-5' thick
5	Other conditions that may support corrosion

Contiguous layers of ash and clay are assigned Priority 1. These conditions caused the corrosion losses in Hartford and can be shown in the laboratory to be potent macrocells. Boring logs for miscellaneous fill often lack detail to determine from a review of the construction documents whether or not they contain aggressive layers. Priority No. 2 to 4 are assigned on the probability that of the occurrence of aggressive layers to be somewhat proportional to thickness of miscellaneous fill, i.e. the thicker the fill the greater opportunity for the existence of aggressive layers. Priority No. 5 is for any other conditions that might produce corrosion.

Every effort should be made to investigate the condition of the piles in Table 1. This might be initiated with a review of the construction drawings and other construction records by CONNDOT personnel to determine if the aggressive layers may have been replaced during the construction process. Another item to consider is the availability of oxygen to the soils, since corrosion only occurs when oxygen is present.

The information in Table 1 has been forwarded to CONNDOT as soon as it was available with the recommendation that the review process begin as soon as possible. Advantage should be taken of every opportunity to determine if these locations do indeed contain aggressive layers. This involves continuous sampling and the testing of contiguous layers for minimum resistivity (4) and contact potential (2) or corrosion potential (5).

Table 1 Priorities of Suspected Corrosion

Town	Project No:	Project Name	Substructure Name	Boring No.	Layer Thck. ft.	Cap Elev.ft	GWT Elev. (ft)	Constituents	Priority
Berlin	85-07	Relocation of Rt.72 over NY,NH & HRR	WB, Abut.	B1	1.9	72.5	54	Cinders and fill	4
	85-07	Same as above	WB, Abut.	B4	0.5	72.5	55	Cinders and fill	5
	85-07	Same as above	West Pier	E4	2	48	46	Cinders, R.R. bed,fill	4
	85-07	Same as above	West Pier	E6	1	48	47	Cinders, R.R. bed,fill	4
	85-07	Same as above	East Pier	E7	3	48	45	Cinders, R.R. bed,fill	4
	85-07	Same as above	East Pier	E9	4	48	43	Cinders, R.R. bed,fill	4
Bridgeport	312-01	G - K Expwy over Central Ave.	SE Wingwall	B-105	10	21.5	4	Black cinders	2
	310-02	I-95 over NY,NH&HRR at Burr st.	Pier	D-15	6	42	5	Cinders	2
	312-01	I-95 over Central Ave.	Pier	B-105	10	21.5	4.5	Cinders	2
	310-01	I-95 over South Ave.	Pier	D-179	3	6	2	Misc.fill	3
	311-01	I-95 over Bridge Port Harbor Bridge	East Abut.	P-50	>10	39	1	Cinders	2
	311-01	I-95 over Bridge Port Harbor Bridge	East Abut.	P-51	10	36	3	Cinders	2
	311-01	I-95 over Bridge Port Harbor Bridge	Ramp D	P-52	>10	21	2.9	Cinders	2
Danbury	34-93	Relocation of Rt.6 over NY,NH & HRR	End Bridge	S4-7	4	469	446.5	Black cinders	4
Haddam	82-118	Relocation of Rt.9	SB Abutment	B-CH11-S	3	138.5	124	Ashes	4
	82-118	Relocation of Rt.9	SB Abutment	B-CH12	5	138.5	121	Ashes and cinders	4
Hartford	63-137	I-84 WB Rdwy over Church St	Abutment	33	2	42		Black cinders&misc.fill	1
	63-137	I-84 WB Rdwy over Church St	Abut.WB	37	3.5	47	37	Black cinders&misc.fill	1
	63-137	I-84 WB Rdwy over Church St	Abut.WB	48	1	42	41	Cinders	4
	63-159	Sigourney Street	Pier S5	47	4.5	43.5	36	Cinders	1
	63-159	Sigourney Street	Wingwall D	56	1.5	56.5		Ash	1
	63-159	Sigourney Street	Pier EBR1	61	4	42.5		Cinders,ash	1
	63-137	I-84	WB, Abut.	37	4.5	47	37	Misc.fill,cinders	1
	63-137	I-84	Pier 1	39	1	35	34	Cinders,Misc.fill	2
	63-137	I-84	Abutment	48	2	42	40	Cinders	4

Table 1 (cont.) Priorities of Suspected Corrosion

Town	Project No.	Project Name	Substructure Name	Boring No.	Layer Thck. ft.	Cap Elev.ft	GWT Elev. (ft)	Constituents	Priority
	63-138	East west I-84 Section III	Pier ML1	12	2	50	15	Black cinders	1
	63-138	East west I-84 Section III	Pier ML9	32	3.5	45.5	20	Ash fill	1
	63-138	East west I-84 Section III	Pier ML11	39	2	44	33	Cinders	1
	63-138	East west I-84 Section III	Pier EBR4	64	5.5	37.5	30	Cinders	3
	63-138	East west I-84 Section III	Pier WBR2	66	1	45	25	Cinders	1
	63-138	East west I-84 Section III	Pier ML16	70	1	45.5	40	Cinders	1
	63-138	East west I-84 Section III	Pier ML17	73	4	44	28	Gray cinders	4
	63-138	East west I-84 Section III	Pier ML19	78	2.5	42.5	37	Black cinders	1
	63-138	East west I-84 Section III	Pier ML20	83	2.5	40	30	Cinder fill	4
	63-138	East west I-84 Section III	Pier ML22	84	4	42	34	Black cinders	4
	63-138	East west I-84 Section III	Pier ML23	86	3	42	32	Black cinders	4
	63-138	East west I-84 Section III	Pier ML26	94	1	41	36	Black ash,cinder fill	1
	63-138	East west I-84 Section III	Pier ML31	106	2	51		Bl.cinders,ashes	1
	63-138	East west I-84 Section III	Pier EW1	107r	2.5	52.5	43	Bl.cinders	4
	63-138	East west I-84 Section III	Pier EW2	110	6.5	51.5		Cinders	1
	63-192	I-84	Pier NS10, B5	23	3	34.5	28	Black cinders	4
	63-192	I-84	Pier NE11, B7	41	3	39.75	32	Black cinders	4
	63-192	I-84	Pier NS14,B5	43	4	39.25	32	Cinders,ashes	4
	63-192	I-84	Pier EW7, B11	48	1	33	32	Misc.fill	4
	63-192	I-84	Pier SW4, B13	49	1	36	34	Misc.fill,ashes	4
	63-192	I-84	Abut, B14	53	16	56.5	30	Misc.fill	4
	63-192	I-84	Pier SW7, B13	55	14.5	45.5	31	Cinders,wood,glass	1
	63-192	I-84	Pier SW9, B13	67	12	49	37	Misc.fill	1
	63-192	I-84	Abut, B13	68	5	67	60	Misc.fill	2
	63-193	Farmington Avenue Connector	Pier NS15, B6	43	4	39.25	32	Misc.fill	4
Hartford	63-193	Farmington Avenue Connector	Pier SN16, B4	44	4	41.75	33	Misc.fill,ashes	4
	63-193	Farmington Avenue Connector	Pier SN19, B4	48	2.5	34.5	32	Misc.fill	3
	63-193	Farmington Avenue Connector	Pier NS21, B6	55	9	33	33	Misc.fill,cinders	1
	63-141	I-84	Pier ES2, B1	14	3	37	34		4

Table 1 (cont.) Priorities of Suspected Corrosion

Town	Project No:	Project Name	Substructure Name	Boring No.	Layer Thck. ft.	Cap Elev.ft	GWT Elev. (ft)	Constituents	Priority
Hartford	63-141	I-84	Pier EN1, B9	36	9.5	38.5	27	Misc.fill	1
	63-141	I-84	Pier NE6, B7	37	15	48	23	Cinders	1
	63-103	The Hartford-Springfield Expy	Pier S7	28	8.5	23.5		Cinders	2
		at Founders Bridge							
	63-103	The Hartford-Springfield Expy	Pier 4R	31	5	18	3	Cinders	3
	63-103	The Hartford-Springfield Expy	Pier 3R	34	12.5	16.5		Cinder,brick fill	1
	63-103	The Hartford-Springfield Expy	Pier 2R	35	5.5	19.5		Cinders	3
	63-103	The Hartford-Springfield Expy	Pier S1	103	2.5	15.5		Cinders	4
	63-103	The Hartford-Springfield Expy	Pier WS1	105	5	19	6.2	Cinder bricks	3
	63-103	The Hartford-Springfield Expy	Pier S4	109	14	17	2.9	Cinder bricks	1
	63-103	The Hartford-Springfield Expy	North Abut.	124	11	34.5		Cinder bricks	1
	63-103	The Hartford-Springfield Expy	Pier S13	125	9	20		Cinders	1
	63-103	The Hartford-Springfield Expy	Pier S12	126	17	19		Cinders	1
	63-103	The Hartford-Springfield Expy	Pier S10	128	7.5	17.5	4	Cinders	2
	63-103	The Hartford-Springfield Expy	Pier S6	131	2	19	17	Cinders	4
	63-103	The Hartford-Springfield Expy	Pier 1L	133	6	18		Cinders	3
	63-158	I-84	Pier EW9	49	9	25	16	Cinders	2
	63-158	I-84	Pier EW10	52	17	29	10	Cinders	1
	63-158	I-84	Pier EW8	47	7	25	18	Ash&cinders	2
	63-158	I-84	Pier EW11	59	17	32.5	6	Cinders	1
	63-158	I-84	Ret. Wall St.#31	95	2	17	5	Ash&coal	3
	63-174	I-84 E-W Section 3	Abutment	185	8	61	31	Coal	2
	63-174	I-84 E-W Section 3	Back Abut.	168	8	67.7	59	Cinders	2
	63-200	River Park road over NY,NH&HRR	Pier	RR-3	4	25	6.5	Cinders	1
	42-133	I-84 Bridge I-10&K-9	South Abut.	I-B2	3	13	10	Cinders	1
Hartford	42-134	I-84 Bridge over Darlin Street	East Abut.	C-B2	1.5	16.5	12	Cinders	4
	63-161	I-91 Retaining Wall A	Retaining Wall A	B-22	4	26.5	12	Cinders	3
Montville	326-01	G - K Expwy over Rt.163	South Abutment	S-27	5	92.5	69.8	Cinders	3

Table 1 (cont.) Priorities of Suspected Corrosion

Town	Project No:	Project Name	Substructure	Boring	Layer	Cap	GWT	Constituents	Priority
			Name	No.	Thck. ft.	Elev.ft	Elev. (ft)		
Hartford	42-134	I-84 Bridge over Darlin Street	East Abut.	C-B2	1.5	16.5	12	Cinders	4
	63-161	I-91 Retaining Wall A	Retaining Wall A	B-22	4	26.5	12	Cinders	3
Montville	326-01	G - K Expwy over Rt.163	South Abutment	S-27	5	92.5	69.8	Cinders	3
New Britai	88-48	I-291 Connector WB Rdwy	Backwall	S1-4	2.4	107	103.5	Cinders	4
		over St. Mary's Cemetery							
New Have	317-02	G - K Expwy over Quinnipiac River	Pier #3	82E	7	-2	-21	Black cinders	1
	317-02	G - K Expwy over Quinnipiac River	Pier #4W	84	1	-2	-3	Cinder fill	4
	92-94	Rdwy OEE over Rdwy OAN&OAE	North abut.	51	10	17	-3	Ashes	1
	92-94	Rdwy OEE over Rdwy OAN&OAE	North Abut.	52	2	17	1	Ashes	4
	92-94	Rdwy OEE over Rdwy OAN&OAE	South Abut.	57	3	24	-9	Ashes	4
	92-94	SB I-91&WB I-95 Rdwys OAE&OAN	North Abut.	A-1	8	14.5	0	Cinders	3
	92-94	SB I-91&WB I-95 Rdwys OAE&OAN	North Abut.	39	3	26.5	0	Cinders	4
	92-94	Rdwys OES&OEW over Water St.	Pier #2	232	4	17.5	3	Cinders&ashes	4
	92-94	Rdwys OES&OEW over Water St.	Pier #4	241	5	4	0	Cinders&ashes	3
	92-94	NB I-91&Rdwy OAN over Water St.	North Abut.	E1	4	18	1	Cinders	4
	92-110	East rock connector under Willow St.	West Abut.	S10.1	14	21.75	-4	Cinders	1
	92-110	East rock connector under Willow St.	West Abut.	S10.2	2	10.5	-3	Ashes	4
	92-110	East rock connector under Willow St.	West Abut.	S10.3	1	-2	-1	Ashes	
	100-60	I-91 over NY,NH&HRR	Pier #2,SB	P3	11	16	13	Cinders	5
	100-60	I-91 over NY,NH&HRR	Pier #2,SB	S3-3	4	16	13	Cinders	1
	100-60	I-91 over NY,NH&HRR	Pier #1,SB	S3-6	5	15.5	14	Black cinders	1
	100-60	I-91 over NY,NH&HRR	Pier #3,NB	S33-9	4	16	15	Black cinders	1
	100-60	I-91 over NY,NH&HRR	Pier #4,NB	S3-10	5	17	16	Black cinders	1
	100-60	I-91 over NY,NH&HRR	Pier #3,NB	S3-13	5	16	11	Black cinders	1
	100-60	I-91 over NY,NH&HRR	Pier #4,NB	S3-14	5	17	16	Black cinders	1
	317-04	Greenwich-Killingly expy over Oak St.	South Abut.	39	5	22	0	Black cinders	1

Table 1 (cont.) Priorities of Suspected Corrosion

Town	Project No:	Project Name	Substructure Name	Boring No.	Layer Thck. ft.	Cap Elev.ft	GWT Elev. (ft)	Constituents	Priority
North Hav	100-57-03B	Relocation of Rt. US. 5A over NY,NH&HRR	Wing Wall	1	1	29	-	Cinders	4
	100-57-03B	Relocation of Rt. US. 5A over NY,NH&HRR	Wing Wall	4	3	29	-	Misc.fill	4
	100-57-03B	Relocation of Rt. US. 5A over NY,NH&HRR	Wing Wall	5	22	29	-	Misc.fill	1
Norwalk	102-114-03B	Relocation of Rt.7	Pier	1	8	38	28	Cinders and coal	3
	102-114-03B	Relocation of Rt.7	Pier	2	16	38	18	Cinders and tr. coal	3
	102-114-03B	Relocation of Rt.7	Wing 1A	3	3	47.5	22	Cinders and fill	4
	102-114-03B	Relocation of Rt.7	Wing 2B	6	3	55	30.6	Cinders and fill	4
	102-114-03D	Relocation of Rt.7 WN Rdwy NE	Pier #1	1	10	38	28	Cinders&coal	2
		Rdwy & Ramp over I-95							
	102-114-03D	Same as above	Pier #1	2	7	38	18	Cinders	3
	102-114-03D	Same as above	South Abut.	3	3	47.5	21	Cinders	4
	102-114-03D	Same as above	North Abut.	6	2	55	29	Cinders	4
	102-114-03	Same as above	Abut. #2	7	7	51.3	-3	Cinders&refuse	3
Seymour	124-99	Relocation of Rt.8 over Derby Ave.	SB, Pier #1	B-22	6	59.5	53.7	Cinders and fill	3
	124-99	Relocation of Rt.8 over Derby Ave.	NB, Abut. #2	B-30	3	70.5	58.8	Cinders and fill	4
Stamford	304-02	G - K Expwy	Wall 5	343	8	3.5	-	Misc. fill	3
	304-02	G - K Expwy	Wall 10	375	5	6.5	1.5	Misc. fill	4
	304-02	G - K Expwy	Wall 8	378	4	10.5	3.5	Misc. fill	4
	304-02	G - K Expwy	Wall 8	389	2	9	6	Misc. fill	4
	304-02	G - K Expwy	Wall 12	401	1	8.75	7.5	Misc. fill	4
	304-02	G-K expy over Lafayette St.	West Abut.	182	3	44.25	10	Cinders&misc.fill	4
	304-02	G-K expy over Lafayette St.	Pier #1	185	4	22	8	Cinders	3
	304-02	G-K expy over Lafayette St.	Ramp P	189	3	43.5	5	Cinders	4
	304-02	G-K expy over Lafayette St.	Ramp P	192	4	43.5	5	Cinders	4
	304-02	G-K expy over Lafayette St.	Pier #6	194	5	24	8	Cinders	3
	304-02	G-K expy over Lafayette St.	Ramp P	198	5	36	8	Cinders	3

Table 1 (cont.) Priorities of Suspected Corrosion

Town	Project No:	Project Name	Substructure Name	Boring No.	Layer Thck. ft.	Cap Elev.ft	GWT Elev. (ft)	Constituents	Priority
Stamford	308-01	Sherwood Island to state highway	B4	1	5	5	-5	Cinders	2
		over NY,NH&HRR							
Watebury	151-87	Structure #9, I-84 EB&WB B1 level	Pier 8N	D349	5	258	253	Cinders	2
		East of Naugatuck River to NY, NH &HRR							
	151-87	Same as above	Pier 8N	D353	15	269.5	254	Cinders	2
	151-89	Retaining Walls 3-3&3-4	Wall 3-4	D326	10	291.5	255	Cinders	2
	151-87	I-84 structure#22&26 NE Rdwys	Pier #7	D216-2	13	281	252	Cinders&ashes	2
	151-87	I-84 structure#22&26 NE Rdwys	Pier #6N	D217	18	290.5	250	Cinders	2
	151-80	Relocation of RT 8 over NY,NH&HRR	Pier	S1-7	6	292.3	263	Cinders	3
	151-80	Relocation of RT 8 over NY,NH&HRR	Pier	S1-8	5	292.3	263	Cinders	3
	151-89	Structure #10, Ramp 10 over relocated Meadow St.	Pier #9	D-378	10	267.5	253	Cinders	2
	151-89	Same as above	Pier #4	D-373	10	281	254	Cinders&coal	2
	151-89	I-84 EB&WB B1 level East over NY,NH&HRR	Abutment	D-326	10	286	255	Cinders	2
	151-89	Same as above	Pier #3	D-304	10	296	255	Cinders	2
	151-88	Route 8 NB&SB B1 level	Pier 1W	D-530	10	259	249	Tr.of coal&cinders	4
	151-87	Route 8 NB&SB B1 level Structure 20	Pier 7W	D-573	17	269	251	Cinders	4

III. Literature Review

A. Difficulties with the Classic Study

At the present time the geotechnical engineer has little guidance in evaluating the corrosion potential of subsurface conditions for steel piles. The conclusions of Romanoff (6) from his study of the corrosion of steel piles stated,

"The data indicate that the type and amount of corrosion observed on the steel pilings driven into undisturbed natural soil, regardless of the soil characteristics and properties, is not sufficient to significantly affect the strength or useful life of pilings as load-bearing structures.

Moderate corrosion occurred on several piles exposed to fill soils which were above the water table level or in the water table zone. At these levels the pile sections are accessible if the need for protection should be deemed necessary."

Although Romanoff (6) noted that the piles that showed moderate corrosion were accessible for protection if deemed necessary, he gave no indication of the subsurface conditions that should alert the engineer to the possibility of corrosion losses from steel piles because he went on to state,

"Properties of soils such as type, drainage, resistivity, pH, or chemical composition are of no practical value in determining the corrosiveness of soils toward steel pilings driven underground. This is contrary to everything previously published pertaining to the behavior of steel under disturbed conditions. Hence, it can be concluded that National Bureau of Standards data previously published on specimens exposed in disturbed soils do not apply to steel pilings which are driven to undisturbed soils."

The conclusions of the second report (7) were similar to those in the first report, and did not address the conditions of piles from the listed locations that may have sustained substantial losses. Romanoff's conclusions that corrosion of steel piles is not a problem became the conventional wisdom and led to published statements such as "The statistical record for the durability of H-piles is perfect. Nevertheless, some designs continue to incorporate protective measures which detract from the economy of steel installations" (8).

TABLE 2

Piles Included in the NBS Study that
Showed Significant Loss of X-Section

Location	Age Yrs	X-Section Loss %	Position of Loss w/GWT	Remarks
Sparrows Pt., MD	18	29	+/- 2 ft	Cinders & Slag
Sardis, Miss. Dam Outlet	20	19	+/- 5 ft	Grav./ Clay
Boardman, NC Lumber River	37	28	-3 ft	Loam/ Clay
Granada, Miss. Spillway	11	16	+3 ft	Clods of Clay
Hartford, CT Dike	23	>10	Varies	Cinders

These conclusions have had a great influence on geotechnical engineers, many of whom probably read the conclusions without examining the data in the reports. A careful reading of the data in the first report (6) shows that the losses that Romanoff referred to as <u>moderate corrosion</u> were as high as 29% of the cross sectional area, and piles from 6 of the 19 sites investigated showed corrosion losses of cross sectional area 11% or greater.

Examples are shown in Table 2. Four of these cases are from the first report published in 1962 (6) and the other is from the 1972 report (7). Column 3 of Table 2 also shows that the losses occurred in the vicinity of the water table. This second report (7) which listed results from 25 additional sites, did not present the detail of the corrosion losses available in the initial report. Specifically, it did not report the amount of cross section lost. Nevertheless, the photo in the report of the piling from East Hartford indicated a loss certainly greater than 10% and the brief descriptions indicate that there may be at least two more locations that experienced losses of 10% or greater. The statements quoted above provide no method to account for the observed losses.

The lack of knowledge about definitive soil conditions that support the corrosion of steel piles has led to confusion among geotechnical engineers. Most textbooks on foundation engineering carry a paragraph or two about the corrosion of steel piles that states the author's feeling that corrosion might occur (9,10,11). The authors do not appear to completely accept Romanoff's conclusions but they have been left without any indication of the proper way to identify conditions that will corrode steel piles. In light of the findings at Hartford, CT and in New York State this is a critical issue especially as the infrastructure is being renovated throughout the United States. It makes no sense to renovate the superstructure unless the foundation is able to continue to function properly. The testing of conditions that support corrosion of steel piles is in its early stages.

Discovery of severely corroded piles raises the questions, Where else has it occurred and where is it occurring now? The answer requires an analysis of the conditions that led to the observed losses. The observed macrocells in Connecticut developed in miscellaneous fills between contiguous layers with differing aeration characteristics and low electrical resistivity. The most powerful macrocells developed between contiguous layers of clay and products from burning processes, such as ash, cinders, and coal. The clay, being a fined grained soil, retains moisture by capillary action for long periods of time after it has been wetted even if it is above the ground water table. In Connecticut where the average rainfall is 45 inches per year, the clay layers in the miscellaneous fill are probably wet most of the time. Having small pore sizes, the clay does not allow oxygen to diffuse readily into it and this layer acts as the anode. The contiguous layer containing ash, cinders, and perhaps coal has much larger pores allowing some of the water to drain away under gravity which is then rapidly replaced by air containing oxygen. The remaining water keeps the resistivity low. This layer becomes the cathode. The corrosion observed in the miscellaneous fills more closely correlates with the loss patterns found by Romanoff with buried metals. The corrosion was greater when the pH was low, and chlorides and sulfates were present indicating that the macrocell has the effect of neutralizing the global cathodic protection that Romanoff hypothesized for steel piles, if it ever existed. The pattern that emerged in New York State indicates that the macro-cell corrosion can develop with the aeration conditions around the water table when the resistivity is low enough. There may also be other mechanisms for forming macrocells that have to do with the location of the ground water table and resistivity of the soil or materials in place. No doubt some of these were at work in the losses shown from the work by Romanoff (6).

B. The Macrocell

The characteristics of the corrosion losses indicated macrocell action and led to a review of literature on this topic which is also known as long-line-corrosion when it occurs in pipelines. There are only a few publications that report systematic investigations of macrocells.

Schaschl and Marsh (12) reviewed the corrosion of steel in soils. They discussed the macrocell action as a function of the degree of water saturation, permeability, availability of oxygen, and soil resistivity. They showed that macrocell and microcell corrosion can occur simultaneously and the role of the anodic/cathodic area ratio on the corrosion rate. They also demonstrated that a steel pile can be corroded by the macrocell established by the ground water table if the resistivity is low enough. A differential aeration cell is developed by the ground water with oxygen available in the partially saturated zone, contiguous to the oxygen deficient saturated zone below the GWT. The macrocell corrosion in the vicinity of the water table depends on the resistivity. If the resistivity is too high, current can not flow, and significant corrosion can not occur.

Other researchers have studied galvanic cell formation of the type STEEL/SOIL1/SOIL2/STEEL/. Schwerdtfeger (13) demonstrated the electrochemical concept that a metal, subjected to the passage of an electrical current, will lose weight at an anodic region of the metal depending upon how much current is passed.

Several investigators associated corrosion problems with soils having fine particles such as clays (1,14,15,16). For example, in 1968 the Swedish Corrosion Institute performed studies with regard to underground corrosion of steel rods in different types of soil. A corrosion rate has been detected as high as 2.8% in weight per 5-year period for steel in contact with some marine clays on the Swedish West coast (17). Unfortunately, the cause of such corrosion acceleration was not determined.

Kasahara (18) proposed that corrosion of buried steel pipes in dissimilar soils resulted from longline and local corrosive attack. He investigated these conditions through corrosion potential. Corrosion potential was measured by positioning a $Cu-CuSO_4$ reference electrode in an immediate vicinity of the test electrode embedded in a soil of interest. He stated that corrosion potential gave as good correlation for the rate of uniform corrosion driven by a local cell action, wherein more negative corrosion potential leads to a higher corrosion rate. As he indicated, corrosion potential is a better, direct indication of soil corrosivity.

Macrocells formed on metal surface as a result of local heterogeneity of soils will depend to a lesser degree on the electrical resistivity. Tomashov and Mikhailovsky (19) concluded that corrosion currents due to the comparatively small size of the soil inclusion are determined mostly by polarization characteristics. At the time the authors could not define the analytical relationship between the probability of macrocell formation, degree of aeration and electroconductivity of soils. But they proposed that the probability of macrocell occurrences, i.e. the formation of potential differences between contiguous portions of the embedded structure increases with the growth of the degree of soil aeration. The magnitude of macrocell current is inversely proportional to the specific resistivity of the soil (ρ). Relating the variations of the soil aeration to the alterations of the cathode current density (ΔI_k), the authors proposed the value $\Delta I_k/\Delta L$ * L/ρ as a reflection of the corrosion rates over a long portion (L) of the underground structure when macrocells function. As a result of their studies, the authors experimentally confirmed actively functioning differential aeration cells on the metal surfaces in soil. The researchers indicated the possibility of comprehensively characterizing the corrosive properties of the soils by measuring the cathode and anode polarization (I_k) of iron in contact with soils and electrical specific resistivity of the soil (ρ).

Other researchers measured the instantaneous corrosion rates of driven steel piles in contact with soil by determining the polarization characteristics of the soils (20)(21). Polarization methods are based on the premise that metals pass current out into the soil at the anode. The process of passing current polarizes the region near the electrodes developing a resistance to the current flow. Corrosion tends to shut itself off and the polarization resistance is a measure of how effectively it is done.

Using this technique, electrical current from an external power source is applied to the steel-soil system. Passing a current from an auxiliary electrode to the pile causes a change in the potential between the pile and a reference electrode attached to pile and embedded in the soil. This potential difference is called overvoltage. When the overvoltage does not exceed 20 mv, plotting corrosion current density, a parameter, usually expressed in amperes per square centimeter, versus the overvoltage, results in a straight line the slope of which is called "polarization resistance."

There is a vast body of literature on the subject of polarization phenomena and measurement methodology. One of the techniques such as linear polarization analysis is defined by Fontana and Green (22). This technique overcomes the disadvantages and difficulties of many other methods. It applies current so that the potential shift is within twenty millivolts of the equilibrium potential, a region of applied current in which the linear function of the working electrode potential. This method has become an ASTM standard Practice for Conducting Potentiodynamic Polarization Resistance Measurements (Designation: G 59-84).

There is concern about the position of the reference electrode with respect to the working electrode. The overvoltage can be shifted by the current flow from the auxiliary electrode past the reference electrode to the working electrode. This shift is called the IR drop. Unless steps are taken to neutralize its effects, the IR drop can cause erroneous readings.

In case of steel/soil interface a large IR drop due to the passage of current through the high resistance of the electrolyte could introduce a large error into the measured potential value of the electrode. To avoid these difficulties, a technique was presented by Kasahara et al. (18) where a galvanostatic square wave current is applied alternatively toward anodic and cathodic directions at a definite frequency. This relatively simple technique was widely employed in the present study to obtain instantaneous corrosion rates for different soil in various stages of saturation.

The macrocell has not been the subject of much investigation; but understanding its function is vital to the protection of steel piles.

IV. Macrocell Corrosion of Underground Structures

A. General

Corrosion requires an anode, a cathode and a soil with low resistivity. Studies of corrosion on underground pipelines has shown that a metal pipe penetrating strata with different oxygen concentrations experiences corrosion along the entire surface. The corrosion rates in different strata were unequal, being higher in regions with low oxygen concentration.

Most reported cases of macrocell corrosion were detected on pipelines, passing through porous, well drained soils into dense, saturated soil (12,14). Corrosion attacks were observed in the saturated, low oxygen soil region, near the interface with a different layer having more oxygen available. Macrocorrosion couples can develop not only because of differential aeration of various sections but also because of soil variation such as differential salt compositions, local density variation, etc.

The character of the metal also plays a role in establishing the degree of activity of the differential aeration couple. This activity can be the result of the ability of a metal to shift its static potential in the positive direction by aeration. Even the shape of embedded steel could influence the corrosion process by forming macrocells due to the "edge effect". The possibility of the formation of such corrosion couples follows from the phenomenon of easier access of oxygen to the edges of iron inserted in the soil. Experimental confirmation of such macrocouples was reported by Tomashov (14).

The geometrical dimensions of macrocells can change considerably, depending on sizes of macro inclusions in the soil (for example, lumps of denser or looser soil), and on resistivity of the soil. The macrocells formed by local small anodic regions and a larger cathodic surface operate at very high anodic current densities, causing extreme deterioration of the metal surface, even perforation.

In microcell corrosion the anode and cathode are very close and the result is often the formation of pits. The anode and cathode of a macrocell are separated by a greater distance, and the loss at the anode covers a larger area. The macrocells that caused the losses in Hartford were caused by contiguous layers of materials having different oxygen availability. There are other conditions that develop macrocells. In fact each steel pile that has a butt above the ground water table and a tip below is experiencing a macrocell because of the differing availabilities of oxygen above and below the water table. The question that must be answered in each of these cases is: How strong is the macrocell? In a sand containing water of high resistivity, the soil will carry little current producing negligible corrosion. A soil of low resistivity might, however, support significant corrosion.

The objective of the present study is to investigate all possible factors that could lead to the occurrence of the macro-cell or could have a significant impact on its strength. The list of factors is as follows:

a. Presence of potentially aggressive contiguous layers.
b. Soil layers with different dgrees of saturation.
c. Availability of oxygen
d. Anode/cathode area ratio
e. Soil resistivity, presence of chlorides and sulfates, the concentration of electrolyte, and pH value.
f. Soil porosity
g. Polarization characteristics of the steel in contact with soil

B. Oxygen Mechanism of Soil Corrosion

The corrosion needs an electrolyte to allow the flow of ions. This electrolyte can be the moisture in soil. Dissolved oxygen is an important factor in the corrosion of steel because it is easily oxidized and reduced allowing the current to enter and leave the metal. It is the most effective cathodic depolarizer in that it controls the corrosion rate of the steel. A moist soil that is less than 100% saturated supplies both the electrolyte and the oxygen.

C. Steel Corrosion in Aqueous Solutions

The electrochemical theory of corrosion relates corrosion to a network of short-circuited galvanic cells on the metal surface. Metal ions go into solution at anodic areas in an amount chemically equivalent to the reaction at cathodic areas. At anodic areas the following reaction takes place (23):

$$Fe \rightarrow Fe^{2+} + 2e \qquad (1)$$

This reaction is rapid in most media. When iron corrodes, the rate is usually controlled by the cathodic reaction, which in general is much slower (cathodic control). In deaerated solutions, the cathodic reaction is

$$H^{+} \rightarrow 0.5*O_2 + e^{-} \qquad (2)$$

This reaction proceeds rapidly in acids, but only slowly in relatively neutral aqueous media. The cathodic reaction can be accelerated by dissolved oxygen in a process called depolarization with the following reaction:

$$2H^{+} + 0.5*O_2 \rightarrow H_2O - 2e^{-} \qquad (3)$$

Dissolved oxygen reacts with hydrogen atoms adsorbed at random on the iron surface, independent of impurities in the metal. The oxidation reaction proceeds as rapidly as oxygen reaches the metal surface. Adding (1) and (3):

$$Fe + H_2 + O.5*O_2 \rightarrow Fe(OH)_2 \qquad (4)$$

Hydrous ferrous oxide ($FeO * nH_2O$) or ferrous hydroxide [$Fe(OH)_2$] composes the diffusion-barrier layer next to the iron surface through which O_2 must diffuse. At the outer surface of the oxide film, access to dissolved oxygen converts ferrous oxide to hydrous ferric oxide $Fe(OH)_3$. Hence, rust films normally consist of three layers of iron oxide in different states of oxidation.

At ordinary temperature in neutral or near-neutral water, dissolved oxygen is necessary for appreciable corrosion of iron. Since the diffusion rate at steady state is proportional to the oxygen concentration, it follows from the Eq. 3 that the corrosion rate of iron is also proportional to the oxygen concentration. Some additional comments should be made about the types of galvanic cells that could initiate a corrosion reaction.

D. Types of corrosion cells

There are many types of cells that are able to initiate corrosion reactions. The concentration cell is of interest in the present study. The differential aeration cell is the most important type of concentration cell. The difference in oxygen concentration produces a potential difference, causing current to flow. It accounts for pitting damage under rust or at the water-air interface. The amount of oxygen reaching the metal that is covered by rust or other insoluble reaction products is less than the amount that contacts other portions.

Salt concentration cells occur when there are differences in salt concentration in the solution. The difference in electrolyte concentration develops a difference in electrical potential and flow of current. Both concentration cells are widely seen in soil corrosion.

E. The electromotive force (emf) of the corrosion cell

In view of the electrochemical mechanism of corrosion, the tendency for a metal to corrode can also be expressed in terms of the electromotive force (emf) that is an integral part of the corrosion process. The tendency for any chemical reaction to proceed, including the reaction of a metal with its environment, is measured by the change of the Gibbs free-energy, ΔG. Since electrical energy is expressed as the product of volts and charge, it is defined by $\Delta G = -EnF$, where n is number of chemical equivalents taking part in the reaction, and F - is the Farady (96,500 C/eq). Accordingly, the greater value of E for any cell, the greater is the tendency for the overall corrosion reaction of the cell to proceed.

In any differential aeration cell the electrode in contact with lower-pressure oxygen tends to be the anode and the electrode in contact with higher pressure oxygen tends to be the cathode, and the value of the operating emf is in correlation with different oxygen partial pressures. As an example, using platinum electrodes immersed in electrolyte with different oxygen concentrations, the potential difference between electrodes is given by equation (23)

$$E = -0.0592 \log \frac{p_1(O_2)^{1/4}}{p_2(O_2)^{1/4}} \qquad (5)$$

where - $p_{1,2}(O_2)^{1/4}$ -oxygen partial pressure in contact with immersed platinum electrode.

If a similar cell is made of an iron electrode instead of platinum, the operating emf of such the cell is much larger. The value of emf in this case also depends on the ferrous ion activity at the anode.

F. The corrosion rates and conductivity of an electrolyte

The corrosion rate of steel in an aqueous solution is also determined by the conductivity of the electrolyte (24). The studies of the corrosion rate of steel in neutral aqueous solutions have shown that steel corrodes by local cell action (microcell), by long cell action (macrocell), or both.

In low-conductivity solutions with local cell action, available oxygen is reduced at microscopic cathodic sites; iron is oxidized at adjacent microscopic anodic sites. As conductivity of the electrolyte increases, corrosion may propagate by long cell action, e.g. macrocell action. In macro cell action, the cathodic and anodic zones are separated by an extended distance. In some high-conductivity solutions this distance can be measured in feet. The major driving force in a macrocell action is difference in oxygen concentration between cathodic and anodic zones of the solution and is independent of the means by which this difference is achieved (12).

G. Steel corrosion in soil

Corrosion of steel in soil is governed by the principles of electrochemistry, and both local cell action and long cell action are possible in soil corrosion.

In low-resistivity soils with different physicochemical properties, such as composition or structure of the soil and different moisture contents, macrocells are possible. Sharp changes in oxygen availability in the soil along the length of the buried metal structure may lead to differences in electrical potential that produces current. The amount of current and its distribution over the surface of the metal depends on the resistivity of the soil and its polarization characteristics. The latter in turn are determined by the degree of oxygen penetration of the soil, moisture and salt content, granulation, and other physicochemical properties of the soil.

Tomashov (14) presented examples of the distribution of corrosion current density and potential in an experimental pipeline that passes through the boundary between clay and sand, containing 10% moisture. The distribution curves show that, because of the variation in oxygen concentrations, the initial potential of iron was 0.15 V more negative in clay than in sand. The initial corrosion current in this case was 28 microAmps/cm^2. The increased corrosion rate observed on these pipe sections is due to the action of macrocells, the cathodic section of which is in the sand and anodic section in the clay. In most cases the anodic regions form under dense soil which have lower oxygen availability. Cathode regions form in soils having high oxygen penetrability.

H. Anode/Cathode Area Ratio

Metal is lost at the anode and oxygen is reduced at the cathode. The greatest loss of cross section occurs when the anode area is substantially smaller than the cathode area. These conditions were present in Hartford, and the concentration of the losses at the anode led to substantial reduction of cross sectional area. When the anode is larger than the cathode, the metal loss occurs over a larger area and cathode experiences a protection that reduces its rate of corrosion. An example of this is shown in Fig.

3. As the ratio of anodic to cathodic area increases, the average rate of corrosion decreases.

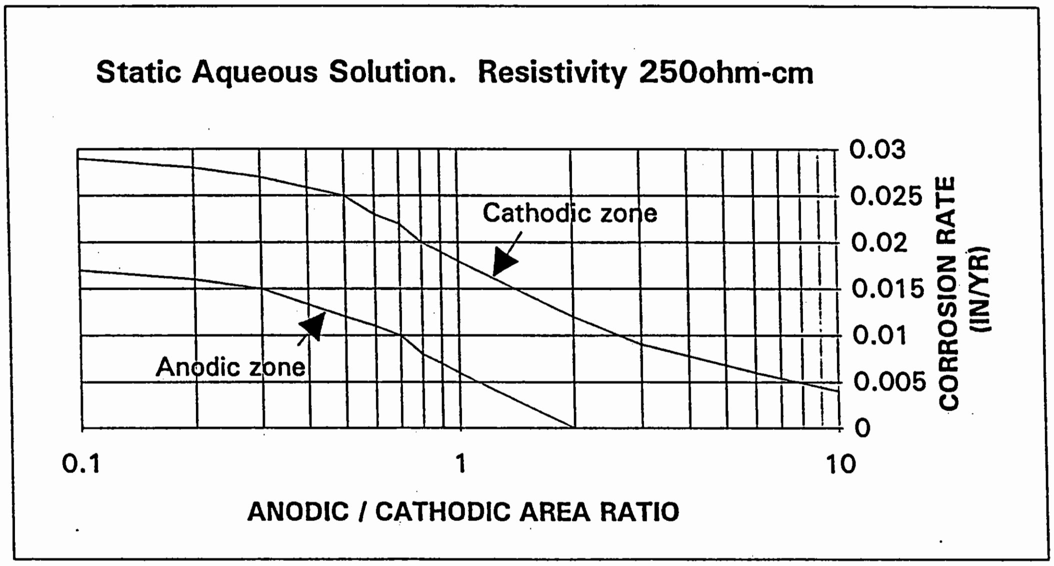

Figure 3

Effect of anode/cathode area ratio on corrosion rate of a macrocell (Schaschl and Marsh (12))

I. Soil Electrical Resistivity

Over the years the electrical resistivity of a soil has been the most commonly used criterion of corrosivity. The resistivity of the soil determines the length of influence of the anode and cathode and has a significant influence on macrocell strength. The resistivity of the soil depends on its chemical content, moisture content, and temperature (15).

J. Chemical content in soil and its effect on the corrosion process

The chemicals in the soil water can be due to the salts in the soil itself, or may have entered through irrigation, fertilization, runoff, etc. Chemical analysis of soil is rarely used alone as the criterion of corrosivity, but the elevated concentration of chlorides and sulfates could be an indicator of higher corrosion rates in some cases.

Corrosion rates in soils with low permeability might be slow, initially, but once the corrosion reaction is initiated, they begin to increase due to several factors which are associated with a higher soluble salt content. The poor protective action of the corrosion product layers has been observed in these soils due to the film breakdown by anions such as Cl^-, SO_4^{2-}, etc. Dilute acids such as HCl or H_2SO_4 which are formed in the immediate vicinity of anodic sites under the pressure of soluble salts; NaCl, or $CaSO_4$ accelerate the corrosion process (25). This process could take place in macrocell corrosion in the low oxygen zone (anode) and will greatly increase local corrosion.

As reported previously (1), one of the observed conditions of macrocell corrosion is that contiguous layers should have specific resistivities less than 1000 ohm-cm. Soil with 1000 ppm of chlorides or sulfates will usually have a saturated resistivity of 650 ohm-cm or less (15). Determination of the presence of chlorides and sulfates in soils by conventional chemical analysis is expensive and time consuming. The salt content of soil can be estimated roughly from electrical-conductivity measurements of a saturated soil (26). A better estimate of soluble salts can be obtained from the conductivity of a solution extracted from the soil. Ground water conductivity analysis gives a good estimate of salt presence, as well. Electrical conductance, which is the reciprocal of resistance, is more suitable for salinity measurements, because it increases with salt content, thus simplifying the interpretation of readings. Electrical conductance is expressed in mhos, i.e., reciprocal ohms, while electrical conductivity has the dimensions of mhos-cm.

The relation between electrical conductivity and the salt content of solutions is shown in Figure 4 for NaCl and Ca SO_4. The curve for NaCl shows higher conductivity than the other salt at an
equivalent concentration.

It is important to note that oxygen solubility in water decreases continuously with sodium chloride concentration. But, at low salt concentrations, on order of 100 ppm, where the conductivity is high and there is still enough oxygen, iron corrodes more rapidly due to the destructive effect of salt ions on the protective corrosive layer. According to Evans (24), the same salt could at different concentrations provoke or inhibit corrosion. Practically all salts are corrosive at very low concentration and inhibitive at very high concentration. This generalization appears to be true in the case of macrocells when clay is in contact with the aggressive layer, however, there may be more than one factor at work.

It is well known that resistivities over 3000 ohm-cm were considered to represent such a low chemical content that analysis would be of no value. Therefore, measurement of resistivity is a first priority, where 1500 ohm-cm should be considered a limit, below which more complete investigation is recommended, and particularly in the case of potentially aggressive contiguous layers.

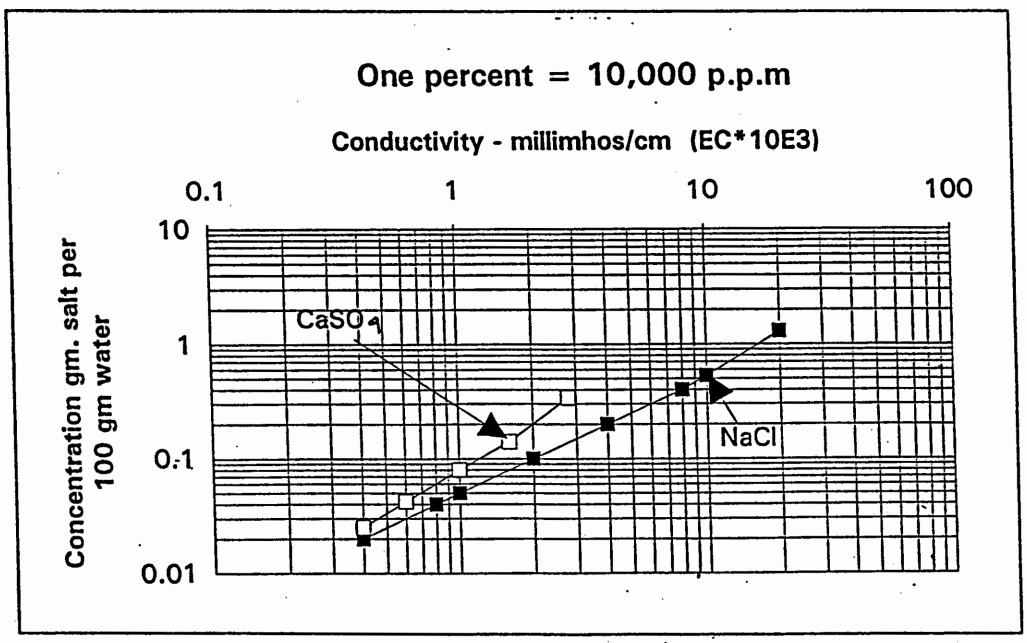

Figure 4
Concentration of single-salt solution in percent as related to electrical conductivity (U.S. Department of Agriculture, 1954 (26)

K. pH as an indicator of soil corrosivity

The use of pH measurements as a criterion of corrosion is of limited value. It has been generally found that metals are most vulnerable to corrosion in soils whose pH is either below 4.0 or above 9.0. For example, the New York DOT has set a range of allowable pH values for backfill materials between 5 and 10 (27).

Schiff (15), however, presented data of six of the most corrosive soils having pH between 4.2 and 9.4. The list includes Montezuma clay having pH equal 6.8 and corrosivity of maximum pit depth of 153 mils per 12 years, and Fargo clay loam having pH equal to 7.6 and corrosivity of maximum pit depth of 119 mils per 12 years.

While the value of pH is a qualitative indicator of hydrogen ion content, total acidity represents the amount of ionizable hydrogen. It is important to stress that the elevated local acidity in low oxygen areas could be an indicator of accelerated corrosion reactions.

L. Moisture content and resistivity of soil

Several investigators have attempted to correlate moisture content, soil resistivity and corrosion rates (12,16). The results have been mixed. Gupta et al. (16) concluded that corrosion rates in the case of water-saturated soil appear to correlate with the fine particle content of the soil. The finer the soil the greater is the corrosivity. The soils with higher content of coarser particles, cause a maximum corrosion rate at comparatively lower moisture content, e.g. maximum corrosion occurred at 65% to 75% of full saturation. This is probably due to the fact that because of reduced capillary porosity, electrical resistivity values of coarser soils decrease rapidly with increasing moisture content, but less oxygen is available. At 65 to 75% there is probably a balance between available oxygen and resistivity.

It is important to stress again that Gupta (16) has found that the maximum corrosion rates of three investigated soils coincident at the point at 65% water holding capacity, which is the degree of saturation. Schaschl and Marsh (12) concluded that corrosion degree of saturation between 50 to 95 percent.

M. Potentially Aggressive Contiguous Layers

Several investigators have described the galvanic cell at the junction of two different soil stratifications as STEEL/SOIL1/SOIL2/STEEL (2,28). Contact potential between the soils with an open circuit could reach 0.5 V (28), and the magnitude of self generated current could be as high as 0.65 milliamps/cm^2 (2). Evans (28) proposed that the reason for electrical potential might be differences of soil chemical composition, water content, resistivity.

Previous reports (1,2) noted the results of two-soil galvanic cells based on cinders in contact with clays from locations which have experienced severe corrosion. Supported by lab experiments and field observation, it was concluded that this combination of two contiguous layers is most conducive to macrocell formation. Long term monitoring of the level of self-generated current in laboratory conditions has shown that the current level was stable in the order of 100 microAmps for 9 months for clay in contact with coal (2). An important observation was made that current could be regenerated in a partially dry cell by adding water. This can be related to the field conditions during snow melting and rainfall. By maintaining the cell in a wetted condition, it is possible to keep up a high self-generated current for an extended period of time.

N. Clays in Contact with Potentially Aggressive Layers

As presented in the literature (2,14), a clay layer <u>always</u> in a combination with a more porous soil above the groundwater table acts as an anode developing a contact-potential generating current that passes between the contiguous layers. The cause of this phenomena is the deferential oxygen availability between the layers. The experiments of the present study investigate the magnitude of current in relationship to the type of clays and electrolyte concentration.

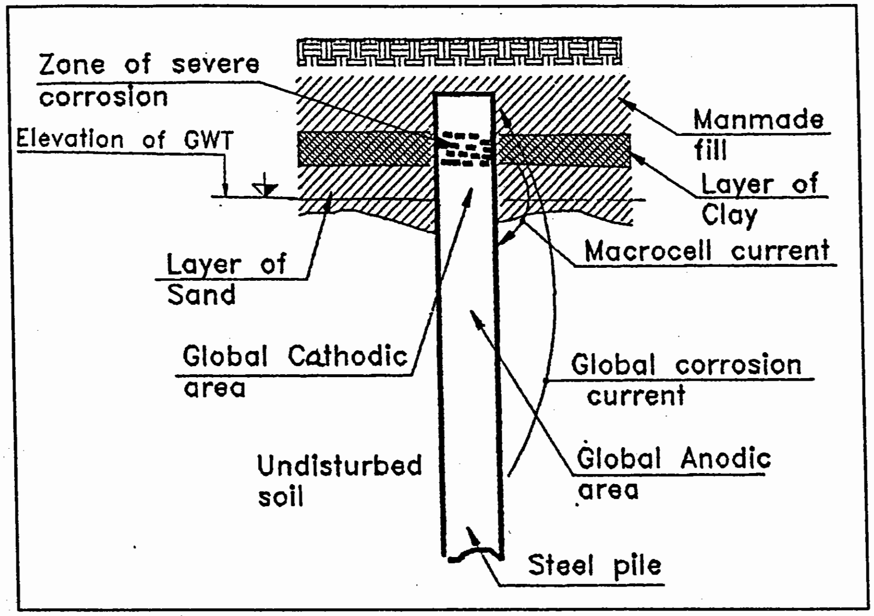

Figure 5

Possible conditions for macro-cell corrosion of steel piles

O. The Effects of Different Degrees of Soil Saturation

The electrical resistivity of a soil will decrease as moisture content increases until the soil is nearly saturated. Beyond that point, the resistivity is fairly constant.

The most serious corrosion problems in a macrocell are usually associated with clay because this fine soil often has high chemical content and can hold moisture for a long time. The water holding capacity and its drainage characteristics are important factors in the corrosion process. The transport of oxygen to the cathodic surface can be facilitated by evaporation or draining of the water in the soil. As the water drains, a thin film is left on the surface of the steel exposed to soil. This film separates the air in the soil from the surface of the steel. In contrast to aqueous solution, where the diffusion film separates the steel from the water that contained a few parts per million of dissolved oxygen, the diffusion film in moist soil separates the steel from 20 percent oxygen of the air. Therefore, cathodic corrosion takes place at a very high rate (12).

Several investigators have studied the corrosion rates with respect to the degree of soil saturation (2,12,20). The summarization of these results are of interest in the present study and presented as follows (12):

1. Metal that remains in a soil at 95 to 100 percent water saturation for a long period of time will not corrode regardless of the soil's resistivity.

2. Long cell (macrocell) action can occur when the soil at the cathode has a water saturation between 50 and 95 percent.

3. A soil that drains slowly keeping the cathode between 50 to 95 percent water saturation for long periods of time will be corrosive, if its resistivity is low.

4. If steel penetrates soil strata and if the upper part of the soil has drained to the 50 - 95 percent water saturation level while the lower part is holding water at 95 - 100 percent of its holding capacity, long cell action will occur. Its effect will depend on the resistivity of the soil.

V. EXPERIMENTAL INVESTIGATIONS

A. The Phenomenon of Polarization

1. General

When a metal is exposed to an aqueous solution containing ions of that metal, both an oxidation of the metal atoms to metal ions, and a reduction of metal ions to metal atoms are taking place. Due to electron exchange, the rate of the two reactions can be expressed by two different current densities. The term "current density" is the ratio of current magnitude to unit of surface area, and is usually expressed in micro Amps/cm^2.

Assuming that no other reaction takes place at the electrode surfaces, the anodic current i_a equals the cathodic current i_c in a state of equilibrium. The "exchange current density" i_o, which is equal to i_a and i_c, is responsible for the disassociation of ferrous ions in steel called "corrosion current density." Using Faraday's law, current can be converted to a corrosion rate. It is important to point out that corrosion current is a direct measure of current flow due to metal oxidation.

Corrosion is an electrochemical direct current process. The flow of current disturbs the equilibrium conditions in the electrolyte by driving the cations toward the cathode and the anions toward the anode. The imbalance caused by the flow of current is called polarization. The passage of current requires electrode reactions, causing a counter electromotive force that can be treated as a resistance. The development of this resistance is important to the corrosion process. If the corrosion current develops a substantial polarization resistance the amount of metal loss will be relatively small, but if the passage of current does not develop much polarization resistance the corrosion loss could be substantial.

The measurement of polarization resistance requires a working electrode, whose polarization resistance in the electrolyte medium is being checked, an auxiliary electrode that completes the circuit in the soil and a reference electrode to measure the change in electrical potential between the working electrode and the electrolyte medium. The polarization resistance is directly related to the change in potential measured with the reference electrode. The passage of current changes the potential between the reference and working electrode from its equilibrium value E_o to the new value E_i. This change in electrode potential is called "overvoltage" and is usually represented by the Greek letter η, where:

$$\eta = E_i - E_o \tag{6}$$

The plot of applied current density versus overvoltage η is called a "polarization curve."

2. Electrolyte polarization

a) Concentration polarization

Concentration polarization is caused by the difference in concentration of ions between the layer of electrolyte nearest the electrode surface and the rest of the electrolyte (30).

b) Activation polarization

Activation polarization is caused by a slow electrode reaction, i.e., the reaction at the electrode requires an activation energy in order to proceed. The most important example is that of hydrogen ion reduction at a cathode, the corresponding polarization term being called hydrogen overvoltage. Activation polarization is also a characteristic of metal-ion deposition or dissolution. This value is predominant for transition metals such as iron. The controlling steps in the reaction are not known precisely, but in some cases it is, probably, a slow rate of hydration of the metal ion as it leaves the lattice, or dehydration of the hydrated ion as it enters the lattice.

At the low polarization values activation polarization η is directly proportional to the current density. At higher polarization values (from approximately 30 to 40 millivolts) there is a linear correlation between activation polarization and the logarithm of the current density. This relationship is given by the "Tafel equation," named after J. Tafel (1904):

$$|\eta| = a + \beta \cdot \log_{10} i \qquad (7)$$

where a and β (Tafel slope) are constants for a given metal and environment.

At low current densities the concentration polarization is often negligible, but it could be predominant at high current densities (30).

c) IR Drop

Polarization measurements include a so-called "ohmic potential" drop through a portion of the medium surrounding the electrode, through a metal-reaction film on the surface, or both. An ohmic potential drop always occurs between the working electrode and the reference electrode. This contribution is particularly large for the steel immersed in soil with high resistivity, and steps must be taken to eliminate it during testing.

d) Basic Concept

The polarization resistance technique, which was first described by Wagner and Traud, and subsequently improved by Stern and Geary (30), is based on the relation:

$$I = 2.303\ I_{corr}[Exp\frac{(E-E_{corr})}{\beta_a} - Exp\frac{(E-E_{corr})}{\beta_c}] \qquad (8)$$

where I and E are current and potential, I_{corr} and E_{corr} are corrosion current and corrosion potential, β_a and β_b are anodic and cathodic Tafel slopes, respectively. This relationship provides a means for determining corrosion current I_{corr} using an externally applied current I_{app}.

To simplify (8) of the exponential function is linearized by expanding it into an infinite series. When the argument is small, only first two members of the series are used neglecting the rest due to their small values, we can make substitution as follows:

$$Exp\frac{(E-E_{corr})}{\beta_a} = 1 + \frac{(E-E_{corr})}{\beta_a} \qquad (9)$$

$$Exp\frac{(E-E_{corr})}{\beta_c} = 1 + \frac{(E-E_{corr})}{\beta_c} \qquad (10)$$

$$(E-E_{corr}) = \frac{I\ \beta_a\ \beta_c}{2.303\ (\beta_a+\beta_c)\ I_{corr}} \qquad (11)$$

Relating the slope of ΔE-I curve at the point of zero current, a first differentiation of Equation (11) yields:

$$(\frac{d\Delta E}{dt})_{t-0} = R_p = \frac{\beta_a\beta_c}{2.303+(\beta_a+\beta_c)\ I_{corr}} = \frac{K}{I_{corr}} \qquad (12)$$

$$\Delta E = E - E_{corr} \qquad (13)$$

$$K = \frac{\beta_a \beta_c}{2.303(\beta_a + \beta_c)} \qquad (14)$$

Where R_p is polarization resistance and to determine the derivative $(d\Delta E/dt)_{t\text{-}o}$, a galvanostatic step can be externally applied to the a function of time. However, an externally applied direct current will introduce several difficulties in the potential measurements as follows:

1. A direct current may cause a modification of the concentration ratios of the anode and cathode couple, which in turn results in the variation of the mixed potential, introducing a large error in the measured E - E_{corr} value.

2. A direct current may give the changes in the surface conditions, because the corroding electrode surface becomes covered by corrosion product layers which results in a very large electrode capacity to cause a transient on the potential variation, therefore introducing a significant difficulty in indicating the exact time when steady state is achieved.

3. A direct current may develop an IR drop due to the passage of current through the high resistance of the electrolyte introducing a large error when measuring potential value.

In order to avoid these difficulties, an alternative technique can be used in which a galvanostatic square wave current is applied alternately toward anodic and cathodic directions at a definite frequency. Kasahara and Kajiyama (25) describe the concept using an equivalent circuit of corroding electrode/electrolyte interface.

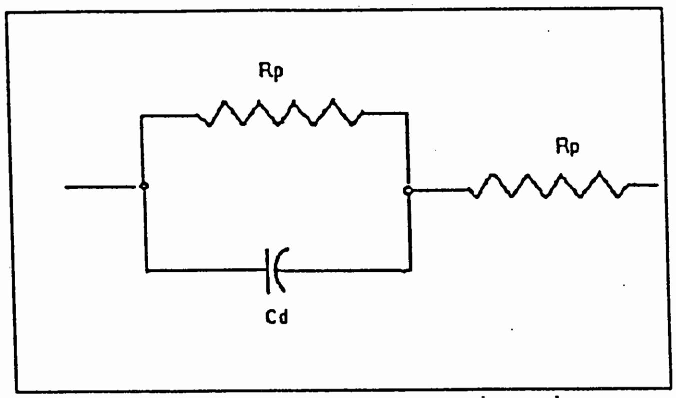

Figure 6

Equivalent circuit of a corroding electrode/electrolyte interface during application of a galvanostatic step

Figure 6 is a schematic representation of a C-R parallel circuit, where R_p = polarization resistance, C_d = double layer capacitance, and R_s = electrolyte resistance. The single galvanostatic polarizing current step can be expressed as follows:

$$I = C_d \frac{d\Delta E}{dt} + I_{corr} \left[Exp \frac{(E-E_{corr})}{\beta_a} - Exp \frac{(E-E_{corr})}{\beta_c} \right] \qquad (15)$$

For a sufficiently small overvoltage, as within 10 to 20 mV of the corrosion potential, equation (15) may be reduced to:

$$I = C_d \frac{d\Delta E}{dt} + \frac{\Delta E}{R_\rho} \qquad (16)$$

If galvanostatic steps are alternately applied in one direction, and then a polarity is reversed at a frequency of "f" (1/sec), equation (16) can be modified as:

$$\Delta E = I\ R_\rho \tanh\left(\frac{1}{4\ R\rho\ C_d} \quad \frac{1}{f}\right) \qquad (17)$$

The actually observed potential variation as a function of frequency, that is ΔE(f), when completely reverse cyclic galvanostatic current steps are applied, can be written as:

$$\Delta E(f) = I\ R_s + \Delta E \qquad (18)$$

$$\Delta E(f) = I\ R_s + I\ R_\rho \tanh\left(\frac{1}{4R_\rho\ C_d} \quad \frac{1}{f}\right) \qquad (19)$$

If frequency f is more than 100 Hz Equation is simplified as follows:

$$\Delta E(f) = I\ R_s \qquad (20)$$

It is noted that at stationary state ($f \rightarrow 0$ or $1/f >> /r_\rho C_d$) Equation (15) reduces to:

$$\Delta E(f) = I\ R_s + I\ R_\rho \qquad (21)$$

Then the polarization resistance can be determined as a difference between Equations (20) and (21). As shown schematically in Figure 7, a typical potential variation with time, when galvanostatic steps are applied alternately toward anodic and cathodic directions. As has been proposed by Kazahara and Kajiyama (24), in order to avoid errors introduced by a potential shift which is caused by electrode capacity, actual measurements can be taken by means of peak-to-peak readings.

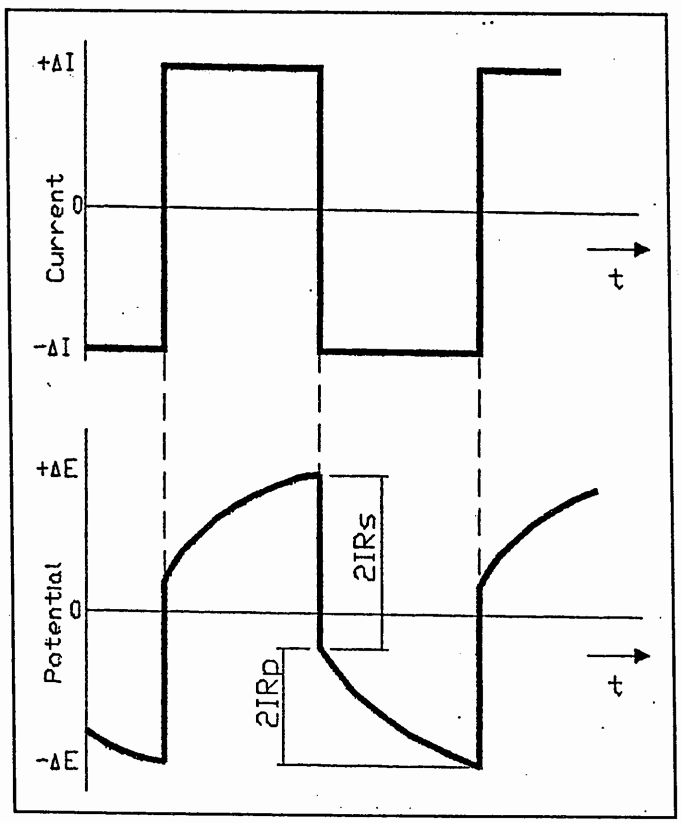

Figure 7

Schematic representation of a typically observed potential response to a completely reverse galvanostatic step

According to equations (20) and (21), at a high frequency of pulses only $2*IR_s$ can be read, whereas at a low frequency of pulses $2*(IR_s+IR_p)$ will be read. Using this method, the effects of corrosion product layers can be minimized by applying alternate galvanostatic steps. The effect of potential shift, which is primarily due to the time required to achieve stationary state in galvanostatic polarization measurements, can be reduced by a peak-to-peak reading.

As mentioned before, in the present polarization resistance methods completely reversed square wave current steps were applied at high cycles to obtain an electrolyte resistance R_s, and at low cycles to obtain total resistance $R_s + R_p$. To determine the optimum conditions, the frequency dependence of potential change was contemplated by Kazahara and Kajiyama (25) and is presented in Figure 8. As evident in Fig. 8, there appeared two plateaus on the log(R) - log(f) diagram. If the frequency of the applied current exceeds 100 Hz, only R_s fully contributes to the effect of electrode polarization. If the frequency is as low as 0.01 Hz, both R_s and R_p contribute to electrode polarization. Based on numerous experiments, the authors have fixed the frequencies, as 0.03 Hz for low and 1000 Hz for high cycles of applied current.

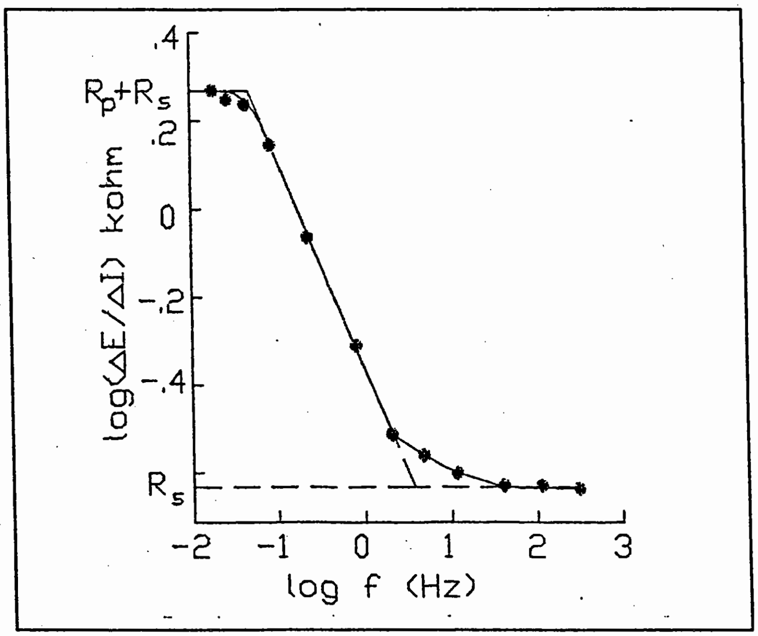

Figure 8

Typical frequency dependence of the amplitude of potential change when completely reversed galvanostatic steps are applied

e) Linear polarization technique

As a step in the simplification of the polarization technique, within 20 mV the value of C_d * $d\Delta/dt$ could be neglected. Formula 16 can be modified as:

$$I = \frac{\Delta E}{R_\rho} \qquad (22)$$

Equation 22 indicated that within twenty millivolts of the equilibrium potential, the applied external current is a linear function of the working electrode potential.

The Stern-Geary equation (30):

$$I_{corr} = \frac{\beta_a \beta_c}{2.303\ (\beta_a + \beta_c)\ R_\rho} \qquad (23)$$

is used in conjunction with a linear polarization plot to obtain a corrosion current. R_ρ is measured from the slope of the polarization plot. Then the value of the slope from the plot is multiplied by 1000 to yield an answer in the units ohm/cm². This is required because I_{app} is plotted in microAmps/cm², and overvoltage is in millivolts.

The β_a and β_b -"beta values" used in the Stern-Geary equation should be recovered from the Tafel extrapolation plot for the steel in contact with the investigated soil. The Tafel extrapolation technique is beyond the scope of the present study. However, the beta values for soil do not vary greatly and the value of $\beta_a = \beta_b = 0.12$ volts has been found to represent an average value (25). In Figure 9, the equilibrium potential was used as an origin point above which overvoltages were measured. A plot of overvoltage versus applied current is presented on a linear scale.

Actually, the calculation of the corrosion current using linear polarization technique is not greatly affected by errors in the beta values. The Stern-Geary equation involves multiplication of the Tafel slope values divided by their sum. In addition, the beta values are typically limited to a relatively small range.

$$I_{corr} = \frac{0.12 \cdot 0.12}{2.303\ (0.12 + 0.12)\ R_p} = \frac{26,053}{R_p} \qquad (24)$$

where:

$$2\ R_p = \left(\frac{\Delta E}{\Delta I}\right)_{0.03HZ} - \left(\frac{\Delta E}{\Delta I}\right)_{1000HZ} \qquad (25)$$

ΔE = is taken as peak-to-peak readings (mV)
and I_{corr} is measured in microAmps/cm^2

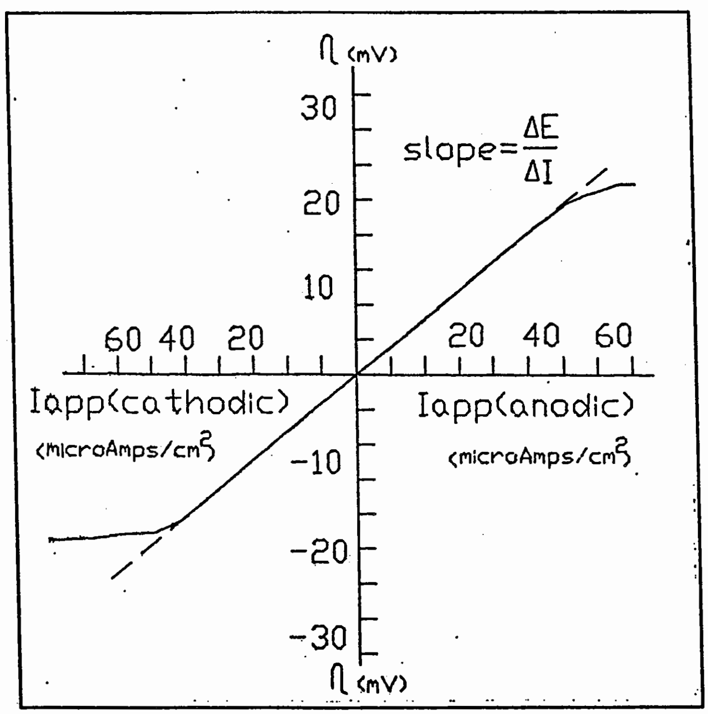

Figure 9

Applied current linear polarization curve (22)

Using long term monitoring of the corrosion process for 40 different soils, ranging from sand to clay, Kazahara and Kajiyama (24) developed the following relationship:

$$\overline{I_{corr}} = \frac{11,200}{\overline{R_\rho}} \quad \left(\frac{\mu Amps}{cm^2}\right) \qquad (26)$$

where a linear relationship has been established between average corrosion current converted from actual metal loss using Faraday's law, and the reciprocal of the average value of polarization resistance for over 300 days.

B. Investigating the Potency of Macrocells

The recently discovered corrosion of steel piles occurred when aggressive layers located above the ground water table contacted the pile (1). There are several combinations of material in contiguous layers that initiate and sustain the corrosive action. One of the objectives of the present study is to determine how the variation in the composition of contiguous layers, moisture content and concentration of electrolyte affects the contact potential and the magnitude of self-generated current in contiguous layers.

1. Contact potential and self-generated corrosion current measurements

It should be noted that self-generated current develops in a galvanic cell of the type STEEL/SOIL1/SOIL2/STEEL. In the research reported here one of the soils was a clay and the other consisted of products of combustion: ash, coal and cinders.

Instantaneous and long term monitoring measurements have been made using a soil box shown in Figure 10. Two different soils are placed in contact with one another, in a plastic box having a steel plate electrode at each end. In order to keep the moisture from evaporating, a second empty box was placed on top of the first and the junction between the two was taped.

The contact potential was measured by reading the "open circuit" voltage on a high resistance digital electrometer connected to both electrodes. Contact-potential measurements were taken at regular intervals during a four day period immediately after putting the soils in the box.

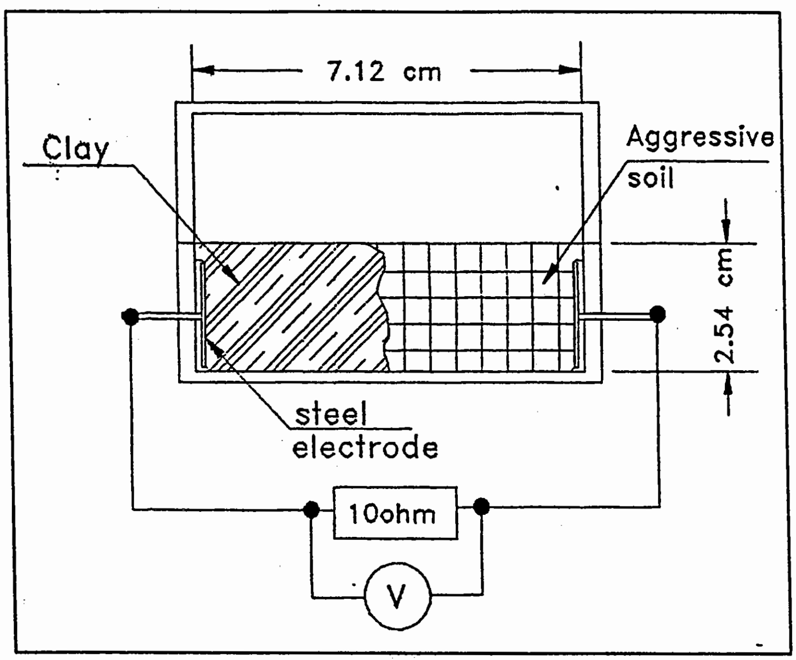

Figure 10

Soil box used for contact potential and self-generated current measurements

The self-generated current was determined by measuring the voltage difference across a 10 Ω resistor and using Ohm's Law, i.e., I = V / R. Current measurements were taken at the same time intervals, which were measured with the circuit shown in Fig. 10. The 10 ohm resistance is negligible compared to the resistance of the soil.

It was of interest to investigate soil type and electrolyte strength using various combinations of clays and the ash layer. Four different types of clays were investigated to make a quantitative analysis of the effect of Cation Exchange Capacity on self-generated current. Variables, such as concentration of electrolyte, and saturation of the layer contiguous to the clay, were examined with respect to their influence on the corrosion process.

Layers to be placed contiguous with the clays were made by a combination of the soil sample from Bridgeport Peck Bridge with addition of ash (5% by weight). Soil from Bridgeport has been chosen due to its demonstrated corrosive nature. This material badly corroded embedded copper clad rod in three weeks.

It was found by experimentation that layers containing coal particles generated higher current than ash alone. Crushed coal, sieved through No. 20 sieve, was added by 25% in one case and 50% in another (by weight) to the ash layer. A chemical analysis of the mixture before adding the coal is shown in Table 3.

Dilute solutions of NaCl in distilled water were used as electrolyte to test the effect of salt concentration on the macrocell strength. The following concentrations were investigated: 0.001M, 0.01M, 0.1M, 0.2M, 0.3M, where M = the molarity of the solution and gives the total number of moles of a solute in one liter. As an example, a 1.0M solution of NaCl indicates that 58.5 g of Sodium Chloride was dissolved in 1 L of distilled water. It is of interest that 0.001 M NaCl concentration could be expressed as 58.5 ppm; 0.3M concentration presents a level of 17,550 ppm.

In order to make a soil sample with specific electrolyte concentration, the following procedure was used:

(1) The soil was dried in an oven for 24 hours.

(2) After placing and lightly compacting soil in a box with a known volume (V_t) the sample was weighted (W_s).

(3) The solids volume $V_s = W_s / (G_s * \gamma_w)$. The value of specific gravity G_s was assumed to be 2.65. The unit weight of water γ_w was taken as 1 g/cm^3

(4) The void ratio was calculated using equation

$$e = (V_t - V_s) / V_s \qquad (28)$$

Table 3

The analytical results of the ash sample used in soil combinations

Parameters	Results	Units
Dissolved Silica	5.942	mg/l
Conductivity	0.177	mMHOS
pH	5.92	-
Chloride	2.7	mg/l
Sulfate	50.5	mg/l
Silver	not detected	mg/l
Aluminum	0.317	mg/l
Arsenic	0.251	mg/l
Barium	0.462	mg/l
Calcium	46.075	mg/l
Cadmium	not detected	mg/l
Chromium	not detected	mg/l
Copper	0.050	mg/l
Iron	0.036	mg/l
Potassium	3.991	mg/l
Magnesium	6.857	mg/l
Manganese	0.176	mg/l
Sodium	1,368.0	mg/l
Nickel	0.025	mg/l
Lead	0.067	mg/l
Selenium	0.089	mg/l
Zinc	0.165	mg/l
Fraction Solid	1.0	-

(5) Required moisture content w could be determined by equation

$$w = e * S / G_s \quad (29)$$

where S = a desirable saturation.

(6) The required amount of electrolyte was computed as

$$W_e = W * W_s \qquad (30)$$

where W_s = a weight of investigated soil sample.

During the experiments all clay samples were saturated, while the saturation of the ash and other layers contiguous to the clay was varied. The same concentration of NaCl solution was used to saturate the clays and bring the ash layer to the desired water content in each test. The experiments also included distilled water as the electrolyte.

2. Corrosion potential measurements

The soil of interest was placed in a soil box between steel electrodes. Corrosion potential was measured by positioning a Cu-$CuSO_4$ reference electrode in the immediate vicinity of the steel test electrode of interest. The Cu-$CuSO_4$ reference electrode is a copper bar in a saturated solution of $CuSO_4$. A plastic 1/2" diameter tube was sealed on the bottom with a Plaster of Paris plug. The plug allows the solution to make contact with the soil by slowly releasing the electrolyte. The measurements were taken by positioning the reference electrode on the top of soil of interest, and reading the potential between the steel electrode and Cu-$CuSO_4$ reference electrode using a digital electrometer. Soils used in this study were Bentonite clay, Hartford clay, Kaolinite clay, Illite clay, aggressive layer, and Medium sand.

3. Determination of Cation Exchange Capacity of clayey soils by the Methylene Blue Test (MBAT)

a) General

Clays contain a net surface charge due to isomorphous substitution in the lattice. This charge attracts cations from the solution. These cations can be exchanged. The Cation Exchange Capacity (CEC) varies with the type of clay. The presence of these cations could strongly influence the strength of any macrocells in which they might be included. In order to distinguish clays by their CEC requires a measurement of this characteristic.

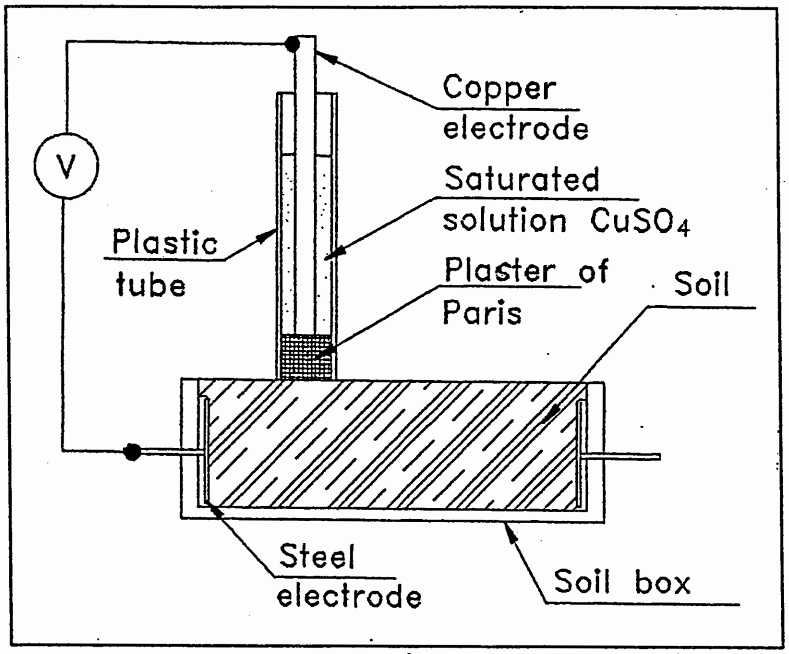

Figure 11

Schematic representation of the test used for corrosion potential measurements

The adsorption capacity of the clay particles could be attributed to two mechanisms:

1. Cation exchange resulting from isomorphous substitution in the alumina-silicate lattice

2. An adsorption mechanism which might be either physical (Van der Waals) adsorption or chemisorption (hydrogen bonding) with the SiOH and AlOH of the alumina-silicate lattice.

When methylene blue is dissolved in water, methylene blue cations and chlorine anions are formed that can replace the existing cations associated with a given clay mineral surface.

[C]$^+$ clay$^-$ + methylene blue$^+$ hydrochloride$^-$ →
methylene blue clay + [C]$^+$chlorite (32)

where:

[C]$^+$ = the exchangeable cation; and methylene blue clay refers to the state in which all of the clay particles are covered by methylene blue. ($C_{16}H_{18}N^3SC1$). [from (31)]

Most of such exchange reactions are reversible. However, organic cations such as methylene blue appear to be the exception.

When a solution of methylene blue hydrochloride is added a little at the time to a sample of clay until the CEC of the clay has been reached, the amount of dye adsorbed is equal to the amount added. Additions of the dye beyond the CEC, however, are not entirely adsorbed.

The nonclay elements (mica, quartz, etc.) of the soil have negligible CEC's and do not participate in the adsorption phenomena. The adsorbed value of methylene blue is predominantly influenced by the clay size fraction of the soil.

Methylene Blue Adsorption Test can be a good indicator of Cation Exchange Capacity of Clays. It is also a helpful method to distinguish different types of clays based on CEC activity.

b) Methylene Blue Adsorption Test

The MBAT has been employed in order to investigate the strength of macrocell current with respect to the CEC of the clay. The following procedure was found to be the most convenient in terms of performing the test.

About 30 g of soil in an oven dry state were mixed were 200 ml of distilled water. Once the ingredients were well mixed, a known amount of methylene blue at a concentration of 10g/l was added to the soil suspension from a burette. The soil water-methylene blue mixture was stirred at 400 rpm throughout the test. After each addition of methylene blue to the soil suspension, a drop of the slurry was placed on filter paper with a glass rod for visual examination.

Initially, a faint blue spot of solids was observed surrounded by a transparent water ring of clear liquid that soon evaporates. As titration proceeds, the color of the inner spot becomes progressively darker blue as the clay adsorbs more dye, but the boundary of the blue spot remains clearly marked and distinct. Eventually, the end point is reached when the outline boundary of the inner blue spot breaks down into a diffuse light blue-green halo, radiating outward.

At the first appearance of the blue-green halo, titration was stopped and the drop test on filter paper repeated five times. If the halo persists, the end point has been reached; if not, titration was continued. Knowing the burette reading at this point, the volume of the methylene blue injected into the soil solution could be estimated. It is worthwhile to carry the additions of methylene blue solution several steps beyond the end point to compare MBAT before and after the end point.

c) Determination of the Cation Exchange Capacity from results of MBAT

The cation exchange capacity of a clay specimen can be found by using the following formula:

$$C = 100/Wm * V_{cc} * Nmb \qquad (33)$$

where:

C = the cation exchange capacity (meq/100 g clay); Wm = weight of clay specimen in g; V_{cc} = the volume of methylene blue titrant (mL); Nmb = the normality of the methylene blue substance (meq/mL).

For 100 g of fine soil, the methylene blue value (MBV) of the soil is given by the following formula:

$$MBV(g/100\ g) = V_{cc} * 10g/1000mL * 100g/Pg \qquad (34)$$

where:

Pg - dry weight of the specimen used (30 g).

The quantity of the methylene blue adsorbed by a mixture is exactly equal to the sum of the quantities adsorbed by the mass of clays present in the mixture. Therefore, the methylene blue test gives a good indication of the presence of any clay soil (31).

Coksa and Birand (31) stated that the level of adsorption capacities of clays obtained from MBAT are reasonably close to those determined by the standard ammonium acetate method. This similarity was particularly noteworthy because the methylene blue adsorption test is simple and rapid.

Table 4 shows data obtained from MBAT for four types of clays used in macro cell test. In Table 4 the values of CEC(1) have been obtained from testing and the range of CEC(2) was obtained from the several publications (31,32).

Table 4 Methylene Blue Adsorption Test Data

Mineralogy (type of clay)	MBV (g/100 g)	CEC(1) (meq/100 g)	CEC(2) (meq/100g)
Bentonite clay	329.0	102	80 - 130
Illite clay	39.48	12.4	10 - 40
Hartford clay (from I-84 sample)	54.13	17.0	
Kaolinite clay	13.67	4.27	2 - 15

4. Concentration Cell Corrosion Experiments

a) General

The corrosion losses observed in Hartford occurred in macro cells in which one of contiguous layers was clay or silt and the other layer contained products of combustion. Steel piles might be subject to macrocells developed by other conditions. One such condition might be ground water that has been contaminated by chemicals lowering its resistivity and rainwater percolating between the soil surface and the water table. In this case there are concentration gradients due to both aeration and chemical gradients. Long term tests were performed in which NaCl was used as the chemical in the part of the test cell that represented ground water. Steel strips simulated the piles.

Similar tests were done across a model ground water table using two versions of a probe that simulates the corrosion action that a pile might experience, but is divided into discreet electrodes so that the behavior of the current with respect to the pile in various locations in the macro cell can be monitored with electrical measurements. Testing was done with both of these arrangements to compare results.

b) Tests using steel strips

The tests were conducted in plastic cylinders (3.5 inches inside diameter and 8 inches high) with tubular inlets through the wall as shown in Fig. 12. Ottawa sand was selected for this test due to the inert nature of the particles.

Two steel washers were buried at elevations corresponding to zones with differing salt concentrations. Wires connected to washers were connected to a 10 ohm resistor outside of the cylinder, in order to monitor current flow. Potential measurements across the 10 ohm resistor were taken at regular intervals over a 3 month period.

In order to reach a full saturation of the lower portion of the sample, the level of NaCl solution was maintained above the elevation of the inlet. As soon as the saturation was reached, the solution flow was stopped. To saturate the lower portion of soil cylinder, 0.5% concentration of NaCl was used. The upper portion of the sample was saturated at about 65% level by tap water. Washers were weighed at the beginning of the test. After removing them from the soil at the end of the test the washers were scrubbed with a steel brush in order to remove corrosion deposits and weighed again.

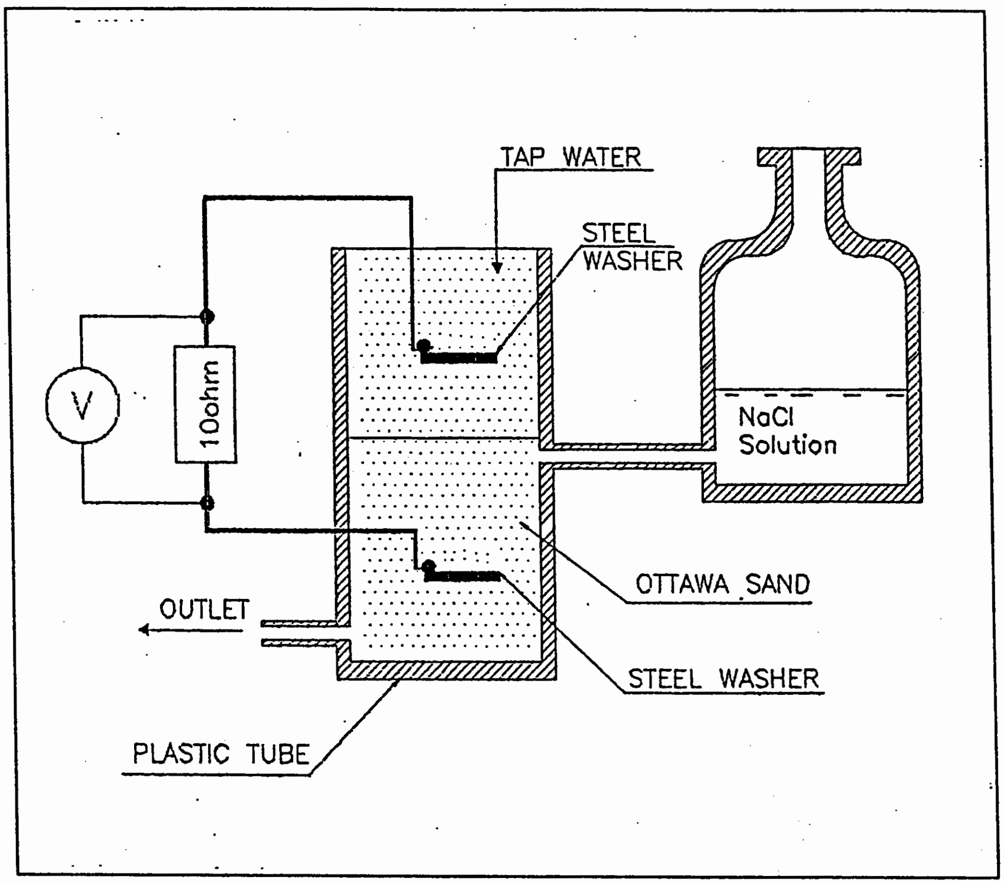

Figure 12

Schematic representation of the concentration cell test

c) Tests with the soil probe

To measure the current intensity at discrete locations within a macro cell, a corrosion probe for soils was developed similar to the device presented by Schaschl and March (12). Two probes of this type were made. The first had 17 flat electrodes glued onto a plastic strip. The second design used 31 short steel cylinders as electrodes. Each cylinder was insulated from its neighbors with plastic rings as shown in Fig. 13. A wire was soldered to each cylinder. The probe simulates a steel pile electrically when all of the wires are short circuited. The design using cylinders can be considered the prototype for a field device. The device used in the laboratory was 38 cm long.

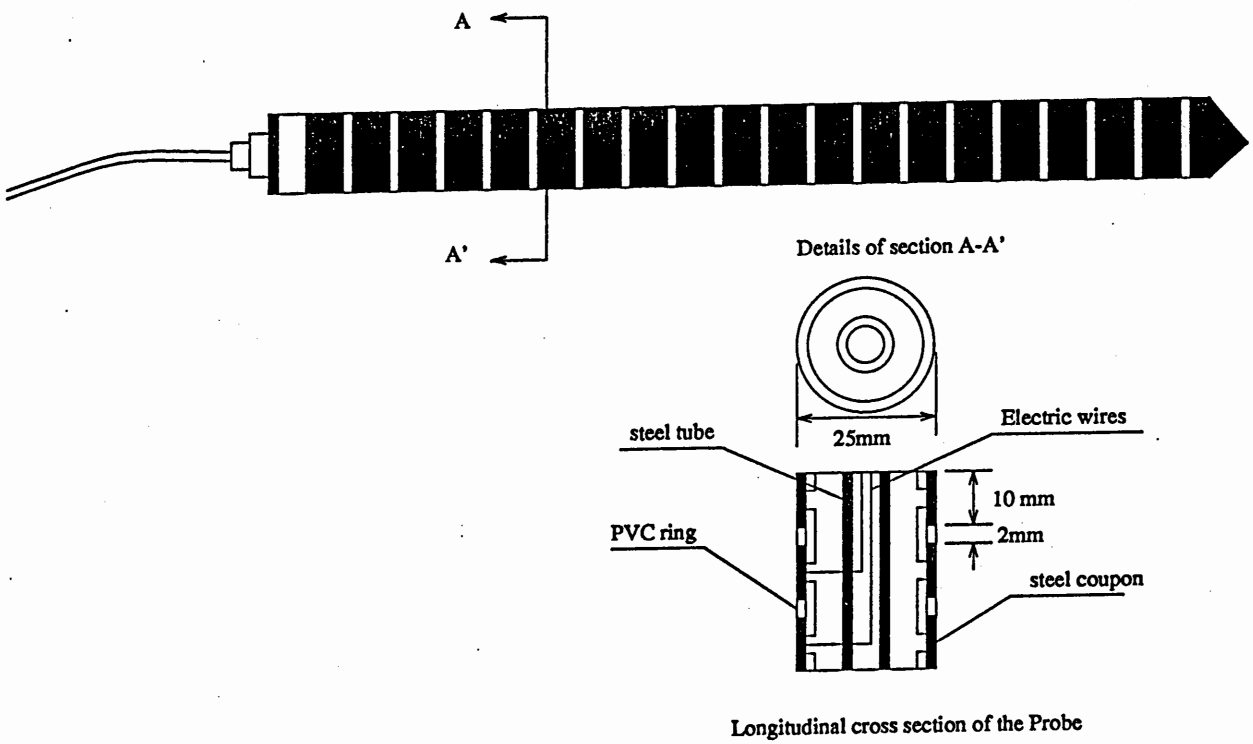

Details of the Corrosion Probe

Figure 13

Corrosion Probe for Soils

The probe was used with soils having a homogeneous soil skeleton, usually sand, in which a macrocell was developed across the water table. Below the water table the supply of oxygen is limited. Above the water table there is much oxygen because the degree of saturation is less than 100%. This difference creates an aeration cell.

Each test was run by placing the probe in the middle of a plastic cylinder and surrounding the probe with the soil of interest. The experimental set up is shown in Fig. 14. A glass tube was cemented into the bottom of the plastic cylinder so that aqueous solutions could be supplied to the soil and a water table established for each experiment. The solution was brought to the top of the cylinder to insure that all of the soil was wetted, then the external reservoir was adjusted to establish the desired elevation of the water table in the cylinder.

The measurements were made after a water table had been established by first shorting all the wires from the electrodes, then removing the wire of one electrode and placing a low resistance system for measuring current between the electrode and the shorting strip. This measurement gives the amount of current handled by this electrode and whether its sense is flow into or out of the electrode. By making systematic measurements on each of the electrodes the complete picture of current developed by the macro cell in the pile simulated by the probe is attained.

The amount of current flowing in this system depends on the dimension of the soil between the probe and the cylinder. The greater the thickness of soil between the probe and the cylinder the more current will flow. Most of the current, however, flows through the soil close to the pile. A study was done using teledeltos paper and an analogue field plotter. It was found that if the thickness of soil between the probe and the cylinder was 2.5 times the height of the electrode, the current flow would be at least 90% of that in an infinite medium. This established 7.6 cm as the minimum radius of the container. The container used was 10 cm in diameter x 42 cm high.

The cylinder used with the probe worked well with homogeneous soils, but contiguous soils of different types were difficult to place around the probe. Measurements with a similar electrical set up were made in a rectangular box placed horizontally. One side of

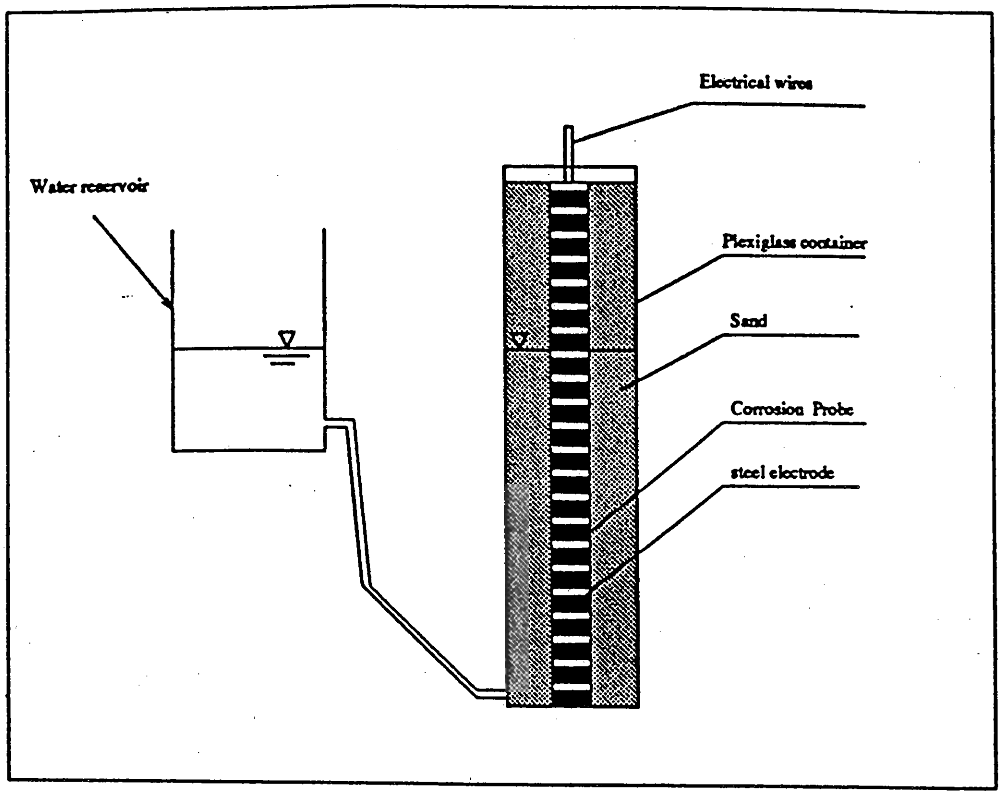

Figure 14

Test arrangement to determine current distribution due to differential aeration

this plastic box was fitted with a series of individual electrodes, insulated from one another and connected to a shorting strip. The soils could be placed the length of the box from the top, making the establishment of contiguous layers relatively simple. The arrangement is as shown in Fig. 15.

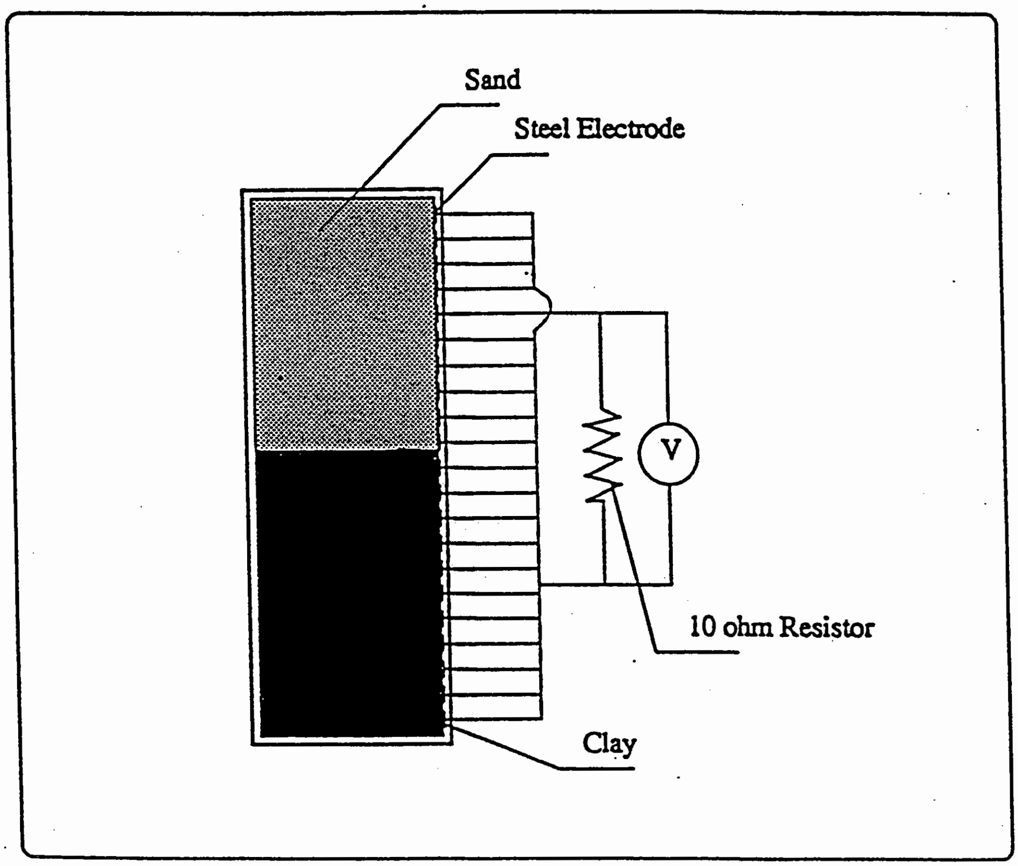

Figure 15

Test set-up to measure the effect of anode/cathode area ratio

5. Influence of the cathode/anode area ratio on corrosion rates in concentration cell environment

a) General

The strength of a macrocell depends on the amount of current that is passing. All of this current must pass out of the metal at the anode and into the metal through the cathode. When the anodic area of the macrocell is much larger than the cathode, the current density at the anode is small and the corrosion rate at any location will be low so that the reduction of cross sectional area due to corrosion is small. In addition the current density into the metal will be great so that the metal in this region receives cathodic protection. When the anodic area is much smaller than the cathode, the effect is opposite. In this case the current in the anodic region is large, producing a high rate of corrosion that results in a substantial loss of cross section. The current density into the metal at the cathode is reduced, decreasing cathodic protection and local corrosion can occur.

For steel piles the portion below the ground water table (GWT) is the anode, the portion in the unsaturated zone above the water table is the cathode. This appears to be the case in which the ratio of the cathode to anode areas is large and should result in no concentrated loss of metal. There is some question as to how much of the pile below the GWT will be effective as the anode. The losses observed by Romanoff (6) were in the vicinity of the GWT. Several experiments investigated the ratio of cathode to anode areas.

b) Experiments with steel strips

The objective of these tests was to quantify the anode/cathode area ratio influence on the corrosion rates of embedded steel strips in a Concentration Cell environment.

There is little oxygen available in the zone saturated with a concentrated solution of NaCl. The assumption could be made that this region will act as an anode. The upper portion of the soil samples maintained at degree of saturation of about 65% with tap water and exposed to the atmosphere will have much more oxygen available and will act as a cathode. Altering the elevations of the inlets of the NaCl solution produces different cathode/anode area ratios.

Medium-density Ottawa Sand has been used as a soil stratum. The test apparatus is shown in Fig. 16. As in the previous tests, 0.5% concentration of NaCl was used in order to fully saturate the lower portion of the soil samples. The solution saturation procedure has been repeated as in previous tests. Tap water was periodically poured on the top of the soil samples.

In order to simulate field driven steel pile conditions, four flat steel electrodes (0.5 inch wide and 10 inches high) were inserted in each soil cylinder. Three small washers were embedded at various elevations as monitoring electrodes. Each inserted steel rod was weighed and labeled.

It was proposed to evaluate the three possible anode/cathode area ratio, such as 1:1, 1:2, and 2:1 by altering the elevations of the sodium chloride solutions inlets.

Three elevations of the NaCl solution inlets were established as follows: 1/3 H, 1/2 H, 2/3 H, where H represents the height of the soil sample. These conditions are shown in Fig. 17.

Potential and current measurements were taken at regular intervals over a four month period. Current values were computed using potential drop across a 10 ohm resistor. At the end of the test the steel electrodes were removed from the soil, brushed free of corrosion deposits and weighed. The zones with high corrosion activity were located.

c) Experiments with electrically shorted electrodes

These experiments were run in the apparatus described in Fig. 15. One side of the box is detachable and has space for 18 electrodes that can be shorted electrically to represent a steel pile. The surface of each electrode is 2 sq cm. Samples of clay and sand were prepared with a solution of NaCl. Clay was placed in contact with 8 of the electrodes and sand in contact with the remaining 10. The effect of the ratio of cathode to anode areas was measured by shorting the appropriate number of electrodes and measuring the current. The anode area was varied from 16 sq cm to

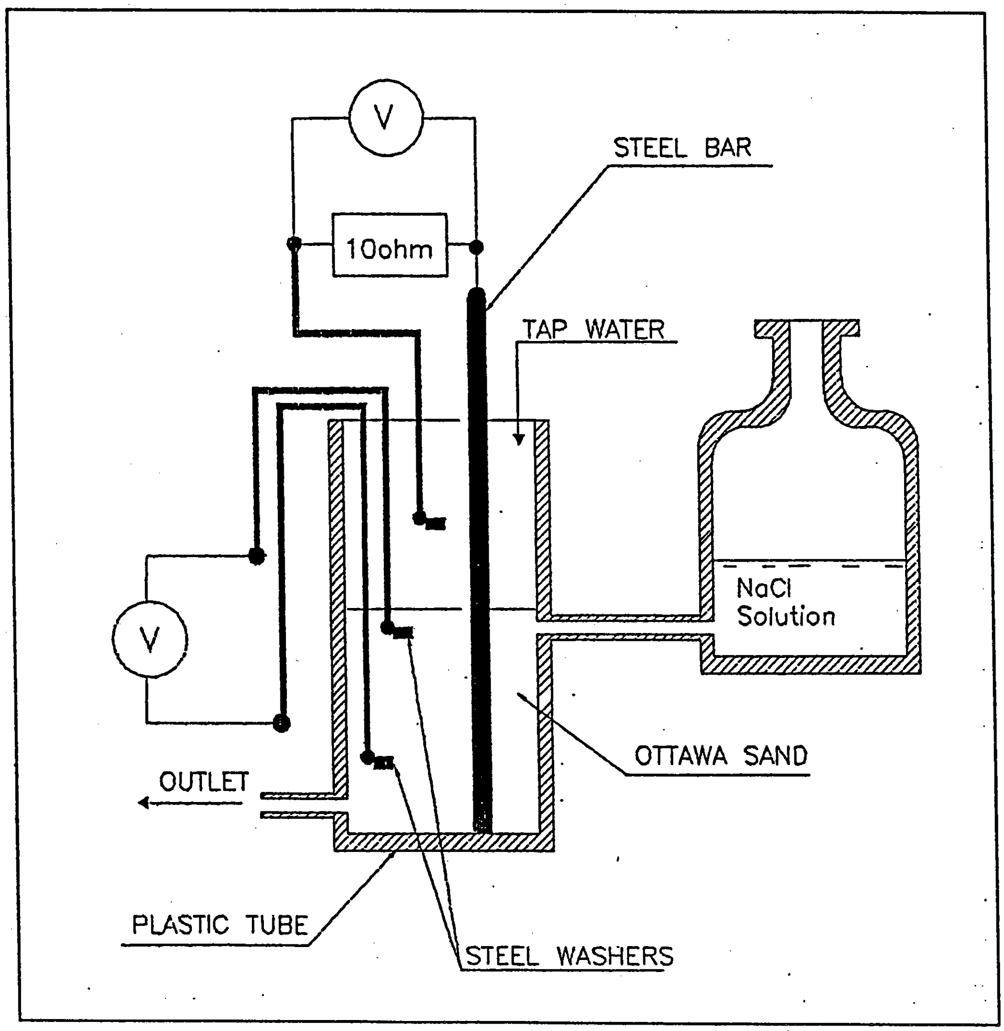

Figure 16
Schematic representation of test used for determination of the influence of different anode/cathode area ratios on corrosion using steel rods

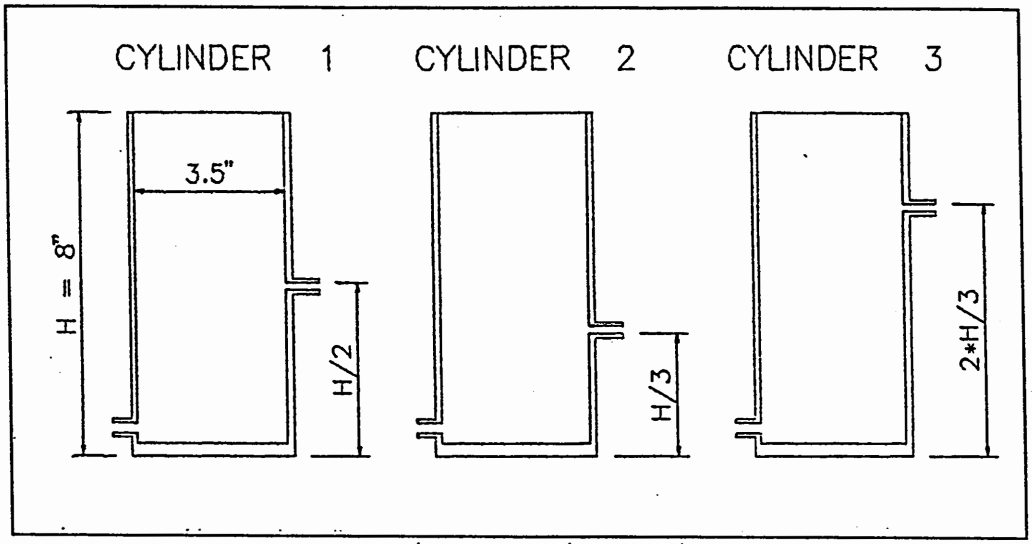

Figure 17

Schematic of soil cylinders with different locations of the solution inlets

2 sq cm, the cathode from 2 sq cm to 20 sq cm. Measurements were taken at various concentrations of NaCl and different degrees of saturation.

d) Effect of soil variation

The corrosion rate in soils varies according to their mineral content and texture. The clay minerals are related to the Cation Exchange Capacity, and the texture of fine grained soils can be varied by adding silts. Clay and silt passed through 100 sieve were used in these tests. Clay is mixed with different amounts of silt to find the variation of current density and contact potential. Clay content was varied from 25% to 100%. The clay/silt samples were tested against ottawa sand at different concentrations of NaCl. In each test contact potential and current density were measured. Clay and sand were tested for long cell corrosion and the current distribution was measured using the box described in Fig. 15. The test set up for long cell corrosion measurement is shown in Fig. 18.

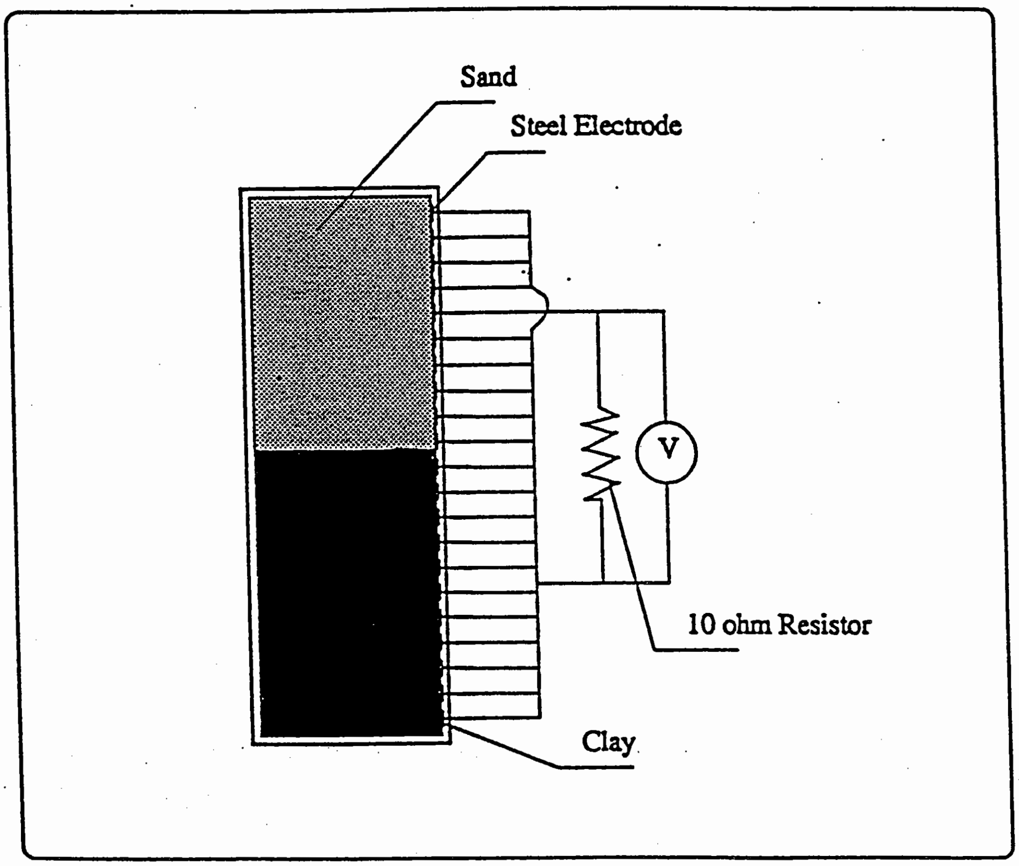

Figure 18

Test arrangement to determine corrosion rates for non-homogeneous soil

C. Determination of polarization characteristics of steel in contact with soils

1. General

Instantaneous measurements of corrosion current and corrosion rates were determined using "Linear Polarization Analysis" (see section Q2d) employing Kazahara's method (2a) of "Completely Reverse Cyclic Galvanostatic Steps." This is a method in which pulse current steps are applied toward anodic and cathodic directions at a predetermined frequency.

Kazahara's method allows the elimination of IR drop without using complicated balanced circuits.

Figure 19 shows the electrical schematic of the unit employed in the present study in order to obtain the instantaneous values of corrosion current and polarization resistance for steel in contact with soil. The electrical unit included the following:

a) Soil box with steel electrodes on the ends (working and auxiliary electrodes). The reference electrode was mounted on the top of the box and inserted into the soil in the immediate vicinity of the working electrode. The moisture of the soil was adjusted to the desirable degree of saturation with known concentration of electrolyte.

b) Power source - Model 362 Scanning Potentiostat.

c) Function Generator FG 501A, as a generator of low distortional pulse waveforms over the frequency range of 0.002 Hz to 2 MHz.

d) Storage oscilloscope, as a recorder of the IR drop between the working and reference electrode.

e) One pen recorder, as a recorder of polarization overvoltage between the working and reference electrode.

f) High resistivity Digital Electrometer Model 616, as an additional recorder of polarization overvoltage between the working and reference electrode.

2. Test Procedure

a. Soil samples were brought to the desired degree of saturation with known concentration of electrolyte and placed in a plastic box with steel electrodes at both ends. The sample was compacted slightly. A reference electrode composed of zinc was positioned by eye close to the working electrode.

b. The Cell Cable (6020-0168) connects to the front panel cell connector. Cable has 4 leads, three of which terminate in a pin jack. It is important that the red clip connects to the auxiliary electrode and the green clip connects to the working electrode. The reference electrode output plugs into the white pin jack. The black clip is a ground (see Figure 19).

c. Potential control output connectors connect to the input of the oscilloscope. Before measurements were taken, the calibration check was performed.

A current of one mA is applied across a 10 ohm resistor and a value of 2*IR drop was seen on the screen of the oscilloscope as 20 mV.

d. A 1000 Hz pulse current was applied across soil box. The initial magnitude of applied current usually was 3 microAmps which corresponded to a current density of about 0.5 microAmps/cm^2 (the working surface of electrode is 6.45 cm^2). The values of 2*IR drop were taken as peak-to-peak readings from the oscilloscope screen.

e. The current magnitude is gradually increased and the values of 2*IR drop are recorded with respect to the applied current.

f. Potential Control output connectors connect to the one pen recorder. Working and reference electrodes connect to the Digital Electrometer.

g. A 0.03 Hz current pulse is applied across the soil box. Pen recorder plots polarization overvoltage versus time (see Figure 20 for a typically observed potential response to a completely reverse galvanostatic step), while readings are taken from the Digital Electrometer visually. Two records are taken to obtain a better test result.

h. Polarization overvoltage is computed using equation:

$$\eta(\text{mV}) = 1/2 * [(\text{peak-to-peak readings})_{0.03\text{Hz}} - (\text{peak-to-peak readings})_{1000\text{Hz}}] \quad (35)$$

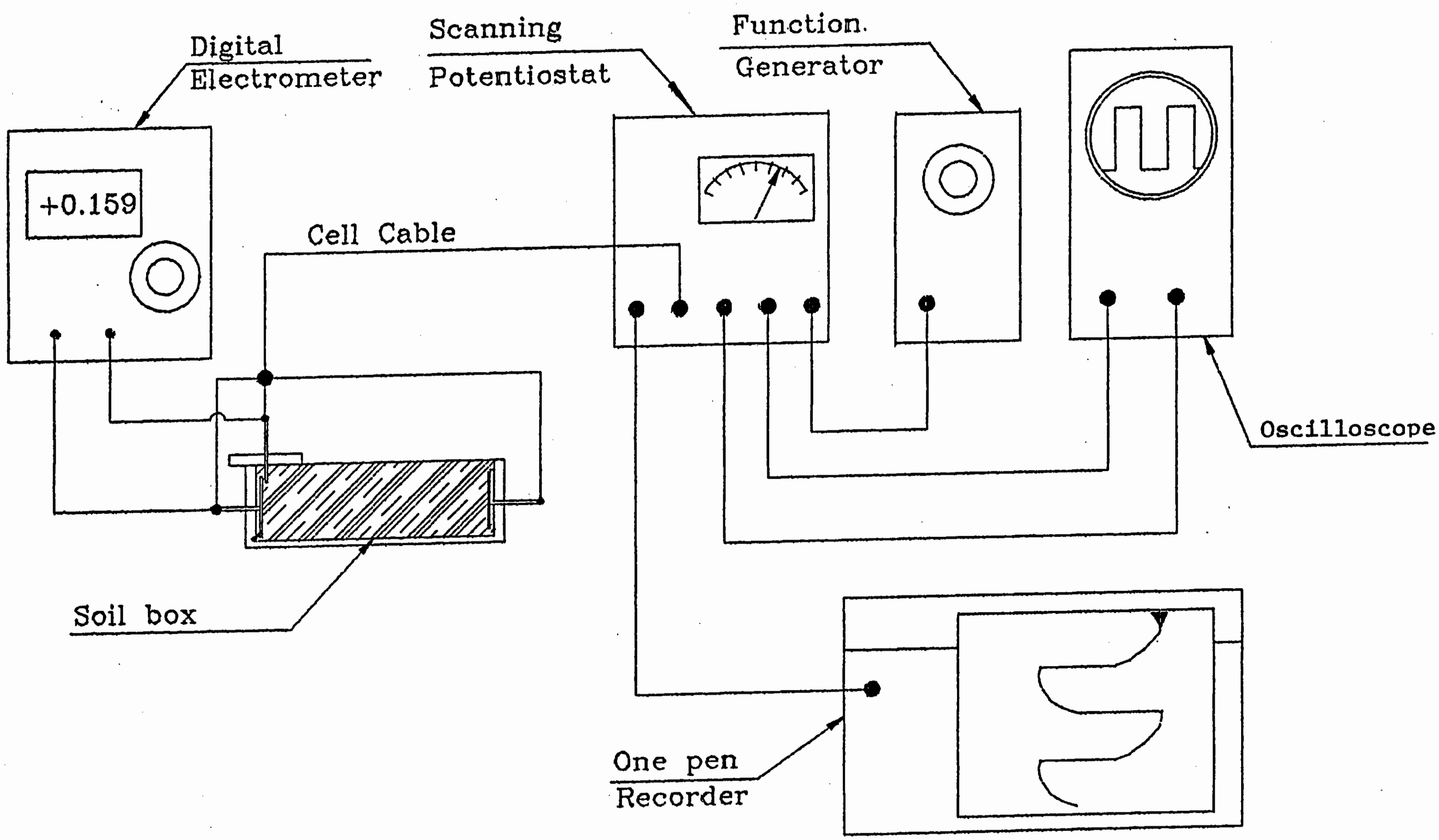

Figure 19

Schematic set-up for linear polarization measurements

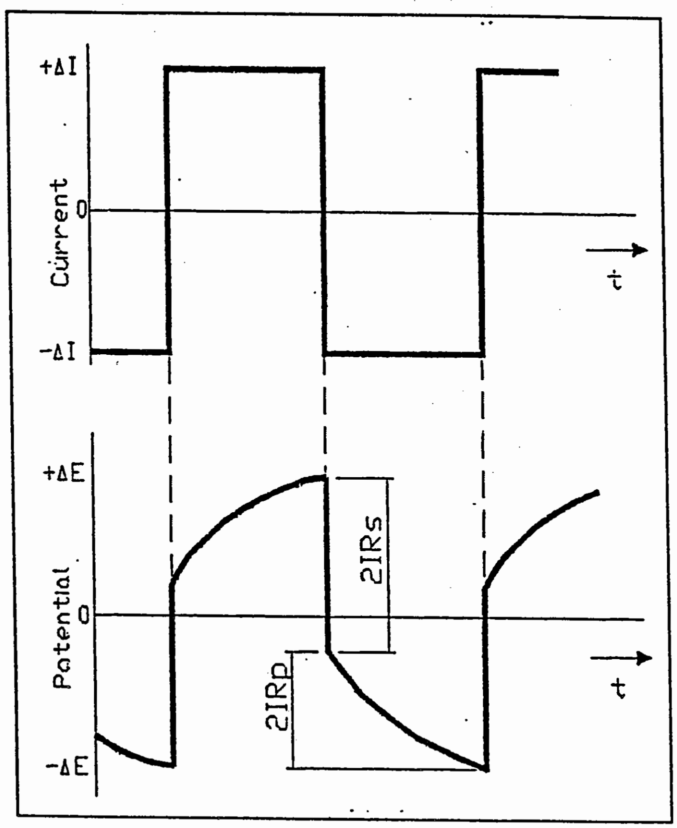

Figure 20

Schematic representation of a typically observed potential response to a completely reversed galvanostatic step

Plot of applied current versus η is drawn. Using least squares a new value of η that is a straight line could be recovered from the results of each test. The slope of the straight line is a desired value of R_p.

D. Macrocell Corrosion on a Pile

1. At the Water Table

Macrocell corrosion needs an oxygen concentration difference to form an aeration cell in a soil with low resistivity. The aeration cell provides the potential gradient and the low resistivity allows the current to flow. Experiments to demonstrate the viability of this type macrocell were carried out with an apparatus shown in Fig. 13. This device consists of individual electrodes insulated from each other that can be connected together to simulate the pile electrically. To measure the effect of the macrocell at any elevation the electrode representing the location of interest is connected to the other electrodes through a low resistance ammeter. In this manner the behavior of the macrocell current at any point in the profile can be measured. Both the magnitude and the direction are obtained.

2. With Heterogeneous Soils

The macrocell effects in heterogeneous soils were measured with the apparatus shown in Fig. 15. The soils used were silts and clay used singly or as mixtures against sands. Solutions of NaCl of various strengths were used as the electrolyte.

VI. DATA AND ANALYSIS

A. Clay in Contact with Potentially Aggressive Layers

Contiguous layers CSC-1 was tested against four clays and a silt. Various electrolyte strengths were used. The clays were fully saturated; the CSC-1 layer was at a degree of saturation of about 65%. Typical results are shown in Fig. 21. Measurements of self-generated current were taken after thirty minutes, two hours, 24 hours, and 96 hours from the beginning of the tests. The strength of the macrocells formed are in direct relation to the Cation Exchange Capacity of the clay.

The self-generated currents at the end of 24 hours are compared in Fig. 22 as a function of concentration of electrolyte. As seen from the Figures 21 and 22, Bentonite Clay generates the greatest current. Apparently, there is a relationship between the current generated and the Cation Exchange Capacity of the clay.

B. Contact Potential and Self-generated Current Measurements

Table 5 lists the contact potentials and self-generated currents measured in soil boxes when clay was placed in contact with various potentially aggressive contiguous layers.

Contiguous layer CSC-1 and CSC-2 have been defined in the previous section. Contiguous layer CSC-3 did not contain any crushed coal and was made up using the same components (95% Bridgeport, 5% ash).

Based on results from Table 5 and Table 6 the current of macrocells made with different types of clays in contact with these aggressive layers decreases with time.
Bentonite clay exhibited the highest self-generated current for four days. It should be noted that this current was generated when the concentration of NaCl in the electrolyte was the lowest at 58.5 ppm of NaCl. The contiguous layer had a degree of saturation of about 65%.

As seen on Figure 21, an initial current level of about 40 microAmps/cm^2 was developed by the macrocell with Bentonite Clay, and a current of about 20 microAmps/cm^2 for a macrocell including the soil from Hartford. The magnitude of self-generated current decreased over time, however, a substantial current was maintained for over 100 hours. A flow of 10 μ amps/cm^2 is sufficient to seriously weaken steel piling in about 25 years.

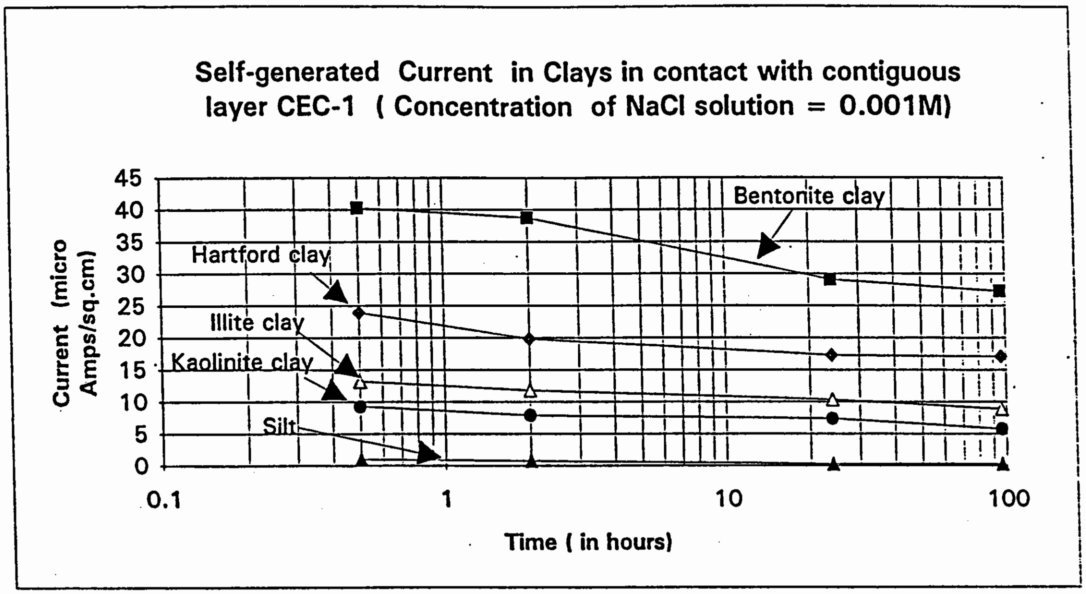

Figure 21

Self-generated current data to contact-potential of contiguous layers in a soil box

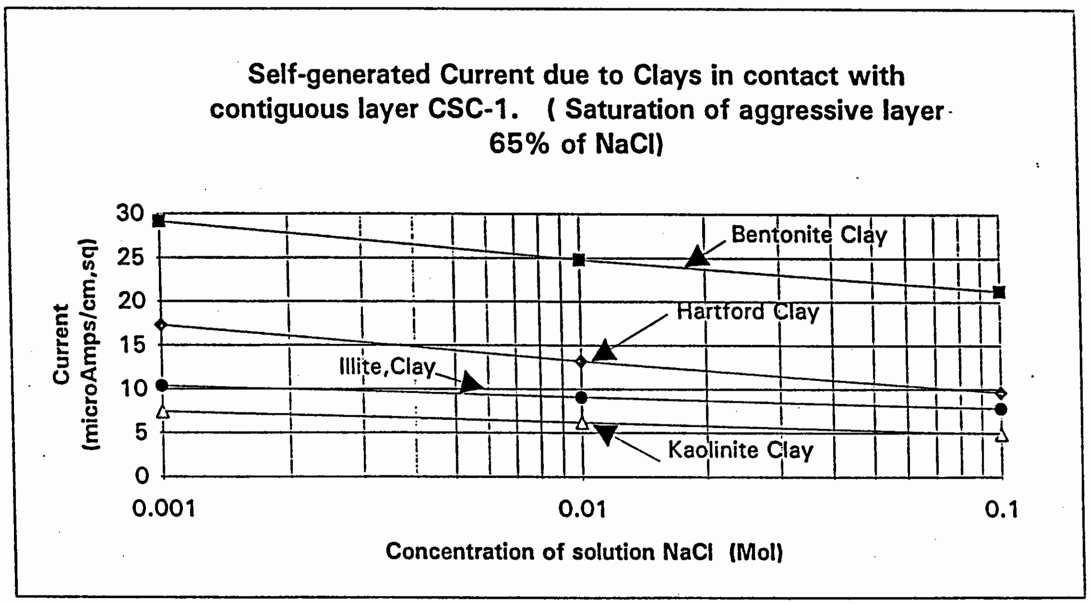

Figure 22

Self-generated current data due to contact-potential of contiguous layers. Concentration of the saturated media has been altered

In the next series of tests the degree of saturation of contiguous layers CSC-1 was varied between 100% to 65%. The results are shown in Fig. 23. The availability of oxygen at the cathode has an important effect on the corrosion rate. As seen in Fig. 23, the corrosion current for all macrocells is greatest at about 65% in these tests, and decreases as the degree of saturation around the cathode increases.

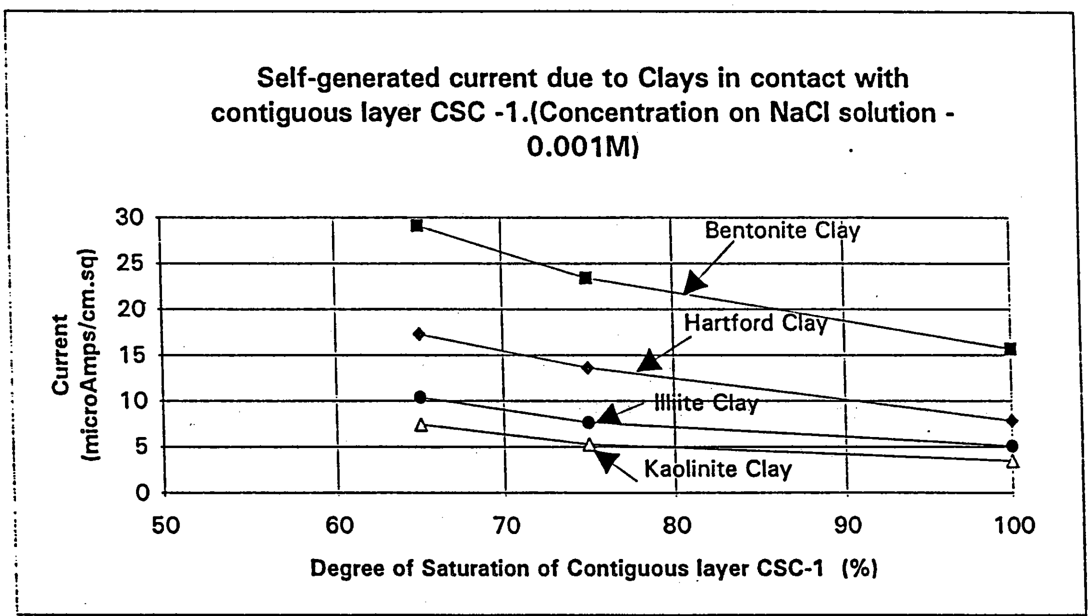

Figure 23

Corrosion current and altered saturation of contiguous layer CSC-1

It was of interest during the present research to determine if inclusions of coal in large volumes could accelerate the corrosion process. Contiguous layer CSC-2 had an addition of 50% by weight of crushed coal, and CS3 contained no coal. As in previous tests, the clay was fully saturated, layers CSC-1, CSC-2, and CSC-3 were maintained at about 65% saturation. As shown in Figure 24, the effect of coal inclusions is not clear. CSC-2, the layer with the greatest amount of coal showed a lower value of self generated current. It is not clear what causes this difference. Layer CSC-3 did not contain any coal inclusions. It seems that additional investigation of these actions is necessary.

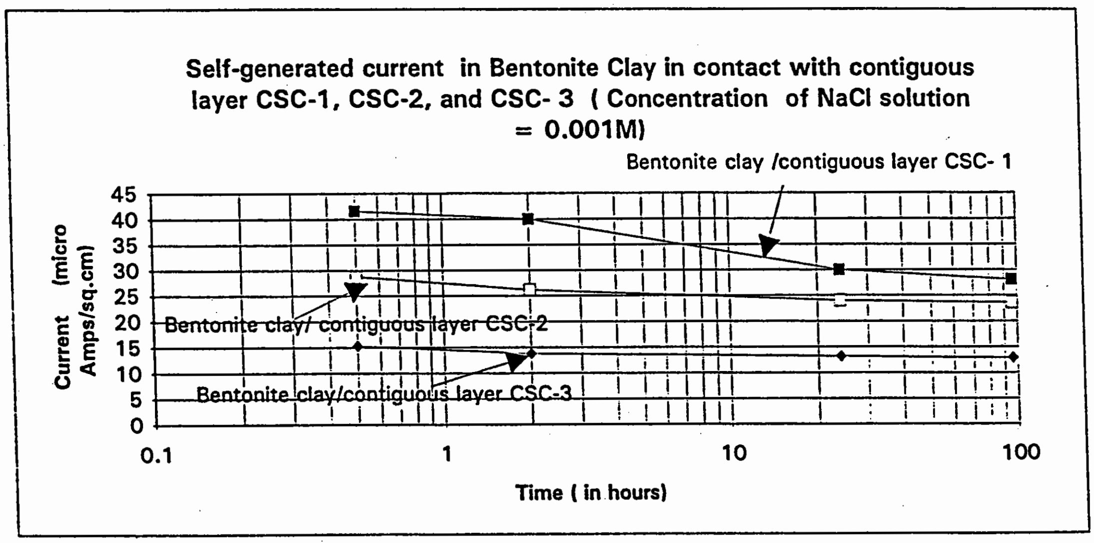

Figure 24

Self-generated current data due to contact-potential of contiguous layers with altered composition of crushed coal

Table 5
Contact potential and self-generated current measurements for clays in contact with layer CSC-1

Contiguous layers composition	Concentration of electrolyte (Mol)	Time	Current	Contact-potential
		(hrs.)	(microAmps/cm. sq)	(mV)
Bentonite Clay Layer CSC-1 Cinders, ashes, crushed coal	0.001M (5.86 ppm)	0.5	40.3	82
		2	38.75	80
		24	29.14	78
		96	27.28	76
	0.01M (58.6 ppm)	0.5	32.55	86
		2	31	84
		24	24.8	82
		96	22.17	82
	0.1M (586 ppm)	0.5	27.9	71
		2	22.79	68
		24	21.24	67
		96	18.91	66
Hartford Clay Layer CSC-1 Cinders, ashes 25% crushed coal	0.001M (5.86 ppm)	0.5	23.9	115
		2	19.8	106
		24	17.3	106
		96	17.05	98
	0.01M (58.6 ppm)	0.5	17.56	92
		2	15.2	88
		24	13.2	80
		96	9.92	76
	0.1M(586 ppm)	0.5	12.4	70
		2	10.6	68
		24	9.6	63
		96	8.84	60

Contiguous layers composition	Concentration of electrolyte (Mol)	Time (hrs.)	Current (microAmps/cm. sq)	Contact-potential (mV)
Kaolinite Clay Layer CSC-1 Cinders, ashes 25% crushed coal	0.001M (5.86 ppm)	0.5	9.3	60
		2	7.91	58
		24	7.44	54
		96	5.74	50
	0.01M (58.6 ppm)	0.5	7.44	58
		2	7.13	55
		24	6.2	50
		96	5.89	50
	0.1M (586 ppm)	0.5	9.15	40
		2	6.51	38
		24	4.88	34
		96	4.03	31
Illite Clay Layer CSC-1 Cinders, ashes 25% crushed coal	0.001M (5.86 ppm)	0.5	13.20	71
		2	11.80	69
		24	10.40	60
		96	8.90	59
	0.01M (58.6 ppm	0.5	11.30	66
		2	10.80	60
		24	9.10	56
		96	8.90	55
	0.1M (586 ppm)	0.5	9.87	59
		2	8.40	54
		24	7.80	50
		96	6.94	49

Table 6

Contact potential and self-generated current measurement data for clays in contact with layer CSC-2

Contiguous layers composition	Concentration of electrolyte (Mol)	Time (hrs.)	Current (microAmps /cm.sq)	Contract-potential (mV)
Bentonite Clay Layer CSC-2 50% crushed coal Cinders, Ashes	0.001M (5.86 ppm)	0.5	27.90	79
		2	25.42	77
		24	23.25	70
		96	22.94	70
Hartford Clay Layer CSC-2 50% crushed coal Cinders, Ashes	0.001M (5.86 ppm)	0.5	18.60	91
		2	17.05	87
		24	16.43	85
		96	16.12	80
Kaolinite Clay Layer CSC-2 50% crushed coal Cinders, Ashes	0.001M (5.86 ppm)	0.5	7.60	48
		2	6.20	45
		24	5.89	40
		96	5.74	40

With the available data it was decided to investigate the relation between the contact potential that was measured with the circuit open to the product of self generated current and the soil resistivity. The results are shown in Fig. 25. As can be seen in Fig. 25, there is a direct relationship for all the soils tested.

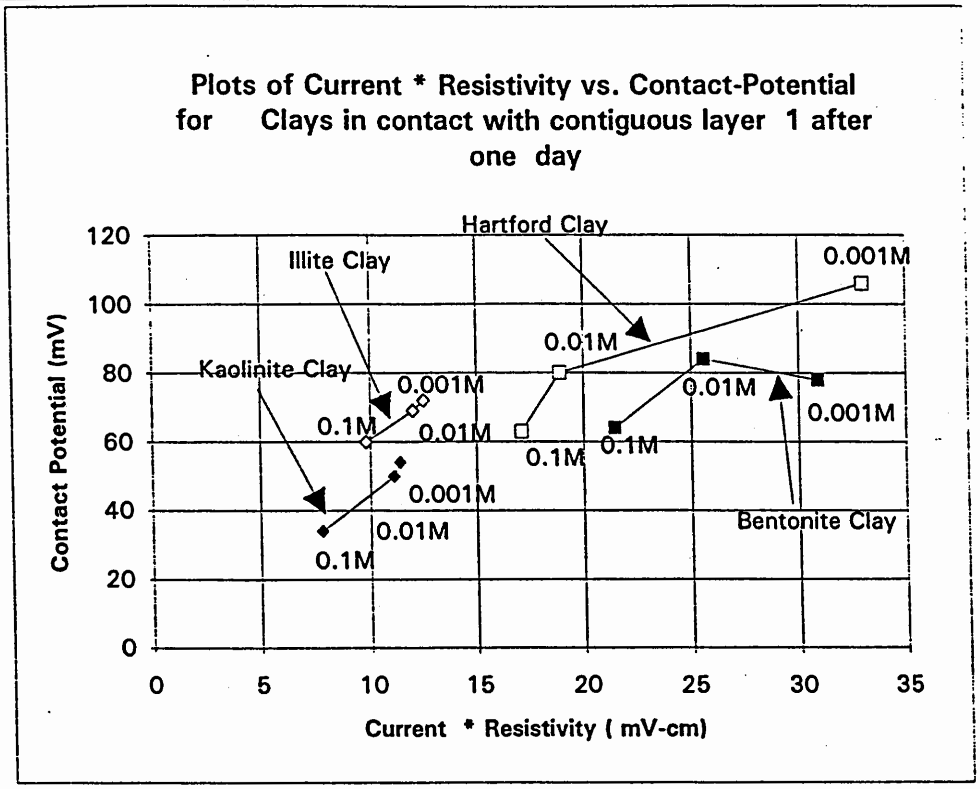

Figure 25
Contact-potential and self-generated current relationship of two contiguous layers

The contact potential decreases with increasing electrolyte concentration, which may be due to the decreased mobility of oxygen.

C. Corrosion Potential Measurements

Corrosion of metals has often been correlated with the potential between the metal and the medium in which it is embedded as measured with a standard Cu/Cu SO_4 half cell. Table 17 shows data obtained from direct measurements of four types of clays used in macrocell tests, along with a medium sand and silt. Corrosion potential was measured using Cu-$CuSO_4$ half cell as the reference electrode as described before.

In Table 7 the values of E_{corr} (1) were obtained by testing. The values of E_{corr} (2) were obtained from the Kasahara (17,24). The value of -760 mV corresponds to an unidentified clay. It should be emphasized that soils characterized by a relatively high negative corrosion potential in order of -700 mV exhibit a relatively small polarization resistance against steel, indicating a relatively high corrosion rate. The measured differences in corrosion potential indicate a possible contact potential of 0.3 to 0.4V, which with sufficiently low resistivity could develop an aggressive macrocell. The contact potentials between contiguous soils in this investigation were lower than indicated by the difference in corrosion potential.

Table 7

Corrosion Potential Measurement Data

Mineralogy (type of soil)	Concentration NaCl solution	E corr (1) (mV)	E corr (2) (mV)
Bentonite clay	0.001M	-780	-760
Illite clay	0.001M	-630	
Hartford clay (from I-84 samples)	0.001M	-670	
Kaolinite clay	0.001M	-600	
Sand from Quick Tank	0.001M	-420	-497
Silt	0.001M	-540	-763

As seen from the Figure 26, the self-generated current reaches its highest level when there is a soil with more negative corrosion potential is the anode of a macrocell. Bentonite clay (Corrosion potential = -780 mV) generated the highest level of self-generated current. Silt (Corrosion potential = -540 mV) did not generate any significant current. In all cases cathodic zone of macro cell was presented the same continuous layer CSC-1.

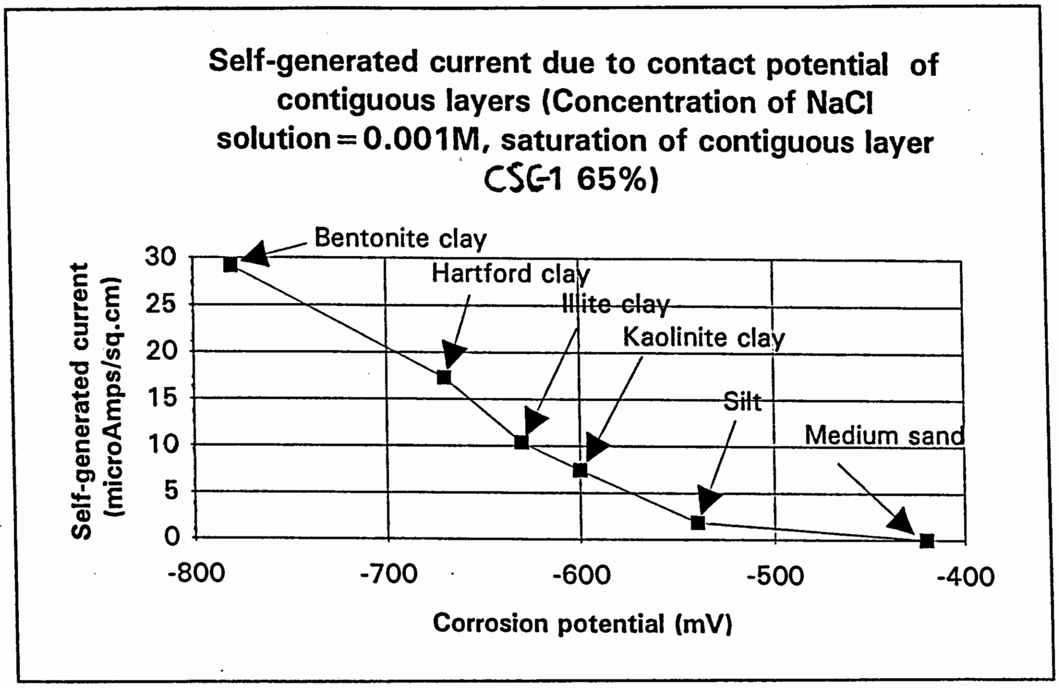

Figure 26

Contact potential and self-generated current relationship of contiguous layers versus corrosion potential of soil.

D. Concentration Cell Corrosion Experiments

1. Concentration Gradient Corrosion Cell Data

This test was performed in order to study the corrosion process in a concentration cell. This test is an extension of tests performed by Long and Lele (2). The current with time is shown in Fig. 27. As can be seen the current decreased slightly with time.

It was desired to calculate the expected weight loss of the embedded steel washers and compare the calculated values to the measured values. Weight loss for the anodic electrode has been calculated applying Faraday's Law using the average value of the detected current. The result is shown in Table 8. Actual loss of weight is higher. Self-generated current made a significant contribution to the corrosion process. The excess of weight loss was probably due to local cell corrosion. The cathode did not experience substantial corrosion losses.

2. Influence of The Anode/Cathode Area Ratio on Corrosion Rates in Concentration Cell Tests Data

This test was performed in order to study the corrosion process on steel rods inserted in a concentration cell environment. The soil was an Ottawa sand, the lower portion of which was saturated with a 0.5% solution of NaCl in distilled water. The upper portion of the soil was left at a degree of saturation of 65%for 110 days. Four steel strips were embedded vertically in each cylinder. The area ratio of the Cathode to Anode differed in each cell. The results plotted in Fig. 28 are the average losses in each cylinder. The smaller the cathode is with respect to the anode the less metal is lost to corrosion.

Table 8

Concentration cell test weight loss data

Test Conditions	Average I corr (microAmp)	Measured Loss (grams)	Calculated Loss (grams)
Medium density Ottawa Sand saturated with: Lower portion- 0.5%NaCl full saturation. Upper portion - tap water at about 65% of full saturation. Steel -two washers	51 (aver. for 90 days)	0.93 (anode) <0.10 (cathode)	0.592

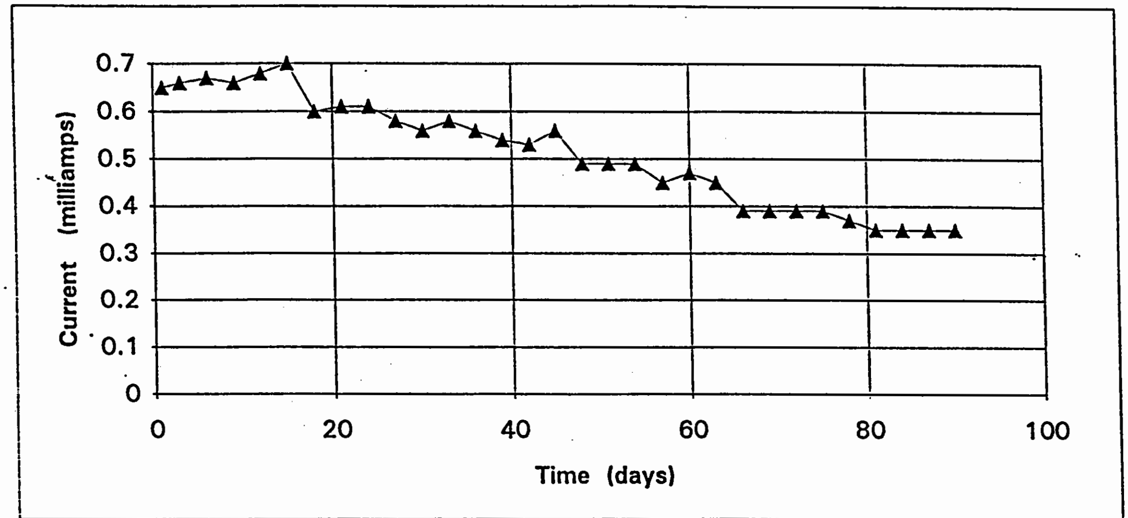

Figure 27

Concentration cell self-generated current versus time

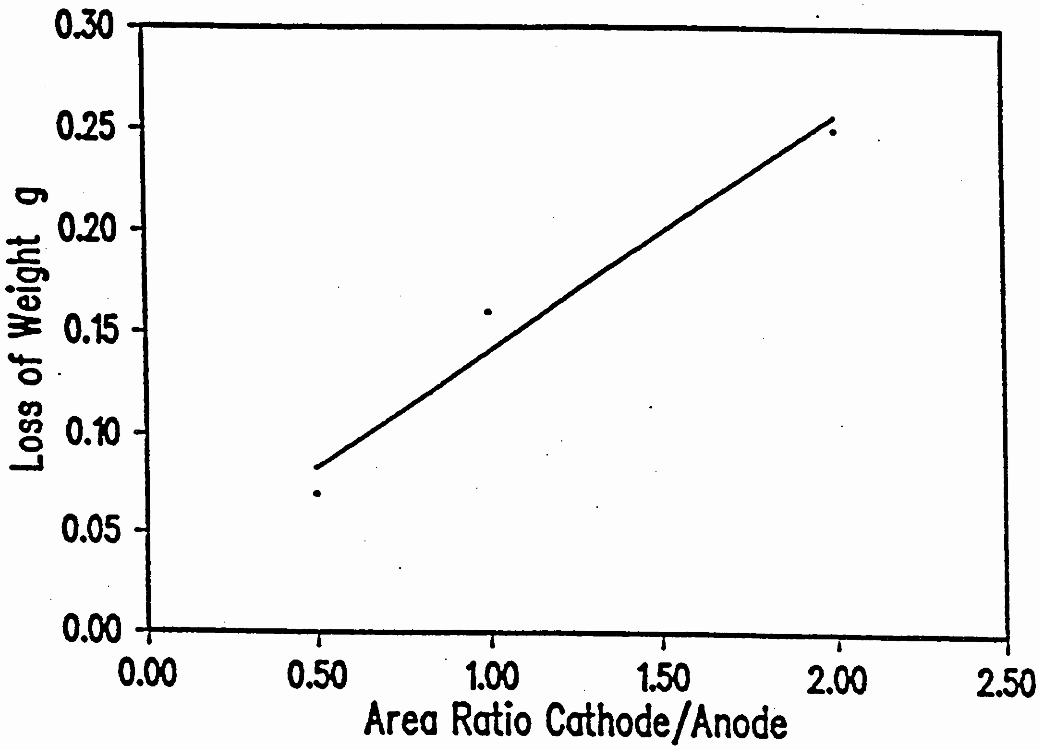

Figure 28

Plot of weight loss of steel strips
vs. cathode/anode area ratio

It should be noted that anode/cathode area ratio was determined by using solution inlet elevations. Actually, the border between the anodes and the cathodes can not be predicted with accuracy if all ion migrations are taken into account. The patterns of loss are shown on Figure 29.

3. Results using various cathode/anode areas with shorted electrodes

The measured current densities are shown in Fig. 30 and 31. As can be seen from these diagrams the current density is greater for the smaller area. As the area decreases the density increases and vice versa. The anodic current density tends to decrease as the degree of saturation of the cathodic soil increases, decreasing the difference in oxygen concentration.

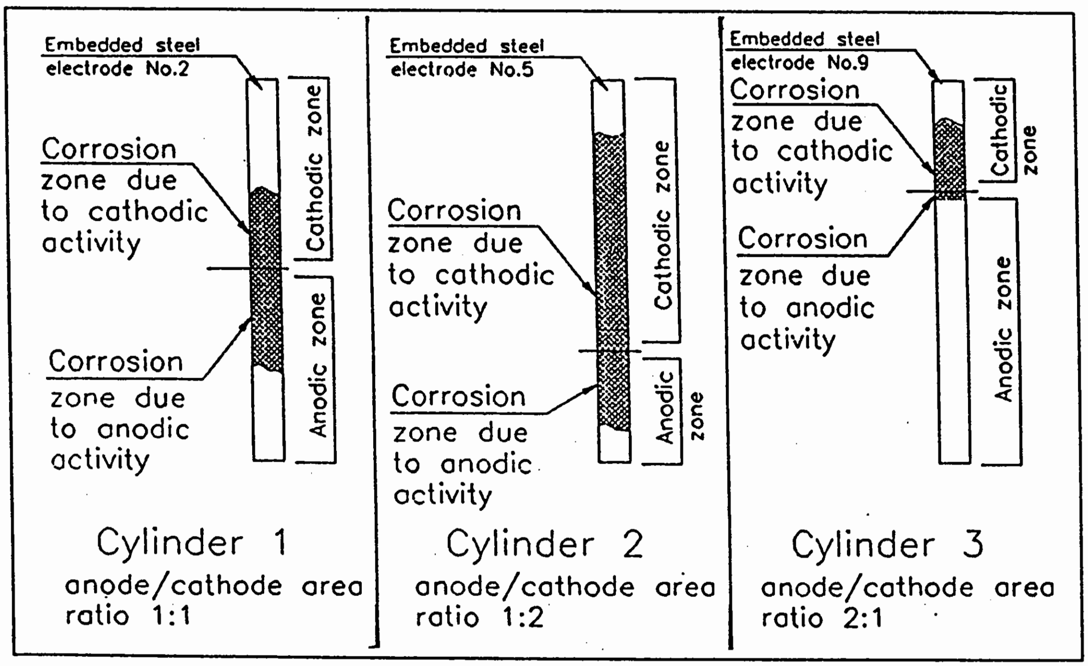

Figure 29

Schematic representation of the corrosion patterns for the anode/cathode area ratio tests

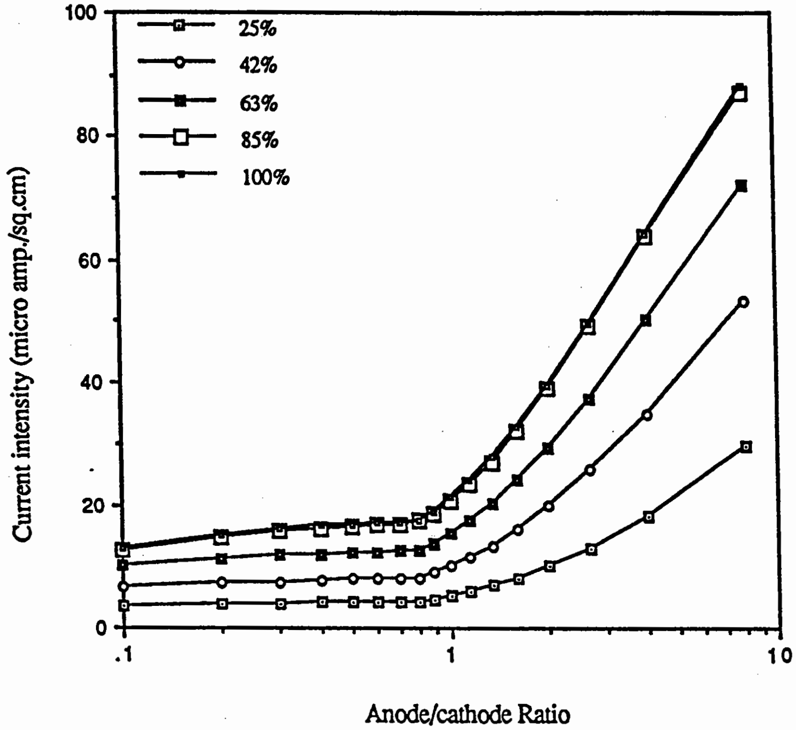

Figure 30
Cathodic current density as a function of anode/cathode ratio

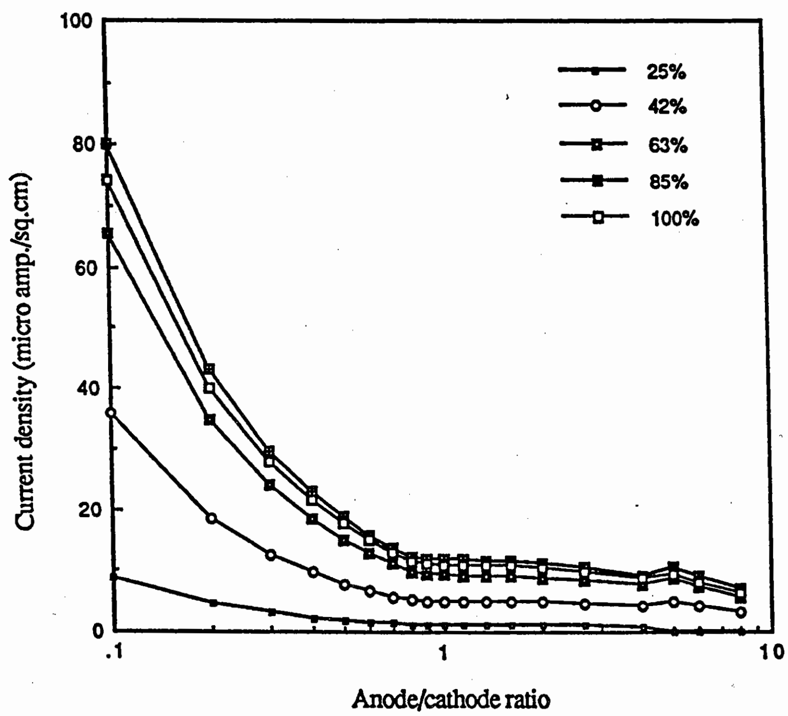

Figure 31
Anodic current density as a function anode/cathode ratio

The effect of concentration of NaCl is shown in Fig. 32. As can be seen the current density peaks at a concentration of about 0.75%.

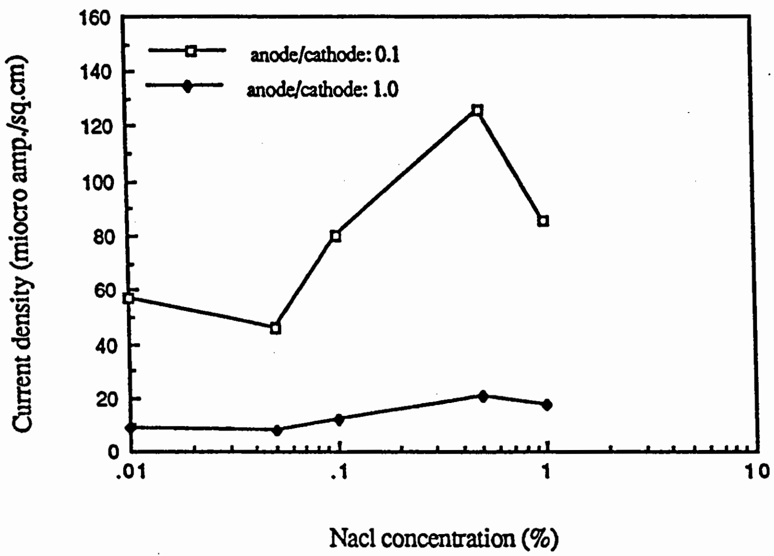

Figure 32

Anodic current density as a function of salt concentration

An example of the effect of the ratio of cathode to anode area as it might affect a steel pile was demonstrated with the corrosion probe. The results are shown in Fig. 33. The ratio of cathode to anode area is 29. As one can see from Fig. 33, the average current density in the anodic area is much smaller than the current density in the cathodic area represented by the plot to the right.

4. Determination of Polarization Characteristics of Steel in Contact with Soil by Kasahara's Method

Polarization characteristics of different type of soil were determined with respect to their saturation conditions. Polarization characteristics of clays have been obtained when clays were saturated with one of two concentrations of NaCl: 0.001M or 0.01M.

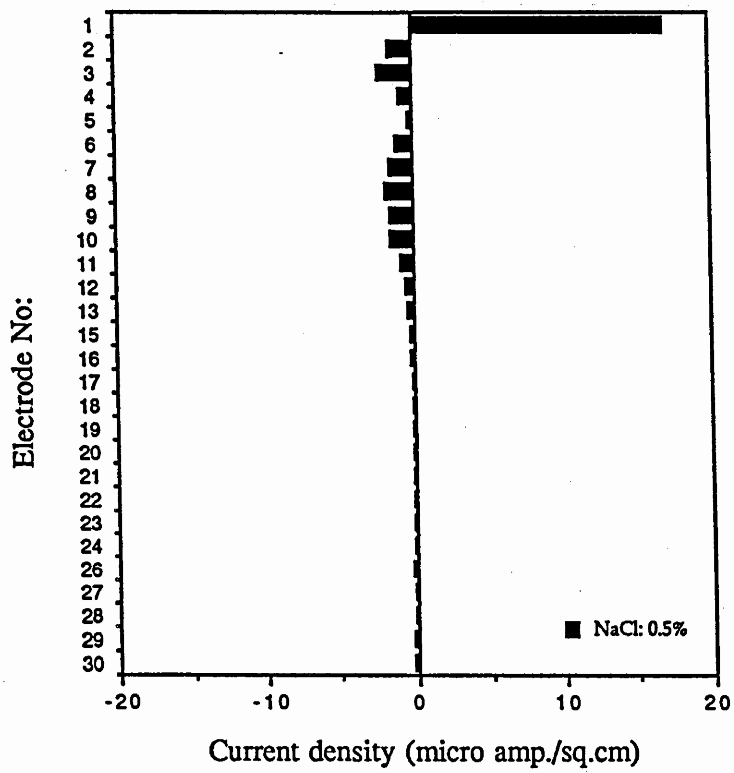

Figure 33

Current distribution along the soil probe simulating a pile with most of its length below groundwater table

The results are shown in Fig. 34. Bentonite clay exhibits the lowest polarization resistance when saturated with a very dilute solution of 0.001M NaCl (58.5 ppm). The effect of increasing concentration of NaCl increasing the polarization resistance was not anticipated.

As seen in Figure 34 there is a direct correlation between CEC of clays and polarization resistance. It should be noted that the highest negative value of corrosion potential for the Bentonite Clay indicates the extreme corrosive behavior of this type of soil which correlates with the low polarization resistance. Soil samples from Hartford show low polarization resistance, therefore it could be listed as a soil with high corrosion potential. It should also be noted that the lower concentration of NaCl yields the lower polarization resistance indicating the greater corrosion current.

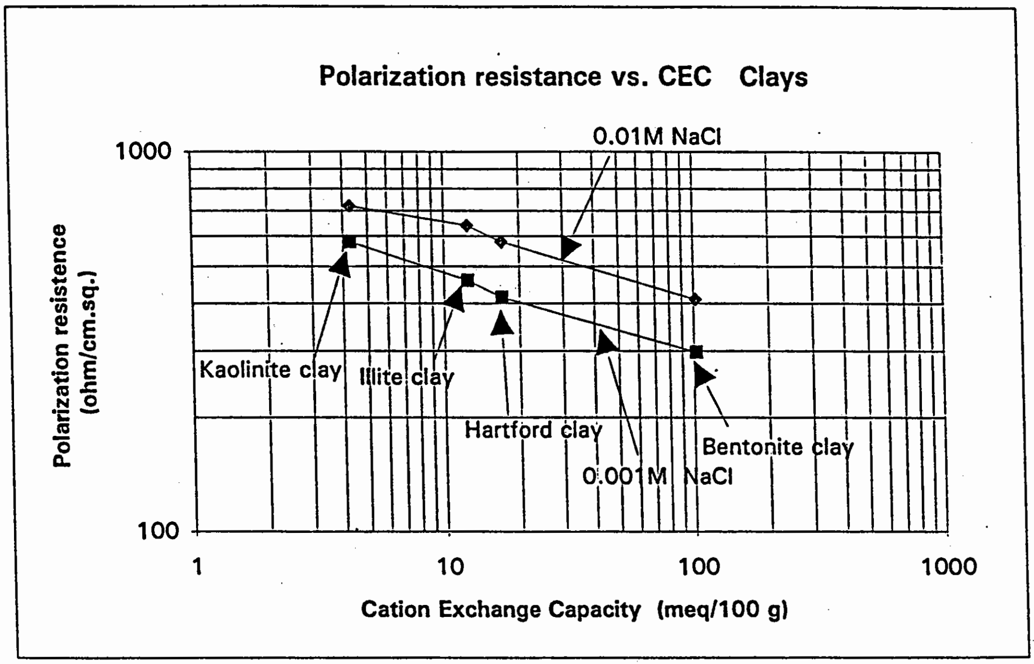

Figure 34

Polarization resistance of clays vs. Cation Exchange Capacity

Hartford Clay has been tested with a wide range of NaCl solutions. The results are shown in Figure 35. It is interesting to note that it has high polarization resistance when there is no salt present (saturated with distilled water), as soon as there is a slight salt concentration of about 50-100 ppm NaCl concentration, the polarization resistance drops sharply to its lowest value. When the concentration NaCl is increased, the resistance also increases.

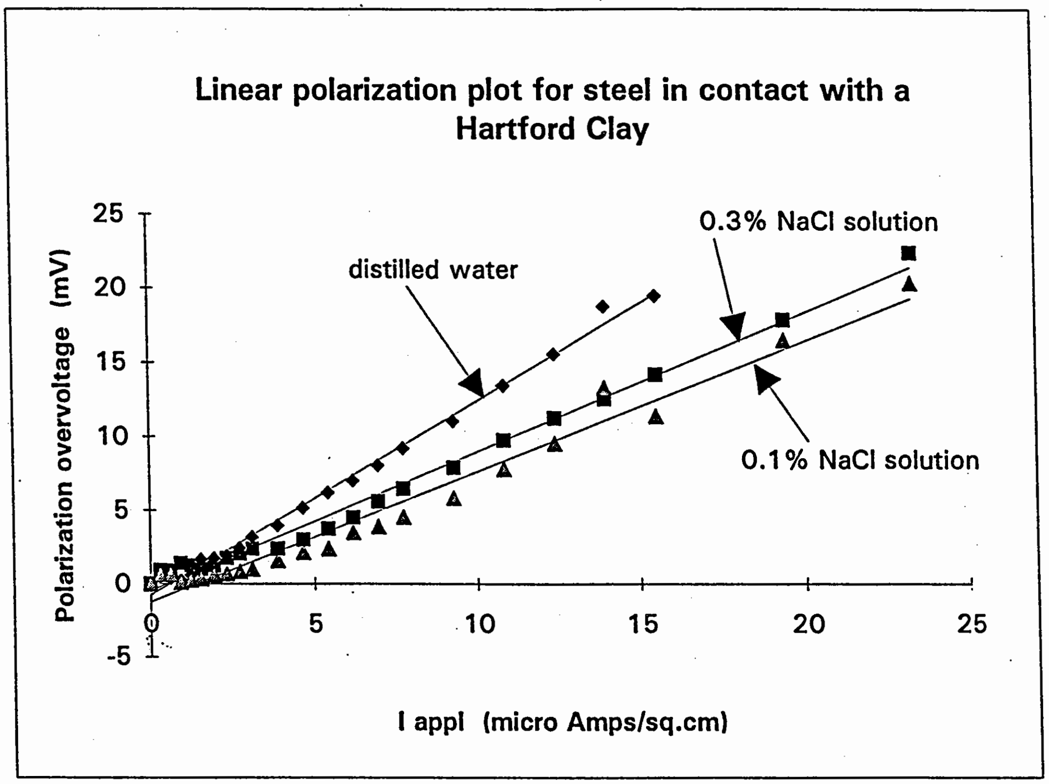

Figure 35

Linear polarization plots for Hartford Clay at various concentrations of NaCl

In terms of polarization resistance measurements, it is important to emphasize the significance of the value of the IR drop. As it is shown in the measurement data, IR drop can have a significant effect in the measurement of polarization resistance of steel even when the reference electrode is placed close to the working electrode in distilled water. As salt is added the IR effect decreases but it must always be accounted for. An accumulation of large errors in R_p may exist without this correction. When the concentration of chemicals in the electrolyte increases, the resistivity of the soil drops, the IR contribution to the total polarization of steel electrode becomes smaller. In this case determination of the IR drop value by the present method has advantages, such as simplicity and more precise values of polarization resistance R_p.

In case of soil with smaller value of negative corrosion potential, the concentration of electrolyte does not significantly alter polarization characteristics. Concentrations of NaCl in case of Medium Density Sand only slightly reduced polarization resistance. The results are shown in Fig. 36. This probably could be attributed to changes in resistivity of the soil.

Polarization characteristics of different types of soil were determined with respect to their saturation conditions. Polarization characteristics of clays have been obtained when clays were saturated with altered concentrations of NaCl such as 0.001M and 0.01M. As shown on Table 9, Bentonite clay exhibits the lowest polarization resistance and, as a result, the highest corrosion rates, when saturated with a very dilute solution of 0.001M NaCl (58.5 ppm). Other clays show the same trend of polarization characteristics.

Table 9

Polarization resistance measurements data

Type of Clay	Concentration of NaCl	CEC	Polarizat. resistance
	(Mol/L)	meq/100 g	ohm/cm.sq
Bentonite Clay	0.001M (5.58 ppm)	102	298
Hartford Clay		17	415
Kaolinite Clay		4.27	580
Illite Clay		12.4	460
Bentonite Clay	0.01M (55.8 ppm)	102	410
Hartford Clay		17	580
Kaolinite Clay		4.27	720
Illite Clay		12.4	640

5. Measurements with the soil probe

Measurements were made with the soil probe to determine the strength of macrocells in the vicinity of the ground water table. All of these measurements were made in a cylindrical container. The water table was established with an external reservoir. Typical results are shown in Fig. 37.

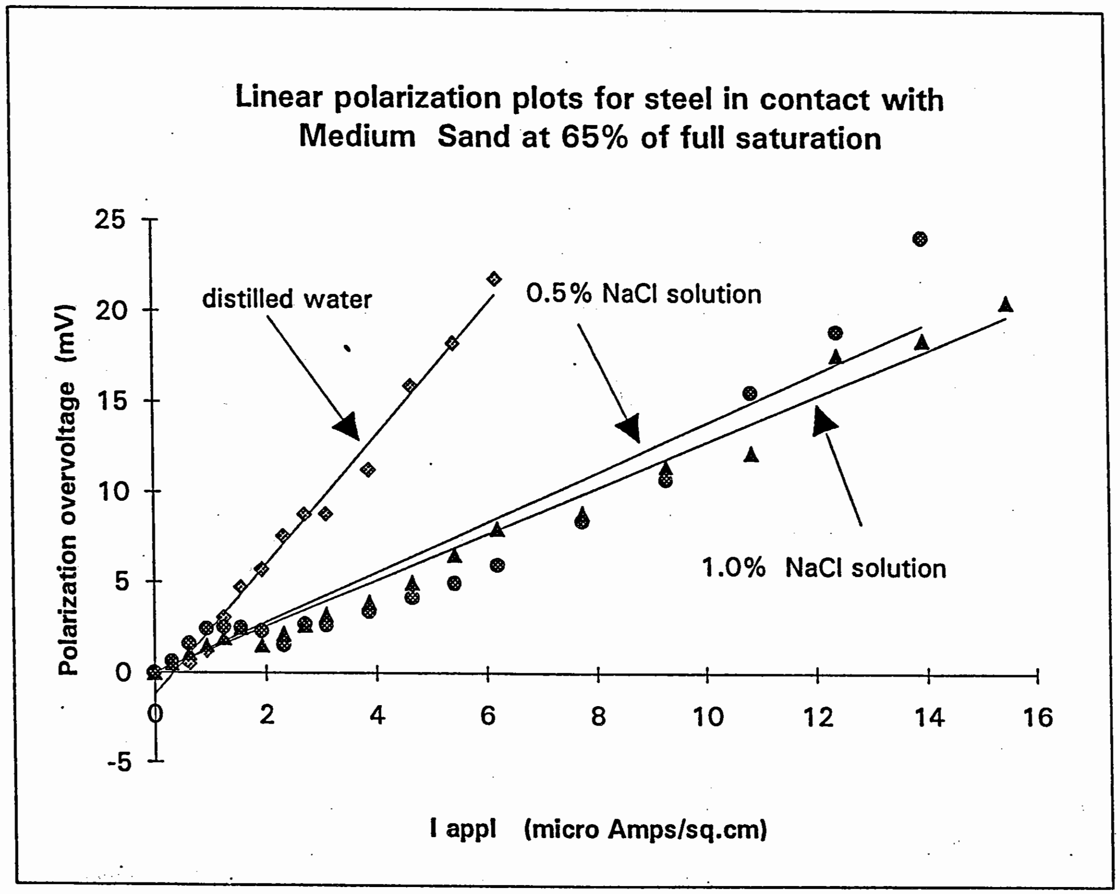

Figure 36

Linear polarization data for medium density sand at various concentrations of NaCl

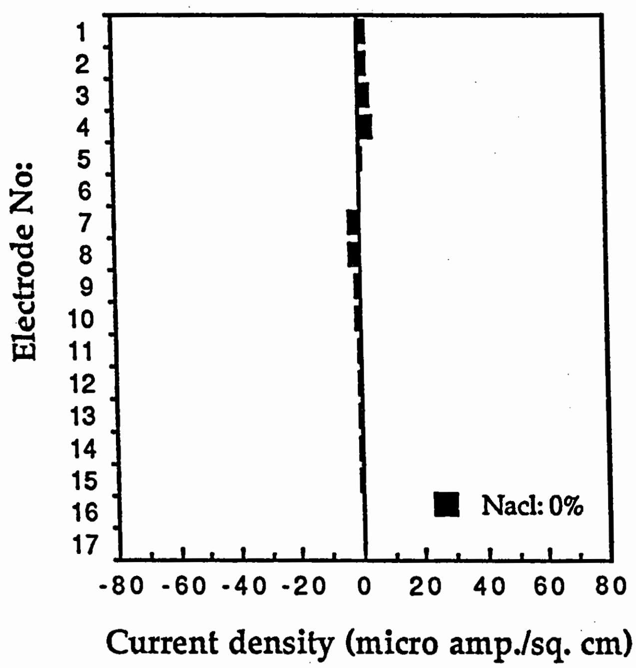

Figure 37

Distribution of current along soil probe in sand containing distilled deaerated water

From this Figure one can see that the flow of current reverses around the water table. Above the water table the current flow is into the probe and below it is out of the probe. The total current in the anodic region equals the current in the cathodic region. The average current in the anodic region is smaller than the average in cathodic region because of the difference in areas. The current tends to decrease with time. The biggest decrease occurs at short times after the current begins flowing.

Fig. 38, 39 and 40 show the effect of various concentrations of NaCl on the current. Fig. 38 shows the current produced when the concentration of NaCl is 0.1%. Fig. 40 shows the current at a NaCl concentration of 1.0% and Fig. 39 at a concentration of 0.5%. This effect of concentration of NaCl is best illustrated with Fig. 41 which shows the variation of current density with concentration of NaCl. The presence of NaCl decreases the mobility of oxygen. At low concentrations the mobility decrease is offset by the decrease in resistivity which allows more current to flow. As the concentration increases the decrease of the mobility becomes evident.

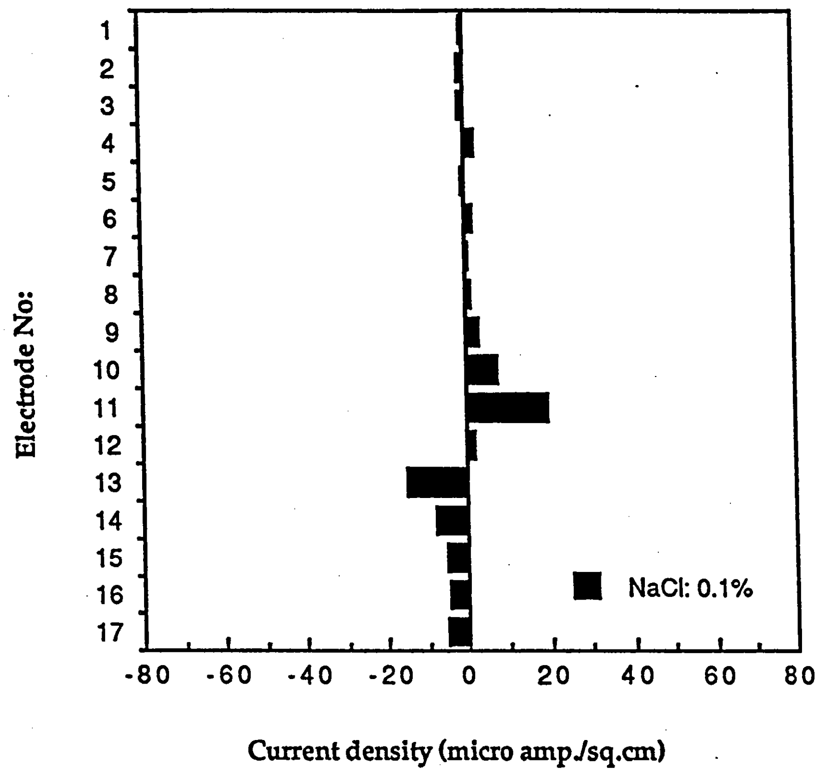

Figure 38

Distribution of current along soil probe in sand containing a solution of 0.1% NaCl

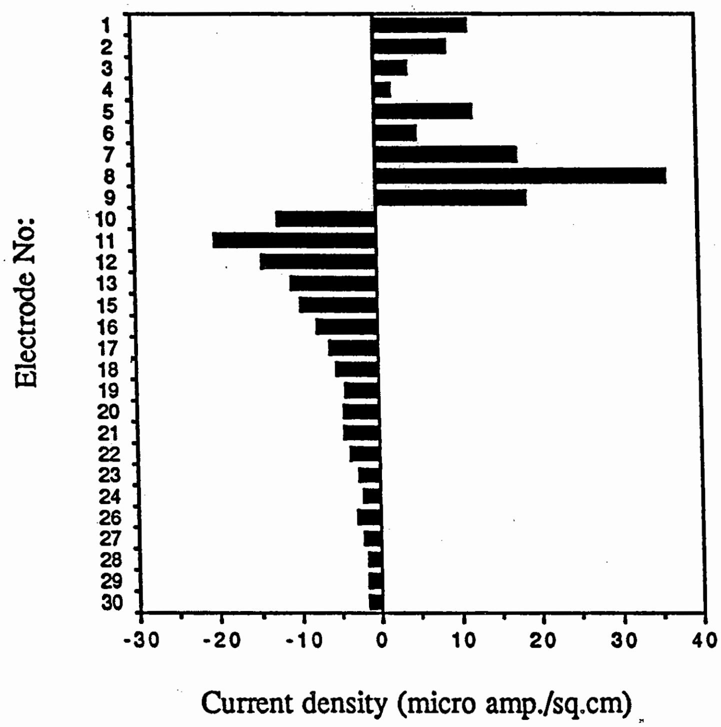

Figure 39

Distribution of current along soil probe in sand containing a solution of 0.5% NaCl

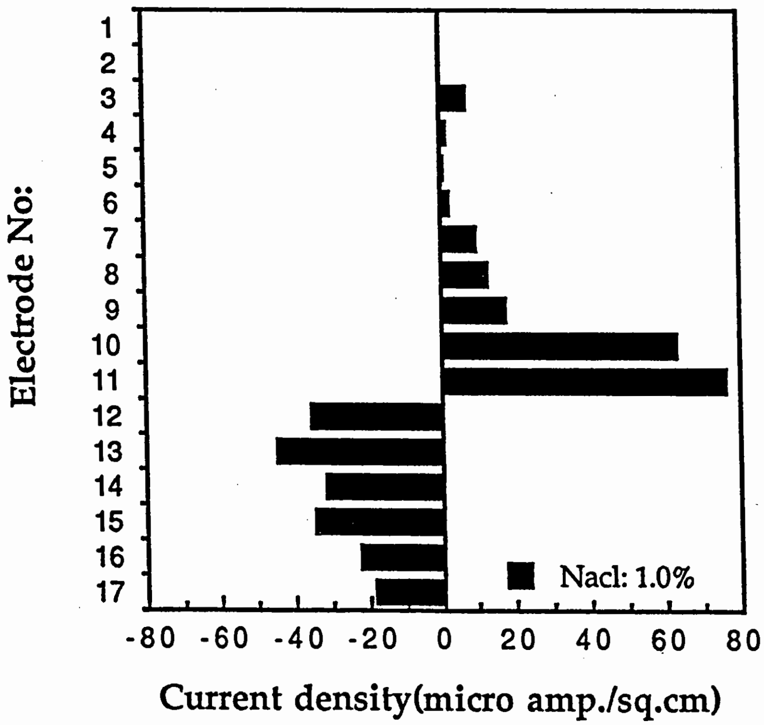

Figure 40

Distribution of current along soil probe in sand containing a solution of 1.0% NaCl

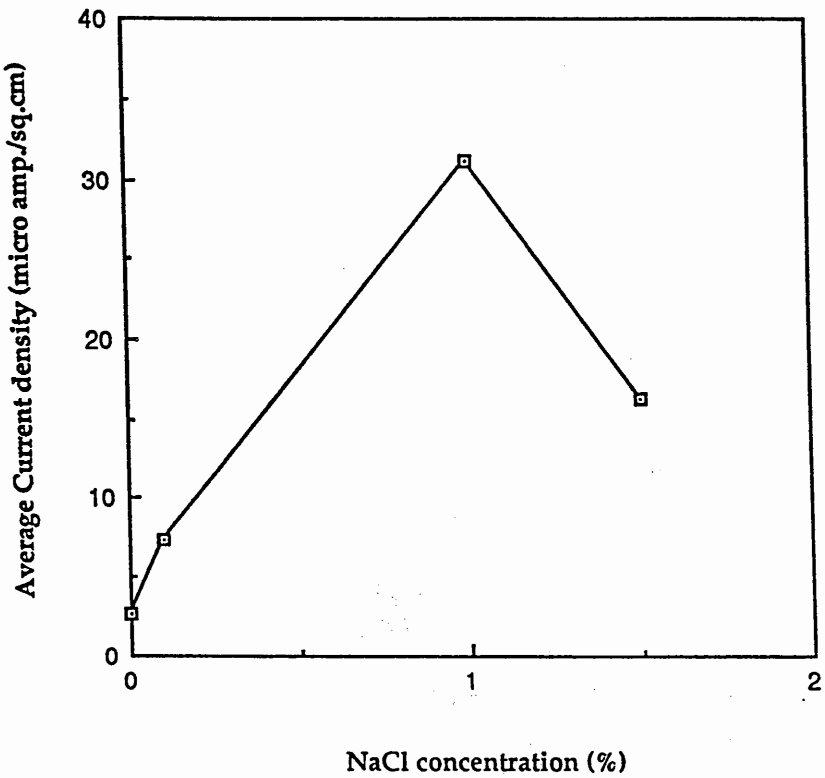

Figure 41

Variation of current intensity in Ottawa sand

E. Resistivity and Contact Potentials from two sites in Hartford

During the process of reviewing the construction drawings for bridges over miscellaneous fills, the boring logs of the I-84 W3 Roadway over Church St. (63-137) and Sigourney St. (63-159) showed cinders. The Soils Division of ConnDOT retrieved continuous samples of the materials at these sites and forwarded them to UConn for laboratory testing.

The jar samples as received were carefully labeled to indicate which came from contiguous layers. Each sample was used in two tests: minimum resistivity and contact potential. The minimum resistivity is the soil's resistivity when saturated with distilled water (1,2,3). The contact potential is the open circuit electrical potential developed by two wet soils in contact (1,2,3). The results are shown in Tables 10 and 11. Table 10 lists the measured minimum resistivities in ohm-cm. In several cases there was not enough recovered sample to conduct the test, as noted in Table 10. About half of the tested samples had resistivities below 1000 ohm-cm, indicating that if a contact potential of about 0.1v is generated, these soils could carry a significant amount of current. The contact potentials in Table 11 are much lower than 0.1v leading to small self-generated currents. The steel piles at these sites should not experience significant corrosion.

Table 10

Contact Potential for Contiguous Layers

No.	Hole No.	Depth (feet) From-To	Contact Potential (mv)	Self-generated Current (μA/cm^2)
1	B-1	3-5(+) 5-7(-)	5.90	0.51
2	B-1	9-11(+) 11-13(-)	24.60	1.73
3	B-2	4.5-6(2)(-) 6-7.5(1)(+)	81.00	7.05
4	B-2	6-7.5(3)(+) 7.5-9(1)(-)	11.33	1.07
5	B-3	2.5-4(-) 4-5.5(1)(+)	72.40	4.20
6	B-3	8.5-10(-) 10-11.5(+)	35.78	3.52
7	B-4	0-2(+) 2-4(1)(-)	8.44	3.60
8	B-4	2-4(1)(-) 2-4(2)(+)	3.55	0.00
9	B-4	4-6(5)(+) 6-8(2)(-)	2.70	0.18
10	B-4	8-10(4)(-) 10-12(1)(+)	35.75	6.51
11	B-5	6-8(2)(-) 8-11(+)	34.20	2.42
12	B-6	0-2(3)(+) 2-4(1)(-)	32.49	1.99
13	B-6	6-8(2)(+) 8-10(-)	0.91	0.21

Table 11

Minimum Resistivity Test

DATE: Sept.7-8,1994

No.	Station	Hole No.	Depth	Resistivity (Ω-cm)
1	Sig. St.	B-1	1-3.	4201
2	Sig. St.	B-1	3-5.	1055
3	Sig. St.	B-1	5-7.	1458
4	Sig. St.	B-1	7-9.	2206
5	Sig. St.	B-1	9-11.	1115
6	Sig. St.	B-1	11-13.	1447
7	Sig. St.	B-1	13-15	1395
8	Sig. St.	B-1	15-17	1557
9	Sig. St.	B-1	17-19	1635
10	Sig. St.	B-2	1-3(1)	3227
11	Sig. St.	B-2	1-3(2)	1508
12	Sig. St.	B-2	1-3(3)	3620
13	Sig. St.	B-2	1-3(4)	2992
14	Sig. St.	B-2	1-3(5)	2538
15	Sig. St.	B-2	3-4.5(1)	1390
16	Sig. St.	B-2	3-4.5(2)	2321
17	Sig. St.	B-2	3-4.5(3)	987
18	Sig. St.	B-2	4.5-6(1)	1253
19	Sig. St.	B-2	4.5-6(2)	792
20	Sig. St.	B-2	4.5-6(3)	Not Enough Sample
21	Sig. St.	B-2	6-7.5(1)	701
22	Sig. St.	B-2	6-7.5(2)	932

Table 11 cont'd

Minimum Resistivity Test

DATE: Sept.7-8,1994

No.	Station	Hole No.	Depth	Resistivity (Ω-cm)
23	Sig. St.	B-2	6-7.5(3)	371
24	Sig. St.	B-2	7.5-9(1)	510
25	Sig. St.	B-2	7.5-9(2)	768
26	Sig. St.	B-2	9-10.5	633
27	Sig. St.	B-3	1-2.5	1912
28	Sig. St.	B-3	2.5-4	1504
29	Sig. St.	B-3	4-5.5(1)	1769
30	Sig. St.	B-3	4-5.5(2)	1783
31	Sig. St.	B-3	5.5-7	1007
32	Sig. St.	B-3	7-8.5	Not Enough Sample
33	Sig. St.	B-3	8.5-10	907
34	Sig. St.	B-3	10.-11.5	840
35	Sig. St.	B-3	11.5-13	1201
36	Sig. St.	B-3	13-14.5	1795
37	Church St.	B-4	0-2	53
38	Church St.	B-4	2-4(1)	124
39	Church St.	B-4	2-4(2)	776
40	Church St.	B-4	2-4(3)	1763
41	Church St.	B-4	2-4(4)	865
42	Church St.	B-4	4-6(1)	942
43	Church St.	B-4	4-6(2)	1121

Table 11 cont'd

Minimum Resistivity Test

DATE: Sept.7-8,1994

No.	Station	Hole No.	Depth	Resistivity (Ω-cm)
44	Church St.	B-4	4-6(3)	Not Enough Sample
45	Church St.	B-4	4-6(4)	1399
46	Church St.	B-4	4-6(5)	964
47	Church St.	B-4	6-8(1)	Not Enough Sample
48	Church St.	B-4	6-8(2)	918
49	Church St.	B-4	8-10(1)	Not Enough Sample
50	Church St.	B-4	8-10(2)	Not Enough Sample
51	Church St.	B-4	8-10(3)	897
52	Church St.	B-4	8-10(4)	619
53	Church St.	B-4	10-12(1)	521
54	Church St.	B-4	10-12(2)	807
55	Church St.	B-4	10-12(3)	814
56	Church St.	B-4	12-14(1)	501
57	Church St.	B-4	12-14(2)	829
58	Church St.	B-4	14-16(1)	692
59	Church St.	B-4	14-16(2)	811
60	Church St.	B-4	16-18	772
61	Church St.	B-5	0-2	370
62	Church St.	B-5	2-4(1)	Not Enough Sample
63	Church St.	B-5	2-4(2)	699
64	Church St.	B-5	4-6.	560
65	Church St.	B-5	6-8(1)	574

Table 11 cont'd

Minimum Resistivity Test

DATE: Sept.7-8,1994

No.	Station	Hole No.	Depth	Resistivity (Ω-cm)
66	Church St.	B-5	6-8(2)	717
67	Church St.	B-5	8-10(1)	770
68	Church St.	B-5	8-10(2)	957
69	Church St.	B-5	10-12.	999
70	Church St.	B-6	0-2(1)	Not Enough Sample
71	Church St.	B-6	0-2(2)	1443
72	Church St.	B-6	0-2(3)	1218
73	Church St.	B-6	2-4(1)	1087
74	Church St.	B-6	2-4(2)	1261
75	Church St.	B-6	4-6(1)	2587
76	Church St.	B-6	4-6(2)	1333
77	Church St.	B-6	4-6(3)	968
78	Church St.	B-6	6-8(1)	2005
79	Church St.	B-6	6-8(2)	425
80	Church St.	B-6	8-10.0	304
81	Church St.	B-6	10-12.0	281

Conclusions

1. Corrosive macrocells develop from contiguous layers of soil that have different levels of aeration. This difference can result from the presence of different soils or from zones of different levels of aeration in the same soil.

2. Resistivity is an important consideration when investigating corrosion in any subsurface profile. A low resistivity allows the current to flow whenever the aeration conditions support an electrical potential between contiguous zones.

3. One of the most potent macrocells develops when a clay layer is contiguous to a layer of combustion products (ash, cinders) especially when they are mixed with coal.

4. The strength of a macrocell containing clay is related directly to the Cation Exchange Capacity of the clay. Clays having greater CEC's develop stronger macrocells.

5. The soil probe is a promising tool for investigating the corrosiveness of subsurface profiles for steel piles.

Recommended Further Work

The soil probe tests reported here show a device that measures the behavior critical to the corrosion of steel piles, i.e., the amount of current and direction of flow. The concept of this probe could be expanded into a field device capable of being pushed into the soil similar to the cone penetrometer. More testing in the field and laboratory is required to determine the most accurate method of use. This investigation would address the methods of inserting the probe and its effects on the readings.

Acknowledgement

This project could not have been completed properly without the contributions of N.D. Greene of the Department of Metallurgy and J. Fikiet of the School of Engineering Electronics Shop. Their help is greatly appreciated.

References

1. R.P. Long and F.C. Huang, "Corrosion of Driven Steel Piles," Final Report, JHR 90-193, Department of Civil Engineering, University of Connecticut, May 1990.

2. R.P. Long and S. Lele, "Insitu Detection of Pile Corrosion," Final Report, JHR 92-207, Department of Civil Engineering, University of Connecticut, April 1992.

3. R.P. Long, "Corrosion of Steel Piles in Some Waste Fills," in Geoenvironmental and Engineering Properties of Rock, Soil and Aggregate, Transportation Research Record No. 1345, TRB, National Research Council, Washington, DC, 1992.

4. State of California, Dept. of Transportation," Method for Estimating the Service Life of Steel Culverts," California Test 643, Sacramento, CA, 1978.

5. J.A. Beavers, N.G. Thompson, and D.C. Silverman, "Corrosion Engineering Applications of Electrochemical Techniques: Laboratory Testing, Corrosion 93," National Association of Corrosion Engineers, Paper No. 348, Houston, TX 1993, pp. 1-29.

6. M. Romanoff, "Corrosion of Steel Pilings in Soils," U.S. Department of Commerce, National Bureau of Standards, Monograph 58, U.S. Government Printing Office, Washington, DC, 1962.

7. M. Romanoff, "Performance of Steel Piling in Soils," In NBS paper on Underground Corrosion of Steel Piling, U.S. Department of Commerce, National Bureau of Standards, Monograph 127, U.S. Government Printing Office, Washington, DC, 1957.

8. Bethlehem Steel, "How Corrosion Affects Steel H-Piles in Earth," Engineering Aids from Bethlehem Steel, December 1977.

9. B.M. Das, Principles of Foundation Engineering, 2nd Ed., PWS-KENT, Boston, 1990, pg. 426.

10. J.E. Bowles, Foundation Analysis and Design, 4th Ed., McGraw-Hill, New York, 1988, pg. 731.

11. M.G. Spangler and R.L. Handy, Soils Engineering, 4th Ed., Harper and Row, New York, 1982, pg. 613.

12. E. Schaschl and G.A. Marsh, "Some New Views on Soil Corrosion," Material Protection, November 1963, pp. 8-17.

13. W.J. Schwerdtfeger, "Laboratory Measurement of the Corrosion of Ferrous Metals in Soils," Journal of Research of the National Bureau of Standards, Research Paper 2422, Vol. 50, No. 6, June 1953, pp. 329-36.

14. N.D. Tomashov, "Theory of Corrosion and Protection of Metal," The Science of Corrosion, The Macmillan Co., New York, 1960.

15. M.J. Schiff, "What is Corrosive Soil," 16th Western States Corrosive Seminar, Proceedings, Pomona, CA, May 1982.

16. S.K. Gupta, and B.K. Gupta, "The Critical Soil Moisture Content in the Underground Corrosion of Mild Steel," Corrosion Science, Vol. 19, pp. 171-179, Pergamon Press, 1979.

17. A. Jerbo, "Underground Corrosion of Steel Piles," 5th Scandinavian Corrosion Congress, Proceedings, October 7-10, 1968, Copenhagen, Danish Corrosion Center, 1969, v. 2, p. 26-2/26-10.

18. Kasahara, K., Adachi, H., Kajiyama, F., "Corrosion of Buried Steel Pipes Driven by Macro-galvanic Cells," 7th Congress of the European Federation of Corrosion, Mainz, Germany, Sept. 6-11, 1981, Proceedings.

19. N. Tomashov and Y. Mikhailovsky, "Corrosivity of the Soil," Corrosion v. 15, p. 77t-82t, April 1959.

20. W.J. Schwerdtfeger, "Polarization Measurements as Related to Corrosion of Underground Steel Piling," Journal of Research of the National Bureau of Standards, and Engineering and Instrumentation, Vol. 75C, No. 2, April-June 1971, pp. 107-21.

21. W.J. Schwerdtfeger and M. Romanoff, "Corrosion Rates on Underground Steel Test Piles at Turcot Yard, Montreal, Canada - Port 1," NBS Monograph 138, National Bureau of Standards, Washington, DC, July 1972, pp. 1-12.

22. M.G. Fontana and N.D. Green, "Corrosion Engineering," McGraw-Hill, New York, 1967, Chap. 2 and 3.

23. H.H. Uhlig, R.W. Revie, "Corrosion and Corrosion Control," John Wiley & Sons, Inc., New York, 1985, Chap. 3 and 6.

24. U.R. Evans, "Corrosion and Oxidation of Metal," St. Martin's Press, Inc., New York, 1960, p. 128.

25. K. Kasahara and Kajiyama, "Determination of Underground Corrosion Rates from Polarization Resistance Measurements," Corrosion, Vol. 39, No. 12, 1983.

26. U.S. Salinity Laboratory Staff, USDA Agricultural Handbook No. 60, L.A. Richard, editor, U.S. Department of Agriculture, Washington, DC, 1954.

27. W.P. Moody, "Corrosion in the Soil Environment: New York's Experience," 13th Central Pennsylvania Geotechnical Seminar "Progress in Geotechnical Engineering Practice," April 12-14, 1993, Hershey, PA.

28. U.R. Evans, "The Corrosion and Oxidation of Metals," Scientific Principles and Practical Applications, Edward Arnold Publishers Ltd., London, 1971.

29. Mattson, E., Basic Corrosion Technology for Scientists and Engineers, Ellis Harwood Ltd., West Sussex, England, 1989, pp. 15-20, 23-25.

30. M. Stern and A.L. Geary, "Electrochemical Polarization, I. A Theoretical Analysis of the Shape of Polarization Curves," Journal of the Electrochemical Society, Vol. 104, No. 56, 1957, pp. 56-63.

31. E. Cokca and A. Birand, "Determination of Cation Exchange Capacity of Clayey Soils by the Methylene Blue Test," Geotechnical Testing Journal, GTJODJ, Vol. 16, No. 4, December 1993, pp. 518-524.

32. R.E. Grim, "Clay Mineralogy," McGraw-Hill Book Company, New York, 1968, pp. 188-225.

APPENDIX

This Appendix contains a list of all the projects by Connecticut towns that were reviewed for steel piles in miscellaneous fill during this research project.

ANSONIA	02_54	Bridge Street Br. over Naugatuck River	No piles
	02_61	Bridge and approaches, Maple St. over Naugatuck River	No problem
	36-48	Naugatuck River Bridge on Divison St.	No piles
AVON	04_79	Rail Road Bridge over Arch Road	No piles
	04_84	Repairs to Rt.44 Bridge over Farmington River	No piles
BEACON FALLS	06_55	Welded composite girder bridge, Pines Br.Rd.	Timber piles
	06_90	Pines Bridge Rd. over Naugatuck River and NY,NH&HRR	No problem
BERLIN	07_42	New Britain - Middletown Road	No piles
	07_77	Route 5	Timber piles
	07_85	Relocation of Rt. 72 over NY,NH&HRR	Has problem
	07_86	Route 72	No piles
	07_103	3 Intersections in Berlin	No piles
	07-111	Relocated Rt.72 over SB rdwy over exist Rt.72	No problem
	21-26	Hartford-New Haven Turnpike	No piles
BETHANY	08_71	Culvert on Route 63	No piles
BETHEL	07_02	Danbury - Bridgeport Road	No piles
BLOOMFIELD	011-72	Relocation of Rt.9	No piles
	011-77	Pipe arch at Tumbul Brook on Rt.184	No piles
	011-80	Bridge repairs on I-91	No piles
	011-89	Rt.187-relocation	No CAM
	011-106	Median barrier on Rts. 187&189	No piles
	148-65	Wharton Brook Connector in Wallingford	No piles
BOZRAH	70-66	Relocation of Route 2	No CAM
	13-68	Bridge replacement on Route 82	No piles
BRANFORD	319-01	NY, NH&HRR Expy	No problem
	320-01	I-95 section.20 in the Towns of Branford, Guilford	No CAM

BRIDGEPORT	15-08	Bridge over Poquonnock River, Stratford Avenue	No piles
	15-39	Stratford Avenue S.R.751	No problem
	15-43	Connecticut Rt. 25	No problem
	15-46	NE&WN Rdwys over CT Turnpike	No problem
	15-47	Relocation of CT Rt.25	No piles
	15-48	Repair of two bridges on Route US 1	No piles
	15-53	Relocation of CT Rt.25	No piles
	15-57	Bridge repairs to I-95	No piles
	15-61	Relocation of Routes 8&25	No CAM
	15-77	Superstructure repairs to various bridges on I-95	No piles
	15-105	Stratford Avenue S.R.751	No problem
	50-93	Rooster River Bridge and approaches on Rt. US 1A	No piles
	310-01	Greenwich-Killingly Expwy	Has problem
	310-02	Greenwich-Killingly Expwy	Has problem
	311-01	Bridgeport Harbor Bridge superstructure	Has problem
	311-02		No problem
	311-03	Greenwich-Killingly Expwy	No problem
	312-01	Greenwich-Killingly Expy over Central Ave.	Has problem
	312-01	Greenwich-Killingly Expwy	Has problem
	313-01	Housatonic River Bridge	No problem
BRISTOL	17-51	North Street in Bristol	No piles
	17-60	Rt.72 in Bristol	No piles
	17-81	Rt.72&229 in Bristol	No piles
	51-105	Bridge over Connecticut River	Concrete pile
BURLINGTON	192-10	4 Bridges	No piles
	203-22	Bridge, Vineyard Road over Burling Brook	No piles
CANTON	20-04	Cherry Brook Bridge	No piles
	23-74	Bridge over Cherry Brook	No piles
	23-102	Reconstruction & wingwall replacement	No piles

	58-09	North Canton Road	No piles
	65-11	Concrete slab bridge	Timber piles
	203-13	Farmington River Bridge	No piles
CHESHIRE	25-74	Cheshire&Wallingford Road#730	No CAM
	25-108	I-691 in Cheshire	No CAM
	151-77	Illumination	No piles
	182-07	Illumination	No piles
	182-21	Illumination	No piles
CHESTER	12_20		
	120-57	Relocation of Route.85 in the Salem	No CAM
	26-83	Route.82-Highway signing	No piles
	26-82	Route.82 extension in Chester & Haddam	No piles
	58-108	Climing lane on Fort Hill	No piles
	58-125	Twin box culvert on SR.649 in Groton	No piles
CLINTON	27-47	Bridge over Hammock River on route.145	No piles
	27-57	Sidewalk on High Street	No piles
	27-19	Kelsey Mill Bridge and approaches	Timber piles
	27-20	Duck Hole Bridge and approaches	No piles
	27-32	Bridge over Menunicetesuck River and approaches on Houpert Rd.	Timber piles
	MC-24	Demolishing and removing old Trolley Bridge	No piles
COLCHESTER	78-68	Route 2	No CAM
	78-36	Culverts on the Colchester-Norwich Road	No piles
	28-109	Relocation of Route 2	No steel piles
	28-37	Jeremy Bridge & approaches	No piles
	28-08	Comstocks Bridge Colchester Road	No piles
	78-36	Relocation of Route 2	No CAM
CORNWALL	21-68	Relocation of Route 63	Timber piles
	21-79	Relocation of Route 63	Timber piles
CROMWELL	33-66	Relocation of Route 72	No piles
	33-79	Relocation of Route 72	No piles

	33-68	Route 72	Steel sheet pi
	33-82	Median barrier	No piles
	82-121	Bridge over Sebethe River	No CAM
DANBURY	34-58	Relocation of Rt.6 at Mill Plain	No piles
	34-60	Construction of White St.	No piles
	34-84	Relocation of US.Rt.6&US.Rt.7	No CAM
	34-86	Construction of Main Street and a section of West.St	No problem
	34-90	Box culvert on Brewster Road	No piles
	34-92	Drainage on Route. US.7	No piles
	34-93	Relocation of US.RT.6	Has problem
	34-95	Resurfacing on Rt.US.6	No piles
	34-101	Route.37	No piles
	34-102	Plan for construction of four structures on the relocation of US.Rt.6	Concrete pile
	34-103	Relocation of US.Rt.6&7	No problem
	34-104	Relocation of Algonquin gas transmission pipeline	Pipeline
	34-105	Relocation of US.Rt.6&7	No problem
	34-106	Relocation of US.Rt.6&US.Rt.7	No CAM
DARIEN	35-19	Old King Highway	Timber piles
	35-36	Bridge & approaches on Locust hill Road	Timber piles
	35-40	Section of Boston Post Road	No piles
	35-48	Stony Brook Bridge & extension	No piles
	35-50	Relocation of US Rt.1 and approaches	No piles
	35-53	Relocation of Route 1	No piles
	35-55	Relocation of US Rt. & overpass and approaches at Rt.136	No piles
	35-56	Relocation of Route 1 overpass	No CAM
	35-58	Relocation of US.1 & overpass over the NY,NH&HRR	No CAM
	35-59	Overpass over Post Road	No piles
	35-60	Bridge over Good Wives River & Stony Brook on the Boston Post Road	No piles
	35-78	Bridge-Tokeneke Road	No piles
	35-79	Five bridges in theTowns of Darien and New Canaan	Sheet piling
	102-10	Five Mile River Bridge & approaches	Timber piles

	135-18	Bridge over Norton River	Timber piles
	135-33	Bridge over Norton River & approaches	No piles
	135-53	Bridge over Norton River on Route US.1	No piles
	135-57	Bridge over Norton River on Rroute 118	Timber piles
	135-83	Norton River Bridge on Route 106 in Stamford	No problem
	35-50121-0	Bridge No.136-090 widening	No piles
DEEP RIVER	49-82	Relocation of Route.9 in Deep River	No CAM
	126-76	Relocation of Route.9	No piles
DERBY	36-58	Bridge over RR siding	No piles
	36-60	Bridge over NY, NH & HRR, Maybrook line	No piles
	36-71	Viaduct over passing Main St. Shelton-Derby-Ansonia Expy	Concrete pile
	36-90	Relocation of Rt.34 Main St. Br. over Naugatuck River	No problem
EASTON	7_02	Danbury - Bridgeport Road	No piles
	26-10	Easton - Monroe Road	No piles
	45-77	Bridge deck repair on Rt.59 over Mill River	No piles
	186-22	2 Bridges in Easton & Wilton	No piles
	187-02	Bridge over Aspetuck River	No piles
	203-M	Concrete box culvert at Mill River	No piles
EAST HARTFOR	42-35	Glastonbury & East Htfd Rd.	Timber piles
	42-40	Hartford Bypass	No piles
	42-53	Forbes st. over approach to Charter Oak	No piles
	42-54	Bridge, Simmons Road	No piles
	42-55	Bridge over Silver Lane	No piles
	42-62	Grading and drainage	No piles
	42-73	East Hartford-Glastonbury Expwy	No piles
	42-74	Beam bridge over Maple Street	No piles
	42-81	Overpass at Sutton Avenue	No piles
	42-83	A section of the East Htfd-Glastonbury Expwy	No piles
	42-87	Overpass & approaches at Main St. on the E.Htfd-Glby Expwy	No piles

	42-105	East Hartford Expressway	No CAM
	42-119	Bulkley Bridge interchange(East)	No problem
	42-132	I-84	No problem
	42-133	I-84 Bridge I-10 & K-9	Has problem
	42-134	I-84	No problem
	42-135	I-84	No problem
	42-136	I-84 Bridge over Main Street	No problem
	42-177	Left turn lanes on Rt.5	No piles
	42-178	Superstructure repairs to bridge on Rt.15	No piles
	63-18	CT River Br. between East Htfd & Hartford	No CAM
	108-08	Glastonbury-East Hartford Rd	Timber piles
	117-07	Hartford Bypass	
	138-03	Bridge over Silver Lane	No piles
	144-04	Forbes St. over approach to Charter Oak	No piles
	145-03	Bridge, Simmons Rd.	No piles
	157-03	Grading and drainage	No piles
	159-08	Beam bridge over Maple St.	No piles
	160-08	East Hartford-Glastonbury Expy	No piles
	160-12	Overpass at Sutton Ave.	No piles
EAST HAVEN	43-11	High Street Road	No piles
	43-34	Bridge over East Haven River & approaches	Timber piles
	319-01	Greenwich-Killingly Expwy over NY,NH&HRR	No problem
EAST LYME	44-19	New London bypass in the Town of East Lyme	No piles
	44-40	Bridge No.156-06 over Niantic River	No piles
	44-57	Flanders-Niantic Road	No piles
	44-74	Rocky Neck connector on I-95	No CAM
	44-76	Route 161	No piles
	44-89	Route.161 in East Lyme	No piles
	44-92	Median Barrier	No piles
	63-106	Rip rap at bridges	No piles
	104-16	A section of US.rt.1,Lieutenant River Bridge	No CAM
	104-19	Black Hall River Bridge and approaches	No piles
	104-43	Relocation of Rt.1	No piles

	104-48	Connecticut River Bridge in Old Lyme	No CAM
	104-52	Bridge on CT River& approaches	No CAM
	104-57	Relocation of Route.3 span arch overpass	No piles
	104-63	Grading&drainage on a section of relocated Rt.1	No piles
	104-63	Grading&drainage on Route US.1	No piles
	104-67	Bridge and approaches	No piles
	104-67	Bridge7approaches at Bridge Lake Road	No piles
	104-74	Paving a section of US Route#1	No piles
	104-75	Paving of a section of the relocation of US.Rt.1	No piles
	104-75	Paving a section of US Route#1	No piles
	104-87	Relocation of Route.156	No piles
	190-14	Route improvement	No piles
	190-17	Culvert at river & approaches on Rt.156	No piles
	324-08	Planting on I-95	No piles
	324-11	Highway illumination	No piles
	324-14	Improvement on I-95	No piles
	324-15	Median barrier on I-95	No piles
	326-01	I-95 in Monteville & Norwich	No piles
EAST WINDSOR	16-23	Bridge over Scantic River	No piles
	46-68	Section of Htfd-Spfld Expwy	Concrete pile
	46-77	Bridge over the CT river deck	No piles
	46-82	Drainage on I-91	No piles
	48-84	Several repairs on bridges	No piles
	165-63	Hartford-Springfield Expressway	No CAM
ENFIELD	48-68	Redecking CT River Bridge	No piles
	63-106	Placing rip bar at bridges	No piles
	129-99	Bridge and approaches over Scantic River on Route 190	No piles
	139-64	Bridge over CT River	No CAM
	139-72	Bridge over CT River	No CAM
ESSEX	49-56	Drainage	No piles
	49-61	Bridge over Falls River	No piles
	49-82	Relocation of Route 9 in the Towns of Essex & Deep River	No CAM

	105-109	Relocation of Route 9 in the Towns of Essex & Old Saybrook	No piles
FAIRFIELD	39-94	Relocation of US.6&RT.25 in Danbury	No CAM
	50-60	Sporthill Road	No piles
	50-93	Rooster River Bridge and approaches on Rt. US1A	Sheet piles
	50-93	Rooster River Bridge and approaches	sheet piles
	50-103	Median barrier on the Merritt Parkway	No piles
	56-81	Median barrier on the Rt.15 in Greenwich, Stamford&NewCanaan	No piles
	56-83	Median barrier on the Rt.15 in Greenwich, Stamford&NewCanaan	No piles
	56-90	Median barrier	No piles
	92-173	Repairs&improvements of service areas on I 95	No piles
	102-68	Wire rope railing	No piles
	102-103	Bridge repair on I-95	No piles
	180-52	Rt.15 rfd.conc.box culvert under Congress St.	Timber piles
	180-57	Rt.15,section 57 in Fairfield	No piles
	180-77	Rt.15, reinforced concrete rigid frame	No piles
	180-84	Sporthill Road Bridge over Mill Road	No piles
	180-85	Rt.15 under Park Avenue	No piles
	305-10	Traffic control signals for the CT Turnpike	No piles
	308-02	Greenwich-Killingly Expressway	No CAM
	309-01	Greenwich-Killingly Expy. in the Town of Fairfield	No CAM
	309-02	Greenwich-Killingly Expy in the Town of Fairfield	No problem
FARMINGTON	51-85	Farmington River Bridge and approaches	Concrete pile
	51-104	Rt.4 at railroad bridge	No piles
	51-106	Relocation of Rt.4	No CAM
	51-144	I-291&I-84	No CAM
	51-145	I-291&I-84	No CAM
	51-146	Rt. I-84	No piles
	51-150	South Road over I-84	No piles

GROTON	58-70	Fender&sidewalks on Mystic River Bridge	No piles
	58-90	I-95 in the Groton & Stonington	No piles
	58-91	I-91 in Groton	No CAM
	58-117	Groton defence access highway	No piles
	58-119	Groton defence access highway	No piles
	58-139	Intersectional improvement	No piles
	104-23	Concrete culvert box at Mile Creek	No piles
	104-54	Paving to Raymond Baldwin Bridge	No piles
GREENWICH	304-01	Greenwich-Killingly Expwy over Ferris Drive	No problem
GUILFORD	14-60	Drainage&shoulders on Rt.US.1	No piles
	59-30	Excavation plan of Channel	No piles
	59-56	Resurfacing & drainage on Rt.US.1	No piles
	59-59	Resurfacing & drainage on Rt.US.1	No piles
	59-80	East River Bridge & approaches on Rt.US.1	No CAM
	59-88	Pedestrian crossing over West River at Rt.US.1	No piles
	75-63	Bridge over Hammonasset River and approaches on Rt.US1	No CAM
	317-01	I-95,Section.17 in New Haven	Concrete pile
HADDAM	60-36	Section of Depot Road	No piles
	60-63	Ponset Brook Bridge&approaches	No piles
	60-88	Relocation of Route.9	No piles
	60-95	Relocation of Route.9	No piles
	60-98	Relocation of Route.9	No piles
	60-100	Beaver Meadow Road interchange	No piles
	60-108	Drainage and improvements on Conn.81	No piles
	82-118	Relocation of Route.9 in Middletown&Haddam	has problem
HAMDEN	185-40	Bridge over W.C.P on Skiff St.	No piles
	185-70	Bridge over Gilbert Avenue on W.C.Pkwy	No piles
	185-71	Separation structures&approaches on Circular Avenue	No piles
	185-86	Bridge on Wilbur Cross Parkway	No piles

	185-125	Wilbur Cross Parkway pavement replacement at structures	No piles
HARTFORD	42-41	Hartford Bypass	No piles
	42-42	Section of Hartford Bypass	No problem
	42-50	Plan for paving of section of Htfd Bypass	No piles
	42-133	I-84 bridge I-10&K-9	has problem
	42-134	I-84 Bridge over Darlin Street	Has problem
	63-18	Connecticut River Bridge	No CAM
	63-30	Grading and drainage on section of the North Meadow Expwy	No piles
	63-32	Front St. Bridge and approaches	Sheet piling
	63-63	Commerce Street Bridge and approaches	No CAM
	63-72	Prospect Bridge & approaches	No piles
	63-72	Park River Street Conduit	No piles
	63-83	Bridge over NY,NH&HRR, Willimantic branch	No CAM
	63-84	Bridge over NY,NH&HRR, Springfield	No CAM
	63-101	Footbridge over North Meadow Expwy	No piles
	63-101	Foot bridge over North Meadow Expy	No piles
	63-103	Founders Bridge	No problem
	63-103	Founders Bridge over the CT River	No piles
	63-103	The Hartford-Springfield Expwy	Has problem
	63-103	State Hartford Bridge	No piles
	63-106	Placing rip rap	No piles
	63-116	Htfd-Spfld Expwy	No problem
	63-124	Founders Bridge	No problem
	63-127	I-91 over Wawarme Ave & Reserve Road	No problem
	63-136	I-84	No steel piles
	63-137	I-84 WB Rdwy over Church Street	Has problem
	63-137	I-84	Has problem
	63-138	I-84	Has problem
	63-141	I-84	Has problem
	63-151	I-84 Trout Brook Connector	No CAM
	63-153	I-84 Bulkley Bridge widening	No piles
	63-158	I-84	Has problem
	63-159	Sigourney Street	Has problem
	63-161	I-91, Dutch Point Viaduct	No problem
	63-162	I-84	Has problem

	63-166	I-91 in the Town of Wethersfield & Hartford	No CAM
	63-174	I-84 E-W section	Has problem
	63-180	Installation of Highway illumination	No piles
	63-180	Installation of Highway illumination	No piles
	63-184	I-84	No problem
	63-185	I-91 Ramps	No problem
	63-190	Columbus Blvd.	No piles
	63-190	Columbus Blvd.	No piles
	63-190	Columbus Blvd.	No piles
	63-192	I-84	Has problem
	63-193	Farmington Avenue Connector	Has problem
	63-200	Median barrier rail on R-91 & Riverside Park Rd.	Has problem
	63-203	I-84 South drain conduit bypass	No steel piles
	63-203	I-84 South east drain conduit bypass Capital Ave.	No piles
	63-219	Traffic control signal	No piles
	63-220	Relocated ramp from I-91	No piles
	63-270	Installation of hydro cushion	No piles
	63-270	Hydro cushion cell	No piles
	115-02	Plan for paving of section of Hartford Bypass	No piles
	119-10	Section of Hartford Bypass	No piles
	130-05	Plan for paving of section of Hartford Bypass	No piles
	159-42	Grade separation structure on Deane Hwy, Htfd Ave.	Sheet piling
	155-45	Construction of New Britain Avenue	Timber piles
	159-91	I-91, Wetherfield Cove Channel	No CAM
	164-58	Relocation of ROUTE US. 5A, the Htfd-Spfld Expwy	No steel piles
	S-1625	Side walk & curb on the Buckley Bridge	No piles
HARWINTON	24-26	Strengthening of bridge over Naugatuck River	No piles
	27-29	Castle Bridge over the Naugatuck River	No piles
	65-62	Relocation of Route 72	No piles
	65-67	Relocation of Route 8	No piles
	65-69	Route 8	No problem
	73-36	Bridge & approaches on Northfield Road	Timber piles

	73-63	Reconstruction of rdwy deck on Castle Bridge over the Naugatuck River on Rt.8	No piles
	73-87	East Litch Road in Litchfield	Concrete pile
	73-88	Northfield Road	No piles
	73-96	Construction of several bridges in Litchfield, Morris	Concrete pile
	73-103	Bridge over Naugatuck River	No problem
	73-108	Turf establishment on Route 8	No piles
	140-105	Route 8 in Thomaston, Litchfield & Harwinton	No CAM
	140-108	Route 8	No piles
	143-68	Construction of several bridges & approaches in Torrington	No CAM
KENT	67-62	Route 341	No piles
	67-77	A section of Route 130	No piles
KILLINGWORTH	69-02	Killingworth-Chester Road	No piles
	69-04	Section of Killingworth-Deep River Road	No piles
	75-85	Bridge over Hammonasset River	No piles
	110-03	Section of the Durham Road	No piles
LITCHFIELD	73-93	Temp. bridge over Bantam River	No piles
	Map.30	Bantam River Bridge, Rt.61	No piles
LYME	13-8	Hamburg-North Plains Rd.-Rt.150 in the Towns of Lyme&Haddam	No piles
	324-01	I-95, Section.24	No CAM
MADISON	75-55-03A	Relocation of Rt. 79 over NY, NH & HRR	Has problem
	75-55	Relocation of Route.79 in Madison	has problem
	75-56	Hammonasset Connector for I-95	No CAM
	75-58	Hammonasset Connector to CT Turnpike in the Town of Madison	No problem
	75-63	Bridge over Hammonasset River	No CAM
	215-79	Metal beam type rail at overhead sign supports	No piles
	321-01	Greenwich-Killingly Expwy	No CAM
MANCHESTER	76-26	Hockanum River Bridge	No problem

	76-33	Separation structure over Charter Oak Bridge	No piles
MARLBOROUGH	44-83	Sealing joints	No piles
	78-66	Structures and approaches on relocated Route 2	No CAM
MERIDEN	79-72	I-91	No CAM
	79-73	I-91	No piles
	79-76	Relocation of Route 6A over ramp " M "	No problem
	79-81	Relocation of Route 6A	No piles
	79-82	Relocation of Route 6A over ramp " M "	No problem
	79-83	I-91	No CAM
	79-87	Signing of I-91	No piles
	79-89	Relocation of Route 6A	No piles
	79-93	Route 6A US.	No problem
	79-93	Relocation of Rt. US 6A over N.Y., N.H & HRR	No problem
	79-93	Relocation of US Rt. 6A over Colony Street	
	185-36	A section of Wilbur Cross Parkway	No piles
	185-37	A section of rt.5 & a structural steel bridge over Wilbur Cross Parkway	Timber piles
	185-56	Wilbur Cross Pkwy under Paddock Avenue	No piles
	185-57	Baldwin Avenue Bridge & approaches	No piles
	185-59	18' Span bridge over railroad & box culvert	Timber piles
	185-58	18' Span bridge over railroad & box culvert	Timber piles
	185-125	Wilbur Cross Parkway	No piles
MIDDLEBURY	80-78	I-84 in Middlebury & Waterbury	No CAM
	80-99	Culvert replacement	No piles
	87-80	Relocation of Route 63	No CAM
	130-96	I-84 in Southbury & Middlebury	No piles
	190-18	Widening of existing bridges	No piles
MIDDDLETOWN	79-79	I-91 in Meriden & Middletown	No steel piles
	82-57	Box culvert at Summer Creek on Rt.9	Timber piles

	82-58	Union Station overpass Middletown Expy	
	82-58	Bridge over NY,NH & HRR and Union St.	No problem
	82-61	East Main Street Bridge	Has problem
	82-73	Drainage extension	No piles
	82-90	Middletown Expy	Has problem
	82-90	Middletown Expy to Union Bridge Station	No problem
	82-98	South Main Street	No piles
	82-103	Sebethe Bridge & approaches	No CAM
	82-104	Bridge over Long Hill Brook and approaches on Rt.17	No CAM
	82-105	Relocation of Route. 5	No piles
	82-106	Relocation opf Route 9	No CAM
	82-118	Relocation of Route 9	No problem
	82-119	I-91	No steel piles
	82-130	I-91 in Middletown and Cromwell	No CAM
	82-135	Protective fencing	No piles
MILFORD	82-61	Relocation of Rt. No: 9	Has problem
	83-98	Fender replacement & placing rip rap	Timber piles
	138-23	Bridge over Housatonic River	No CAM
	138-172	Rehab. of I-95, Bridge 135 over Housatonic River	No piles
	314-01	Bridgeport Ave. Bridge	No CAM
	314-01	Milford Pkwy(G-K Expy)	No CAM
	314-01	G-K Expy over NY, NH & HRR	No problem
	BM1750	Replacement of ends of piers	No piles
MONROE	16-13	Bridgeport-Newtown Road	No piles
	17-14	Stevenson Road	No piles
	18-15	Stevenson Road	No piles
	19-16	Easton Road	No piles
	96-91	Route 111	No CAM
MONTVILLE	326-01	Greenwich-Killingly Expy over Rt. 163	Has problem
	326-01	I-95	No CAM
MORRIS	9-6,7	Thomaston Road	No piles

	86-78	Superstructure repairs to Rt.109, Bridge 01309	No piles
NAUGATUCK	87-08	Long Meadow Creek Bridge	No piles
	87-68	Bridge over ELM Street	No piles
	87-74	Bridge repair	No piles
	87-76	Construction of Rt. 63	No piles
NEW BRITAIN	07_85	Relocation of Route 72 in New Britain & Berlin	No problem
	07-111	Relocation of Rt. 72	No problem
	88-48	I-291 connector WB Rdwy over St.Mary's Cemetry	Has problem
	88-53	Route 72	No piles
	88-65	Reconstruction of South Street	No piles
	92-111	I-91 over NY,NH&HRR	Concrete pile
NEW CANAAN	89-38	Smith Ridge Road	No piles
	89-49	Relocation of channel of Five Mile River	No piles
	89-58	Route 123	No piles
	89-63	Route 123	No piles
	161-70	Bridge over Silvermine River	Timber piles
NEW HARTFORD	23-37	Section of Winsted-Hartford Road	No piles
	91-11	Townhill Road	Timber piles
	91-27	Nepaug River Bridge on Rt. 219	No piles
	91-30	Section of Winsted-Hartford Road	No piles
	91-72	Section of Rt. US 44	No CAM
	91-74	Bridge & approaching road over Nepaug River	No piles
	91-76	Relocation of Rt. 219	No CAM
	91-77	Misc. constructions in Torrington	No CAM
	91-78	Bridge over Troy Brook on Brook St.	No piles
	91-81	Bridge & approaches on Stub Hollow Rd. over Nepaug River	No piles
	91-85	Bridge over Nepaug River	No CAM
	91-105	Replacement of Bridge	Concrete pile
NEWINGTON	93-81	Relocation of Route 175	No piles

NEW MILFORD	95-77	Housatonic River Bridge and Bridge Street	No CAM
	95-112	The intersection of Route 25 & ELM Street	No CAM
	189-02	Construction of location no:44 Bridge and approaches	Concrete pile
	189-05	Location no:25 Bridge repair and approaches	No piles
NEW HAVEN	92-37	Piles bents under trolley area at West River Bridge	Timber piles
	92-46	Relocation of US.Rt. 1	No CAM
	92-47	Bridge over Stiles St. Relocation of US.Rt.1	No piles
	92-69	Underpass & approaches in New Haven & East Haven	No piles
	92-80	Relocation of Route US.1	No piles
	92-94	SB I-91 & WB I-95 Rdwys OAN&OAE	has problem
	92-99	Relocation of Route 34	Concrete pile
	92-110	East Rock Connector under Willow Street	Has problem
	92-111	I-91 in New Haven	No problem
	92-111	I-91 over NY, NH & HRR	concrete piles
	92-117	I-91	No CAM
	92-123	I-91	Concrete pile
	92-144	Route 17	No piles
	92-150	Median barrier	No piles
	92-151	Pedestrian overpass at Southern CT College	No piles
	92-167	Pavement marking	No piles
	100-60	I-91 over NY, NH & HRR	Has problem
	156-78	Temporary bridge-Kimberly Avenue	No piles
	156-77	Kimberly Avenue Bridge	Concrete pile
	182-21	Relocation of US. 6 from Marion Road	No piles
	185-64	Fountain Street Bridge & approaches	No piles
	185-65	Grade separation structure at Rt.67&Wilbur Cross Pkwy	No piles
	185-66	Grade separation structure at Rt.69	No piles
	185-123	Illumination	No piles
	189-07	Relocation of US Rt.6	No CAM
	317-02	Greenwich-Killingly Expy over Central Ave.	Has problem

	317-04	Greenwich-Killingly Expwy over Oak Street	Has problem
NEWTOWN	34-94	Relocation of Rt. US 6&25	No CAM
	60-15	Mile Hill Road in Fairfield State Hospital Grounds	No piles
	60-18	Bridge over Great Brook Newtown	No piles
	96-39	The relocation of US Route 6 in the Town of Newtown&Southbury	No piles
	96-49	Housatonic River Bridge and approaches on the relocation of US Rt.6	No CAM
	96-59	Overpass at Centre Street on the relocation of US Rt.6	No CAM
	96-60	Overpass at Alpine drive on the relocation of US Rt.6	No piles
	96-70	Relocation of Rt. 6	No piles
	96-74	School house hill road, relocation of US Rt.6	No CAM
	96-74	Relocation of Rt. US 6, School House Hill Rd.	No CAM
	96-112	Bridge over Pootatuck River	No piles
	125-98	Resurfacing of bridges	No piles
	193-02	Relocation of US Route .6	No piles
	199-03	Bridge over Great Brook at Fairfield State Hospital	No piles
NORWALK	102-57	West Avenue in Norwalk	No piles
	102-114	Relocation of Rt. US.7 in Norwalk	No problem
	102-114-03	Relocation of Rt. 7	Has problem
	102-114-03	Relocation of Rt.7 WN Rdwy NE Rdwy&ramp over I-95	Has problem
	102-114-03	Relocation of Rt.7 EN Rdwy over NY,NH&HRR	Has problem
	102-115	Relocation of Rt. US.7 in Norwalk	No piles
	304-01	Greenwich-Glenville	No problem
	306-01	Grade separation structures on G-K Expy	No piles
	306A-01	Greenwich-Killingly Expy in Norwalk	Has problem
	306-03	Greenwich-Killingly Expy over NY,NH&HRR Danbury Branch	Concrete pile
NORWICH	103-51	Relocation of Route 12	No piles
	103-63	Shetucket River Bridge on Rt.12	Timber piles

	103-67	Culvert on Route 2	No piles
	103-68	Laurell Hill Bridge over Shetucket River	No piles
	103-74	Relocation of Routes 2&32	No CAM
	327-01	I-95	No CAM
NORTH BRANFO	98-25	Concrete slab bridge & approaches on Durham Road	No piles
	98-37	Road No. 80&139 Quarry Road	No piles
	100-85	Shoulder reconstruction on Route 17	No piles
	135-69	Sealing joints on Route 104	No piles
NORTH HAVEN	18-36	Broadway Bridge over Quinnipiac River	No piles
	100-11	NY, NH, & HRR, New Haven to Springfield	No problem
	100-57-03B	Relocation of Rt. US 5A over NY, NH & HRR	Has problem
	100-59	I-91 in North Haven	Concrete pile
	100-60	I-91 over NY, NH &HRR	Has problem
	100-61	Route. 22	No piles
	100-72	Relocation opf Route. 10	No CAM
	100-85	Shoulder reconstruction	No piles
	100-87	Relocation of Route. 10	No CAM
	185-74	Relocation of State Street	No piles
	185-76	Bridge over Toelles Road	Timber piles
	185-81	Concrete bridge over Mill River	Timber piles
	185-105	Hamden Dixwell Avenue over Mill River	Timber piles
NORTH STONIN	101-85	Bridge and approaches over Green Falls River on Route 216	No CAM
	113-85	Route 2	No piles
	190-09	Bridge over Assekomk Brook & approaches on Rt.119	No piles
OLD LYME	104-19	Black Hall River Bridge and approaches	Timber piles
	104-23	Box culvert and approaches	Timber piles
	104-29	Relocation of Route.156 in Old Lyme	No CAM
	104-52	Drainage on Routes.80&144	No piles
	104-87	Relocation of Rt.156	No piles

OLD SAYBROOK	22-30	Proposed bridge on Oyster River cut-off over Oyster River	No piles
	86-125	I-95, section.22	No CAM
	104-48	Construction of Connector of river bridge in Old Lyme	No CAM
	104-53	Paving approaches to Raymond E. Baldwin Bridge	No piles
	105-20	Construction of Federal aid project#17,section A	No piles
	105-56	New floor&curbs on the Bridges over the CT River	No piles
	105-107	Reconstruction of bridge over railroad on Rt.166	No piles
	322-01	I-95, section.22	No CAM
ORANGE	106-68	CT Turnpike ramps at March Hill Road	No piles
	158-106	Pavement markings	No piles
	185-22	Wilbur Cross Pkwy Grassy Hill Rd. Bridge	No piles
	185-28	Cast stone faced arch bridge at Derby Avenue	No piles
	185-79	Wepawauc River Bridge and approaches	Timber piles
	315-01	I-95	Concrete pile
	315-02	I-95	Concrete pile
OXFORD	12_12	Proposed bridge over Little River	No piles
	13-13	Proposed arch bridge, 8 Mile Brook	No piles
	39-08	Proposed bridge over 8-Mile Brook	No piles
	39-09	Proposed bridge over Little River	No piles
	39-11	Seymour - Southbury Rd.	No piles
	104-05	Concrete box culvert	No piles
	107-09	Seymour-Southbury Road	No piles
	107-27	Concrete box culvert	No piles
	124-04	Seymour-Southbury Road	No piles
PLAINFIELD	88-46,51-12	Rt.84 in New Britain and Farmington	No piles
	109-30	Requabick River Bridge	No piles
	109-51	Drainage	No piles
	109-68	Railroad grade separation&approaches	sheet piling
	109-92	Route.72	No piles
	131-80	Rt.84 in Southington and Plainville	No problem

PLAINVILLE	109-74	NE Rdwy over relocation Rt. 72	No problem
PORTLAND	82-67	Repairs to CT River Bridge	No piles
	112-26	Bridge over Cox's Brook on Rt.15A	Timber piles
PRESTON	113-67	Route 2	No piles
	113-78	Turn establishment on railroad	No piles
REDDING	116-45	Overpass at NY,NH&HRR &Connectors between US.7&53 at Wilson&Redding	No piles
	116-60	Route 107	No piles
	116-69	Norwalk River crossing on Route 53 & 465	No problem
	117-94	Joints sealing	No piles
RIDGEFIELD	117-93	Intersection of Route 102 & US.7	No piles
ROCKYHILL	33-66	I-91 in Cromwell & Rocky Hill	No problem
	118-58	Ferry slips	No piles
	118-61	Cromwell Avenue	No piles
	118-68	I-91 in Rocky Hill & Wethersfield	No CAM
	118-74	I-91	No piles
ROXBURY	119-27	Box culvert	No piles
	119-72	Reconstruction of Routes 199&67	No piles
	119-76	Location 12 Bridge and approaches	No CAM
	119-77	Bridge over Shepang River and approaches on Route 199	No piles
SEYMOUR	02_20	Ansonia-Seymour Road	No piles
	24-24	Abutment & slab bridge over Hoppe River	No piles
	25-30	Wood Bridge Paynes Seymour extension Rt.147	No piles
	36-73	Shelton-Derby-Ansonia Expressway	No CAM
	124-04	Seymour-Southbury Rd.	No piles
	124-11	Relocation of Rt.8 in Seymour	Timber piles
	124-24	Broad street bridge in Seymour	No piles
	124-49	Seymour - Beacon Falls Road	No piles

	124-54	Brdge over Little River	No piles
	124-80	Reconstruction of Rt.8	No problem
	124-91	Foot Bridge at Broad Street over Naugatuck River	Timber piles
	124-94	Relocation of Rt.8 over Rt.67	No CAM
	124-99	Relocation of Rt. 8 over Derby Ave.	Has problem
	190-10	Culvert replacement on Rt.8,79&144	No piles
SHARON	125-76	Sharon-Lakeville Road	No piles
	125-81	Rt.4 over Mudge Pond Brook	No piles
	125-98	Resurfacing of bridges	No piles
	125-100	Bridge replacement on Rt.4	No piles
	125-101	Restoration of the covered bridge over the Housatonic River	No piles
SHELTON	36-37	Housatonic River Bridge in Shelton	No problem
	36-37-03A	Housatonic River Bridge	No problem
	126-13	Section of birid turnpike	No piles
	126-34	Nichols-Shelton Road	No piles
	126-54	Grading and drainage on Shelton Expy	No piles
	126-56	Prospect Avenue Bridge & approaches	No piles
	126-57	Coram Avenue Bridge&approaches over Shelton-Derby Expy	No piles
	126-58	Bridge over Sullivan Avenue on Shelton-Derby-Ansonia Expwy	No CAM
	126-60	Paving a section of the Shelton-Ansonia Expy	No piles
	126-68	Howe Ave. Bridge Rt.110	No piles
	138-76	Bridge over Far Mill River and relocation of Rt.110	No piles
	185-79	Wepawaus River Bridge	No piles
	126-81	Route.110	No piles
	126-95	Installation of barrier rail on Rt. 8	No piles
	126-99	Route.108 realignment	No piles
	158-19	Reinforced concrete deck of Housatonic River Bridge	No piles
	160-05	Bridge over Sullivan Avenue	No CAM
	S-2176	Indian Well Road in Shelton	No piles
	S-3186	North and Thompson Streets	No piles
SIMSBURY	04_68	Two cable railing	No piles

	48-06	Reinforced concrete T-beam bridge	No piles
	48-62	Bridge over Scantic River and approaches	No piles
	48-80	Corrugated str.steel plate pipe arch at Terry Brook	No piles
	48-82	Htfd-Spfld Expy in the Town of Enfield	No CAM
	48-84	Several bridges and approaches in Enfield	No piles
	113-07	Various culverts in Enfield	No piles
	128-24	Avon road	No piles
	128-59	Bridge and approaches over Farmington river	Concrete pile
	128-67	Bridge over Hop Brooks on Rts. 10&202	No piles
	128-68	Reinforced concrete box culvert on state road	No piles
	128-69	Corrugated structural plate pipe arch at Minister Brook	No piles
SOUTHBURY	14-17	Proposed alterations to Abutments & piers	No piles
	43-13	Proposed alterations to abutments and piers	No piles
	107-09	Seymour-Southbury Road	No piles
	124-04	South Britain Road	No piles
	130-24	Bridge over Pomp River	No piles
	130-69	Underpass at station 190+76 on Rt. US 6	No piles
	130-83	Bridge over Pomperaug River on Rt.67	No CAM
	187-08	Bridge over Pomp. Rd	No piles
SOUTHINGTON	27-37	Federal aid project.19	No piles
	131-69	Dunham Bridge	No piles
	131-75	I-84 under West Street	No problem
	131-75	I-84 over Eight Mile River	No CAM
	131-75	I-84 under Prospect Street	No CAM
	131-75	I-84 under Jude Jane	No CAM
SPORT HILL	26_01	Superstructure for proposed bridge	No piles
STAMFORD	56-81	Median barrier on the Merritt Parkway	No piles
	56-83	Median barrier	No piles
	56-91	Median barrier	No piles

	56-90	I-95 in Groton & Stonington	No CAM
	135-75	Planting on Rt.137	No piles
	135-83	Noroton River Bridge and approaches on Rt.106	No CAM
	135-85	Culvert replacement on Rt. US.1	No piles
	135-87	Widening of Rt.104	No piles
	135-88	Reconstruction of Rt.104	No piles
	304-01	Greenwich-Killingly Expy in Greenwich&Stamford	No problem
	304-02	Greenwich-Killingly Expy	Has problem
	305-01	Greenwich-Killingly Expy	No piles
	308-01	Sherwood Island to state highway over NY,NH&HRR	Has problem
STRATFORD	83-98	Fender replacement & placing rip rap	Timber piles
	97-01	Merritt Parkway	No piles
	98-12	Barnum Ave. Cutoff & Ferry Blvd.	No piles
	138-04	Stratford South Route	No piles
	138-44	Sidewalk on Decks Mill Bridge over Yellow George Brook on Rt.8	No piles
	138-71	Box culvert at Bruce Brook & approaches, Nichols Ave.	No piles
	138-80	Removal of remains of old piers	No piles
	138-105	Truck weighing station	No piles
	138-114	Box culvert under Rt. US 1	No piles
	138-167,168	Bridge substructure repair	Timber piles
	138-172	Rehab. of I-95, Bridge 135 over Housatonic River	No piles
	138-N3	Nichols-Shelton Road	No piles
	180-01	Merritt Highway section #1	Concrete pile
	313-01	Greenwich-Killingly Expy over Housatonic River Bridge	No problem
	313-03	Greenwich-Killingly Expwy	No problem
	BM 1750	Replacement of ends of piers	No piles
STONINGTON	58-70	Mystic River Bridge	No boring log
	58-90	I-90	No CAM
	137-71	Relocation of Route US.1	No CAM
	137-74	I-95	No piles
	137-75	I-95	Concrete pile

THOMASTON	26-24	East Main Street Bridge & approaches	No piles
	110-76	Several bridges in Plymouth	No piles
	140-05	East Main Street Dry Bridge and grade crossing	No piles
	140-11	Bridge & approaches-Moosehorn Brook	No piles
	140-46	Bridge over Northfield Brook on Center St.	No piles
	140-47	Marine St. Bridge over Northfield Road	No piles
	140-84	Repairs Reynolds Bridge	No piles
	140-90	Bridge over Branch Brook	No problem
	140-90	Bridge over Thomaston & Watertown	No CAM
	140-91	Bridge over Northfield Brook	No piles
	140-92	Draining & truck climbing on Plymouth Hill Rt. US 6	No piles
	140-98	Retaining wall at Northfield Brook on Route 8	No piles
	140-99	Jackson Street widening	No piles
	140-108	Route 8	No piles
	140-111	Route 8 over relocated river and railroad	No CAM
	151-65	Route 8 in Waterbury & Thomaston	No piles
	151-69	Route 8 in Waterbury & Thomaston	No piles
	151-80	Relocation of Rt.8	No problem
	190-20	Section of pavement replacement	No piles
	MC 34	Repair to Bridge on Main Street	No piles
TOLLAND	142-31	Wilbur Cross Parkway	No piles
	142-38	Wilbur Cross Pkwy Bridge over Willimantic River & approaches	No piles
	142-42	Paving of section on Wilbur Cross Parkway	No piles
	142-61	Wilbur Cross Highway underpass & approaches at Merrow Rd.	Concrete pile
	142-65	Wilbur Cross Highway & overpass at Cider Mill	No CAM
	142-68	Grading & drainage and 3 bridges on the Wilbur Cross Highway	No piles
	142-69	I-84 Eastbound Roadway	No piles
	142-76	The Intersection of Cider Mill Road & Merrow Road	No piles
	160-25	Bridge over Willimantic River	Timber piles

TORRINGTON	143-56	Bridge over W.Branch Naugatuck River	No piles
	143-64	Bridge & approaches Brass Mill Dam Rd. over Naugatuck River	No piles
	143-66	Bridge & approaches over West Branch Naugatuck River	No piles
	143-77	Relocation of Rt. 77	No piles
VERNON	76-41	Section of I-84	No piles
	146-47	I-84 Overpass	No CAM
	146-47-03	I-84 over NY,NH & HRR	No piles
	146-58	Wilbur Cross Highway and approaches	No piles
	146-61	Wilbur Cross Highway underpass & approaches at Dobson Rd & Campbell Ave.	Concrete pile
WALLINGFORD	100-60	I-91 in North Haven & Wallingford	No problem
	148-26	Bridge over Quinnipiac River	No piles
	148-55	Route I-91 in Wallingford&Meriden	No piles
	148-65	Wharton Brook Connector	No piles
	148-70	Route US.5 & Bridge over Meeting House Brook	No piles
	148-75	Relocated Connecticut Route.68	No piles
	185-78	Grade separation structure	No piles
WATERBURY	05_74	Two-cable guide railing	No piles
	19-21	Waterbury-Watertown-Thomaston Road	No piles
	87-88	Relocation of Route 8	No problem
	130-120	Median barrier on I-84	No piles
	151-05	Mad River Bridge & approaches	No piles
	151-12	Thomaston Avenue	No piles
	151-47	South Leonard Street Bridge over Naugatuck River	No piles
	151-61	Bridge & approaches Washington Ave. over Naugatuck River	No piles
	151-63	Bridge & approaches, Bristol Rd. over Naugatuck River	Concrete pile
	151-69	Route. 8 in the Towns of Waterbury & Thomaston	No piles
	151-79	Relocation of CT Route. 8 & Watertown Connector	Concrete pile
	151-80	Relocation of CT Route 8	No CAM

	151-86	Relocation of CT Route. 8 & Watertown Connector	Concrete pile
	151-87	I-84 & relocation of CT road	Has problem
	151-88	I-84 & relocation of CT road	Has problem
	151-89	I-84	Has problem
	151-90	Relocation of CT Route 8 & Grading of I-84	No problem
	151-91	Viaduct superstructure	No piles
	151-102	Relocation of CT Route. 8 & Watertown Connector	Concrete pile
	151-112	Reconstruction of I-84	No CAM
	151-126	Median barrier on I-84	No piles
	151-173	Thomaston Avenue Sr.847 bridge replacement	No piles
	151-177	West bound entrance ramp	No piles
	151-202	Rehabilitation of bridges	No piles
	151-203	Rehabilitation of bridges	No piles
	151-208	Crack arrestment	No piles
	151-214	Infrastructure renewal program	No piles
	182-02	Silver Street connection to relocation of US Route 6A	Timber piles
	182-04	Viaduct River Mill Street Baldwin St, Mad River	No piles
	182-06	Waterbury Expwy from Mill St. Viaduct to Silver St.	No piles
	182-07	Relocation of Route US. 6 from Scott Road to Marion Road	No CAM
	182-13	Harper's ferry & Scott Roads and a section of the Service Road	No piles
	182-19	The Waterbury Expwy from Silver St. to Hamilton Avenue	
	182-20	The Waterbury Expwy from Hamilton Avenue to Scott Road	No CAM
WATERFORD	85-75	Thames River Rd. & approaches Route 2A	No piles
	94-65	Frontage Road & approaches on Rt. US 1	No CAM
	152-35	New London Bypass	Timber piles
	152-61	I-95, WB Rdwy and Frontage Road	No CAM
	325-01	I-95	No CAM
	325-06	I-95	No piles

WATERTOWN	15-129	Thermoplastic pavement	No piles
	125-98	Resurfacing of bridges	No piles
	153-56	Buckingham Street & widening on Main Street	No piles
	153-61	Bridge over Steel Brook Rt. US 6	No piles
	153-68	Buckingham Street	No piles
	153-73	Extension of Route 72	No piles
WEST HARTFOR	53-64	East Hartford-Glastonbury Expy,Rt.17	No piles
	53-65	East Hartford-Glastonbury Expy	No piles
	53-77	East Hartford-Glastonbury Expy,Rt.17	No piles
	53-100	Relocation of Rt.2, Reconstruction of Hebron Avenue	No piles
	53-104	Relocation of Rt.2, Reconstruction of Hebron Avenue	No piles
	63-151	I-84 connector Trout Brook	No CAM
	155-63	I-84	sheet piles
WEST HAVEN	18-65	Housatonic River Bridge&approaches at Southville	No CAM
	83-87	Sea wall on Route 122	No piles
	92-32	Bridge over West River	Timber piles
	156-28	Drainage system on James Hill Road	No piles
	156-70	Saw Mill Rd. underpass & approaches	No steel piles
	156-75	Concrete barrier installation	No piles
	156-78	Temporary bridge - Kimberly Avenue.	No piles
	156-85	Resurfacing I-95	No piles
	316A-01	Grade separation structure on I-95	No CAM
WESTON	012-12	Georgetown Road	No piles
	012-13	Cobb's Mill Bridge Road	No piles
	116-59	Relocation of Route 57	No piles
	151-14	24' Span rfd. concrete bridge	No piles
	157-58	Route 57	No piles
	158-74	Bridges & approaches in the Town of Weston	No piles
WESTPORT	35-79	Five Mile River Bridge Rt.123	No piles
	56-90	Median barrier on the Merritt Pkwy	No piles
	158-44	Sherwood Island Connector to CT Turnpike	No piles

	158-46	Repairs to bridge No. US.1-1189 over Saugatuck	No piles
	158-55	Stony Brook Bridge on Rt.33	No piles
	158-66	Removal of movable span on the Naugatuck River	No piles
	158-79	The relocation of Hilland Rd. over Sherwood Island Connector	No piles
	307-01	Greenwich-Killingly Expy in Westport	No problem
	307-02	Greenwich-Killingly Expy in Westport	No piles
	308-01	Construction of G-K Expy in Westport	No problem
	308-02	Greenwich-Killingly Expy in Westport	No CAM
WETHERSFIELD	007-77	Route. 5	Timber piles
	93-37	US.5 Route	No piles
	118-68	I-91 in Wethersfield & Rocky Hill	No CAM
	159-30	Hartford Bypass	No piles
	159-31	Hartford Bypass	No piles
	159-32	Bridge on Ridge Road	No piles
	159-34	Bridge over Folly Brook Boulevard Bypass	No piles
	159-38	Hartford Bypass bridge	No piles
	159-40	Hartford Bypass	No piles
	159-42	Silas Deane Highway Hartford	Sheet piles
	159-43	Bridge over US. Rt.5	No piles
	159-61	Section of Berlin Turnpike	No piles
	159-90	Maple Street Interchange	No piles
	159-92	I-91 & US.5 over Avery Point	No problem
	159-96	Median barrier on I-91	No piles
	159-111	Resurfacing of I-91	No piles
WILTON	107-74	Bridges over 8 Mill Rd. over Norwalk River	No piles
	116-45	Overpass at NY, NH & HRR and connections between Rt.7&53 at Georgetown	No piles
	161-19	Bridge over Norwalk River on Ridgefield Road	No piles
	161-69	Bridges over Norwalk River, Five Mile River & Still River	Timber piles
	161-70	Several bridges and approaches in Ridgefield & Wilton	Timber piles

	161-72	Bridge over West Branch Saugatuck River	No piles
	161-78	Passing Line on Rt.7	No piles
	161-79	Intersection of Rt.7&33	No piles
	161-86	US Rt.7	No problem
WILLINGTON	142-43	Paving of a section of Wilbur Cross Parkway	No piles
	159-75	Painting on Route 15	No piles
	160-25	Bridge over Willimantic River	Timber piles
	160-26	Bridge & approaches over Roaring Brook on Rt.32	Timber piles
	160-51	The relocation of Rt.32	No CAM
	160-63	Wilbur Cross Hwy underpass approaches & Frontage Roads at Ruby Rd.	data missing
	160-65	Wilbur Cross Hwy underpass & approaches at Potter School Road	No piles
	160-99	Reconstruction of Rt.320 Ruby Road	No piles
WINDSOR	164-58	Relocation of Rt. US 5, Htfd-Spfld Expwy	No piles
	164-74	Grading Rt. US 5A	No piles
	S2863D	Roadway approaches	No piles
WINDSORLOCK	39-64	Bradley Field connector	No piles
	63-106	Placing rip rap at bridges	No piles
	165-53	Bridge over canal	No steel piles
	165-64	Bradley Bield connector	No piles
	164-81	I-84	No CAM
	164-87	I-84 over Hayden Sation Road	Concrete pile
	164-117	Drainage on Route US. 5A	No piles
WOODBRIDGE	167-50	Ansonia Road & Fountain Street	No piles
	185-29	Race Brook Road Bridge and approaches	No piles
	185-30	Johnson Rd. Br. & approaches, Wilbur Cross Pkwy.	No piles
	185-90	A twin bore tunnel through West Rock	No piles